

The Role of WH2-containing Proteins in Regulating Actin-MRTF-SRF-mediated Transcription

Dissertation

zur Erlangung des
Doktorgrades der Naturwissenschaften (Dr. rer. nat.)

der

Naturwissenschaftlichen Fakultät I
– Biowissenschaften -
der Martin-Luther-Universität Halle-Wittenberg

vorgelegt

von Frau Julia Weißbach
geboren am 24.06.1987 in Querfurt

Gutachter:

Prof. Guido Posern

Prof. Mechthild Hatzfeld

Prof. Bernd Knöll

Verteidigungsdatum: 15. November 2017

Content

I Summary.....	3
Zusammenfassung	4
II Introduction	5
II.1 Serum Response Factor - SRF	5
II.2 Myocardin-related Transcription Factors – MRTF-A/-B	6
II.3 Actin and Actin-Binding Proteins	9
II.4 Nucleation Promoting Factors – NPF	12
II.4.1 Neuronal Wiskott-Aldrich Syndrome Protein – N-WASP	14
II.4.2 WASP Family Verprolin-homologous Protein 2 - WAVE2.....	15
II.4.3 Junction-mediating and Regulatory Protein - JMY	15
II.5 Structure of MRTF:Actin Complexes and Aim of the Study	16
III Materials and Methods.....	18
III.1 Materials	18
III.1.1 Equipment.....	18
III.1.2 Chemicals and Reagents	19
III.1.3 Common Buffers and Solutions.....	22
III.1.4 Antibodies and Staining Reagents	23
III.1.5 Oligonucleotides	26
III.1.6 Plasmids	29
III.1.7 Cells and Culture Media	34
III.2 Methods	35
III.2.1 Molecular Cloning and DNA Manipulation Methods	35
III.2.2 Cell Culture Methods.....	39
III.2.3 Protein Analytical Methods	41
III.2.4 Immunofluorescence Staining and Microscopy	44
III.2.5 Luciferase Reporter Assay.....	44
III.2.6 Isolation of total RNA.....	45
III.2.7 cDNA Synthesis and Quantitative real-time PCR.....	45
III.2.8 Calculation and Statistics.....	46

IV Results.....	47
IV.1 Actin Polymerization inside the Nucleus	47
IV.2 WH2 (V) Domain-containing N-WASP and WAVE2.....	49
IV.2.1 N-WASP and WAVE2 activate MRTF-SRF-dependent Target Gene Transcription.....	49
IV.2.2 N-WASP and WAVE2 induce Nuclear Accumulation of MRTF-A.....	51
IV.2.3 N-WASP and WAVE2 compete with MRTF-A for Actin-Binding independently of ARP2/3 Interaction	52
IV.2.4 N-WASP and WAVE2 induce MRTF-A Nuclear Accumulation and Target Gene Expression independently of ARP2/3-mediated Actin Polymerization	55
IV.2.5 Serum-stimulated Actin:MRTF-A Complex Disruption is mediated by a <i>Trans-Acting</i> Factor.....	66
IV.3 WH2 (V) Domain-containing JMY	70
IV.3.1 Full length JMY has a slight Impact on MRTF Activation and Nuclear Translocation	70
IV.3.2 C-Terminal truncated JMY competes with MRTF-A for Actin-Binding....	73
IV.3.3 C-Terminal truncated JMY induces Nuclear MRTF-A Accumulation	76
IV.3.4 C-Terminal truncated JMY activates MRTF-SRF-dependent Gene Expression.....	78
IV.3.5 C-Terminal truncated JMY activates MRTF-SRF-dependent Gene Expression independently of ARP2/3-mediated Actin Polymerization	79
V Discussion	83
V.1 Nuclear Actin Polymerization.....	83
V.2 MRTF-A Activation by N-WASP and WAVE2	84
V.3 MRTF-A Activation by Competition with WH2 (V) Domains for Actin-binding..	85
V.4 JMY CA-Region mediates intramolecular Inhibition.....	91
VI Bibliography.....	93
VII Abbreviation List.....	106
VIII Appendix.....	109
IX List of Publications.....	117

I Summary

The complexity of eukaryotic organisms and the vast diversity of cellular functions result from spatiotemporal regulated gene expression. Transcription factors such as the serum response factor (SRF) and myocardin-related transcription factors (MRTF) therefore act as essential signaling nodes and coordinate cellular functions. They are controlled by cytoskeletal actin dynamics which critically affect transcription of target genes through the MRTF-SRF module. MRTF-A activation requires its dissociation from an inhibitory complex with globular actin. The molecular reason for complex disruption is still controversial. Changes in G-actin availability is the most common model, but it is challenged by the immense excess of monomeric actin over MRTF-A. Another possibility which is proposed by this work is a direct competition of representative WH2 (V) domains with MRTF-A for actin-binding. Analysis of transcriptional activation, *in vitro* competition assays and immunofluorescence studies in NIH 3T3 mouse fibroblasts show that MRTF-A is induced by the WH2-containing nucleation-promoting factors (NPF) N-WASP and WAVE2 independently of altered actin dynamics. Moreover, mutations of the ARP2/3-interacting central acidic (CA) region and inhibition of the ARP2/3 complex by CK-666 or ARP3-siRNA hardly reduce N-WASP- or WAVE2-mediated MRTF-A activity. Biochemical complementation experiments point towards a transferable factor which is responsible for impaired *de novo* association of actin and MRTF-A upon serum-stimulation. The results demonstrate that MRTF target gene transcription can occur by a competitive mechanism through N-WASP and WAVE2 which is independent of their role in actin dynamics. The WH2-containing protein JMY confirms this competition hypothesis by activating the MRTF-A-SRF reporter independently of actin nucleation. Elevated activity upon truncation of the C-terminal CA region reveals an as yet unknown auto-inhibition of full length JMY. Therefore, this work additionally contributes to better understand the complex regulation of the nucleation-promoting factor JMY. Various NPF are known to be inhibited by intramolecular back-folding which occludes their WH2 domains. This study suggests a novel mechanism of MRTF target gene activation by unfolded NPF involved in physiological signal transmission in mammalian tissue.

Zusammenfassung

Die Komplexität eukaryotischer Organismen und die funktionelle Diversität ergeben sich aus einer räumlich-zeitlich regulierten Genexpression. Dabei fungieren Transkriptionsfaktoren, wie der *serum response factor* (SRF) und *myocardin-related transcription factors* (MRTF), als Signal-Schaltstellen, welche zelluläre Funktionen koordinieren. Sie werden durch die Aktin-Dynamik des Zytoskeletts kontrolliert, die über das MRTF-SRF Modul Einfluss auf die Transkription von Ziel-Genen nimmt. Zur Aktivierung von MRTF-A muss die Dissoziation von einem inhibierenden Komplex mit Aktin erfolgen. Die molekulare Ursache dieser Dissoziation ist bisher ungeklärt. Ein verbreitetes Model stützt sich auf die Reduktion des verfügbaren globulären Aktins, was aber aufgrund des zellulären Überschusses an G-Aktin gegenüber MRTF-A zu bezweifeln ist. Diese Arbeit schlägt daher als möglichen Grund eine direkte Konkurrenz zwischen WH2 (V)-Domänen und MRTF-A um die Bindung an Aktin vor. Untersuchungen der transkriptionellen Aktivität sowie *in vitro* Kompetitions- und Immunfluoreszenz-Analysen in NIH 3T3 Fibroblasten zeigen, dass die WH2-enhaltenden *nucleation-promoting factors* (NPF) N-WASP und WAVE2 MRTF-A aktivieren ohne dabei die Aktin-Dynamik zu ändern. Zudem führen Mutationen der ARP2/3-interagierenden *central acidic* (CA)-Region sowie die Inhibierung des ARP2/3-Komplexes durch CK-666 oder ARP3-siRNA nur geringfügig zur Verminderung der N-WASP- und WAVE2-vermittelten MRTF-A Aktivität. Biochemische Komplementations-Experimente weisen auf einen übertragbaren Faktor hin, welcher die *de novo* Aktin-MRTF-Assoziation nach Serum-Stimulation reduziert. Die Ergebnisse belegen, dass die MRTF-A-vermittelte Genexpression durch Konkurrenz von N-WASP und WAVE2 induziert werden kann und unabhängig von einer veränderten Aktin-Dynamik ist. Das WH2-Protein JMY bestätigt diese Hypothese durch eine ebenfalls Polymerisations-unabhängige MRTF-SRF Aktivierung. Eine gesteigerte Aktivität nach Mutation der C-terminalen CA-Region deutet auf eine bisher unbekannte Auto-Inhibierung von *full length* JMY hin. Somit trägt diese Arbeit dazu bei, die komplexe Regulation von JMY besser zu verstehen. Auch für andere NPF ist bereits bekannt, dass sie durch intramolekulare Faltungen reguliert werden, die z.B. zur Verdeckung der WH2-Domäne führen. Diese Arbeit schlägt daher einen neuen Mechanismus zur Aktivierung von MRTF Zielgenen vor, bei dem aufgefaltete NPF an der physiologischen Signalübertragung in Säuger-Gewebe beteiligt sind.

II Introduction

II.1 Serum Response Factor - SRF

The complexity of eukaryotic organisms results less from their genomic layout. Rather, genetic and functional diversity of cells is due to a spatiotemporal regulation of gene expression. Transcription is one essential regulatory center which has to be controlled by various signaling pathways and cooperation of regulatory proteins, especially transcription factors and their co-factors.

The serum response factor (SRF) is a versatile transcription factor that influences essential cellular functions such as cell proliferation, differentiation and migration in a vast diversity of cell types and tissues by regulating numerous target genes (Posern & Treisman, 2006; Philippar *et al*, 2004; Miano *et al*, 2007; Selvaraj & Prywes, 2004; Sun *et al*, 2006a; Stritt *et al*, 2009). SRF is conserved from fly to human and encoded by a single gene. It was originally characterized as nuclear protein that binds the promotor region of the proto-oncogene *c-fos* in response to serum-stimulation (Greenberg & Ziff, 1984; Treisman *et al*, 1985; Prywes *et al*, 1986; Norman *et al*, 1988; Posern & Treisman, 2006). Richard Treisman described the SRF-binding site in *c-fos* as serum response element (SRE) which is a conserved DNA sequence of 23 bp (Treisman *et al*, 1986; Olson & Nordheim, 2010). The promotor region of SRF target genes harbors the SRE-specific consensus sequence CC(A/T)₂A(A/T)₃GG which is called CArG box (Boxer *et al*, 1989; Taylor *et al*, 1989). SRF binds the CArG box through its MADS box (MCM1, Agamous, Deficiens, SRF) which is a 56 amino acid DNA-binding motif conserved from plants to mammals. The C-terminal part of the MADS consensus facilitates homo- and hetero-dimerization of various MADS box transcription factors for potential multi-component complexes and differential regulation of target genes (Shore & Sharrocks, 1995; Pellegrini *et al*, 1995). Moreover, binding of SRF to DNA and its regulation of target gene transcription depends on diverse phosphorylation of various phosphorylation sites located at the amino terminus of SRF (Iyer *et al*, 2003).

Target gene expression through SRF in fibroblasts is mediated by two classes of signaling pathways and thus recruitment of distinct SRF co-factors. The mitogen-activated protein kinase (MAPK) cascade activates ternary complex factors

(TCF) like Elk-1, Net or Sap-1 which is a subfamily of Ets-domain transcription factors (Posern & Treisman, 2006; Dalton & Treisman, 1992). A complex of SRF and TCF contacts Ets-motifs next to the CA₂G box of immediate-early genes (IEG) thereby regulating IEG transcriptional activity (Treisman, 1994, 1995; Posern & Treisman, 2006). IEG like *c-fos*, *Arc* and *Egr1* mainly encode signaling molecules and transcription factors and are involved in cell cycle regulation, proliferation and cell differentiation (Philippar *et al*, 2004; Sun *et al*, 2006a; Dalton & Treisman, 1992; Dalton *et al*, 1993).

Members of the myocardin family, myocardin and myocardin-related transcription factors (MRTF), belong to the second class of SRF co-activators (Pipes *et al*, 2006; Wang *et al*, 2001, 2002). Their activity is regulated through activation of Rho-family GTPases like RhoA, Rac1 or CDC42 as well as altered actin dynamics (Gineitis & Treisman, 2001; Hill *et al*, 1995; Sotiropoulos *et al*, 1999). The association of SRF with class II co-factors controls cytoskeletal-specific genes like β -actin, vinculin or gelsolin and cardiac, smooth and skeletal muscle-specific genes as well as genes involved in cell proliferation and migration (Pipes *et al*, 2006; Eden *et al*, 2002; Boxer *et al*, 1989; Norman *et al*, 1988; Wang *et al*, 2001, 2003; Leitner *et al*, 2011).

Furthermore, knockout studies revealed an important role for both co-factor classes and signaling pathways on SRF-regulated neuronal response, migration and dendritic branching (Knöll *et al*, 2006; Stritt & Knöll, 2010; Kalita *et al*, 2012). The serum response factor therefore is an essential signaling node for regulating a vast diversity of cellular functions.

II.2 Myocardin-related Transcription Factors – MRTF-A/-B

Myocardin-related transcription factors (MRTF) belong to the myocardin family of transcriptional SRF co-activators. The family includes myocardin (MYOCD), which is expressed in cardiac and smooth muscle tissues, as well as widely expressed MRTF-A (MAL/BSAC/Mk11) and MRTF-B (Mk12/MAL16) (Cen *et al*, 2003; Miralles *et al*, 2003; Wang *et al*, 2001, 2002). All members belong to the SAP (SAF-A/B, Acinus, PIAS) family of proteins and share homology in a number of functional domains. SAP domains are 35 amino acid DNA-binding motifs and are often responsible for transcriptional activation, chromatin remodeling and chromosomal organization. But,

their role in MRTF is controversial (Wang *et al*, 2001; Aravind *et al*, 2000; Miralles *et al*, 2003). C-terminal to the centrally located SAP domain myocardin-family members possess a dimerization-mediating leucine zipper and a transcriptional transactivation domain (TAD). At the N-terminal part MRTF-A, -B and the cardiac isoform of myocardin contain three binding motifs for globular actin (G-actin) with a conserved RPxxxEL sequence, called RPEL motifs. Adjacent to the RPEL motifs there is a basic B-box and a glutamine-rich Q domain both responsible for SRF interaction (Posern & Treisman, 2006; Miralles *et al*, 2003).

Myocardin is located inside the nucleus and activates SRF following homo-dimerization. Due to the cardiovascular-restricted expression myocardin-SRF-mediated transcription exclusively affects cardiac and smooth muscle-specific promoters including SM22 α as well as smooth muscle myosin heavy and light chain (Miralles *et al*, 2003; Wang *et al*, 2003, 2001).

MRTF-A was initially described for acute megakaryoblastic leukemia in infants and children. In this disease a chromosomal translocation leads to the fusion of two genes: the gene encoding MAL (megakaryocytic leukemia) on chromosome 22 and the gene encoding the RNA-binding motif protein-15, RBM15 (also named OTT, one twenty two) on chromosome 1. The translocation t(1;22)(p13;q13) results in the expression of the fusion protein OTT-MAL. This fusion protein induces abnormal chromatin organization (Ma *et al*, 2001; Mercher *et al*, 2001; Posern & Treisman, 2006). Later, MAL was described as myocardin-related transcription factor A (MRTF-A). MRTF-A and its close relative MRTF-B are ubiquitously expressed in many cell types and required for SRF-mediated transcriptional activation (Wang *et al*, 2002). Whereas in primary neurons and some breast cancer cells MRTF-A is constitutively located in the nucleus, in fibroblasts MRTF-A shuttles between the cytoplasm and the nucleus.

The regulatory mechanism of this nuclear-cytoplasmic translocation was well studied in mouse NIH 3T3 and muscle cells and is restricted by G-actin binding (Kalita *et al*, 2006; Medjkane *et al*, 2009). Depending on the isoform, the N-terminus of MRTF-A harbors two or three RPEL motifs which are separated by linkers thereby having a binding capacity for three to five G-actin molecules, respectively. RPEL motifs adopt a helix-loop-helix conformation and contact a hydrophobic surface on actin monomers (Miralles *et al*, 2003; Posern *et al*, 2004; Mouilleron *et al*, 2008). Furthermore, subcellular localization of MRTF-A is determined through a bipartite

nuclear localization signal (NLS) inserted in the RPEL domain which is blocked during actin-MRTF binding. Thereby, cytoplasmic MRTF-A is hold in an inactive state (Kalita *et al*, 2012; Pawłowski *et al*, 2010). Lysophosphatidic acid (LPA) or serum activates Rho-mediated actin polymerization resulting in depletion of the cytoplasmic G-actin level and the dissociation of the inhibitory actin:MRTF complex (Fig. II-1). Released MRTF translocates into the nucleus to activate SRF-mediated target gene transcription (Posern *et al*, 2002, 2004; Miralles *et al*, 2003; Olson & Nordheim, 2010; Mouilleron *et al*, 2011).

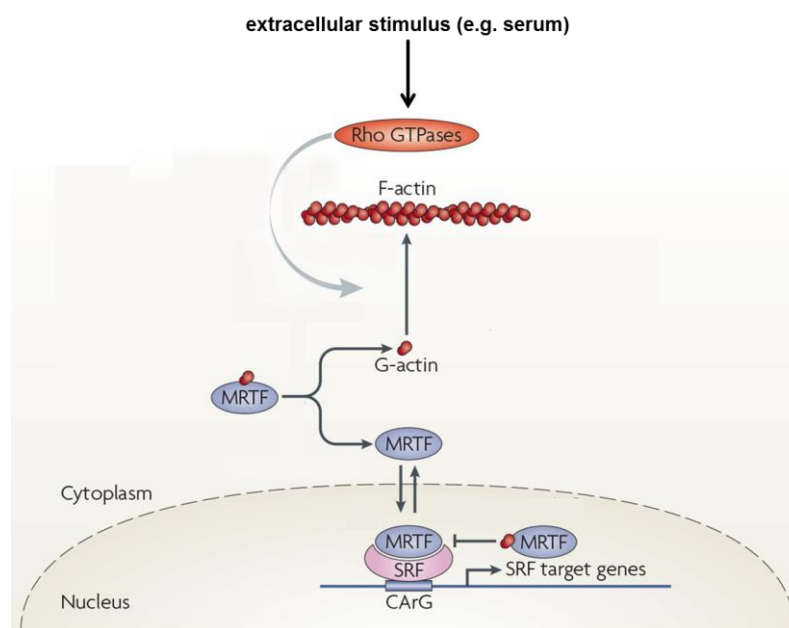


Figure II-1: Principal regulatory pathway for expression of SRF target genes through actin-MRTF interaction in NIH 3T3 mouse fibroblasts. Stimulation of the Rho-GTPases signaling pathway leads to altered actin dynamics and MRTF/SRF activation in NIH 3T3 cells. MRTF-SRF-mediated transcription is prevented by a repressive actin:MRTF complex. The inhibitory complex can be dissociated by competitive G-actin-binding proteins leading to the recovery of MRTF/SRF activity. Modified from (Olson & Nordheim, 2010).

Nuclear MRTF accumulation occurs upon exposing the bipartite NLS and binding to importin- α - β 1 heterodimers (Guettler *et al*, 2008; Pawłowski *et al*, 2010; Hayashi & Morita, 2012). Because β -actin transcription itself is regulated by MRTF/SRF the G-actin level will be restored to ensure re-formation of actin:MRTF complexes which induces nuclear export of MRTF and downregulation of the SRF response. Nuclear export signals (NES) are leucine-rich sequences in the MRTF-A Q-domain and are specific for exportin Crm1. From there, MRTF-A nuclear-cytoplasmic-shuttling is facilitated by complex formation with nuclear G-actin enhancing Crm1-dependent export and inhibiting transcriptional interaction with SRF (Vartiainen *et al*, 2007;

Guettler *et al*, 2008; Pawłowski *et al*, 2010). ERK-mediated MRTF-A phosphorylation on serine 454 following serum-stimulation promotes complex formation with actin and nuclear export thereby presenting an additional off-switch mechanism for MRTF-SRF activity (Muehlich *et al*, 2008).

According to the functional diversity of SRF, MRTF and MRTF-SRF-mediated gene transcription plays an essential regulatory role for many cellular processes including adhesion and migration especially tumor cell migration and metastasis (Morita *et al*, 2007; Miralles *et al*, 2003; Medjkane *et al*, 2009; Yoshio *et al*, 2010). Furthermore, MRTF-A knockout mice are unable to nurse their offspring due to defects in mammary myoepithelial cell differentiation and function (Li *et al*, 2006; Sun *et al*, 2006b). MRTF-B null mice suffer extended cardiac defects like endocardial fibrosis or altered organization of cardiomyocytes (Li *et al*, 2005; Oh *et al*, 2005). Mice with brain-specific deletions of MRTF-A,-B or SRF exhibit defects in neuronal migration and neurite outgrowth as well as morphological abnormalities in the cerebral cortex and hippocampus resulting in embryonic lethality (Mokalled *et al*, 2010; Knöll *et al*, 2006; Shiota *et al*, 2006).

II.3 Actin and Actin-Binding Proteins

The cytoskeleton component actin is essential for a wide range of biological processes including cell motility and cell morphology (Pollard & Cooper, 2009). Together with the motor protein myosin it was originally discovered in muscle tissues as responsible for muscle contraction (Straub, 1942). Actin polymers, together with microtubules and intermediate filaments, are central for cytoskeleton structures to maintain cell shape and to move cells (Heuser & Kirschner, 1980). Actin and myosin both have ATP-hydrolysis activity to generate force which is required for muscle contraction, cell migration or transport of intracellular materials, vesicles and DNA (Heuser & Kirschner, 1980; Richards & Cavalier-Smith, 2005; Geeves & Holmes, 2005).

Hence, actin is the most abundant constituent of eukaryotic cells with a highly conserved sequence across the species (Gunning *et al*, 2015). In mammals there are six actin genes encoding three functional isoforms. The α -isoform is muscle-specific whereas β - and γ -actin co-exist in most cell types for cytoskeleton-related functions (Gunning *et al*, 2015; Ponte *et al*, 1983; Machesky *et al*, 1994; Vandekerckhove &

Weber, 1978).

Actin is present in a globular (G-actin) and filamentous (F-actin) state, both in the cytoplasm and inside the nucleus (Olson & Nordheim, 2010; Vartiainen *et al*, 2007; Kokai *et al*, 2014). A dynamic equilibrium between both states and the interaction of actin with actin-binding proteins (ABP), RNA-polymerases and the transcriptional co-activator MRTF enables its functional diversity as cytoskeleton component and transcriptional regulator of gene expression (Olson & Nordheim, 2010; McDonald *et al*, 2006; Grummt, 2006; Miralles & Visa, 2006; Philimonenko *et al*, 2004).

Translocation into the nucleus occurs via importin-9 and in complex with the ABP cofilin. Nuclear export together with profilin is exportin-6-mediated (Dopie *et al*, 2012; Hendzel, 2014). Beside the interaction with MRTF transcription factors and all three RNA-polymerases, nuclear actin is linked to histone acetylation and chromatin-remodeling (Hofmann *et al*, 2004; Hu *et al*, 2004; Miralles & Visa, 2006; Olave *et al*, 2002; Shen *et al*, 2003; Bettinger *et al*, 2004).

Because actin dynamics regulate essential cellular functions the G-/F-actin treadmilling has to be controlled. Globular actin is structurally divided into four subdomains with a centrally located hydrophobic cleft which contains the nucleotide/ATP-binding motif (Graceffa & Dominguez, 2003; Kabsch *et al*, 1990; Oda *et al*, 2009). During filament assembly ATP is hydrolyzed to ADP (Straub & Feuer, 1989). Hence, each actin molecule is bound to ATP or ADP and Mg^{2+} resulting in the most common forms ATP-G-actin and ADP-F-actin (Graceffa & Dominguez, 2003; Reisler, 1993). Monomer addition occurs on both sides of an actin filament, called the pointed and the barbed end, but is faster at the barbed end.

Globular actin is mostly in complex with the sequestering proteins profilin or thymosin. Profilin-binding occurs on actin subdomain 1 and 3 thereby inhibiting polymerization at the pointed. Profilin favors ATP-actin and promotes nucleotide exchange from ADP to ATP (Posern *et al*, 2004; Schutt *et al*, 1993; Jockusch *et al*, 2006; Pollard & Cooper, 2009). Binding of thymosin- β 4, the predominant thymosin isoform in mammals, generally inhibits actin polymerization by occupying essential actin-actin contact sites on subdomain 1, 2 and 3 (Safer & Nachmias, 1994).

Polymerization of actin requires a minimal association of three actin monomers forming the nucleation core. Initially, these small oligomers are unstable and the polymerization process is slow. ATP-hydrolysis results in altered G-actin conformation and stable oligomer association, thereby accelerating polymerization (Mitchison &

Kirschner, 1984; Pollard & Cooper, 2009). Capping proteins such as gelsolin and cofilin regulate filament length by de-polymerization or termination of elongation at the pointed and the barbed end. Cofilin covers G- and F-actin and de-polymerizes ADP-F-actin at the pointed end (Jockusch *et al*, 2006; Winder & Ayscough, 2005; Lappalainen & Drubin, 1997). Gelsolin is a high-efficient actin severing protein acting at the barbed end of the filament (Sun *et al*, 1999; Burtnick *et al*, 2004). Polymerization is initiated by extracellular stimuli activating formins, actin-related proteins (ARP) or nucleation-promoting factors (NPF) (Fig. II-2, upper part). Numerous receptor classes, including integrin receptors, receptor tyrosine kinases, TGF- β receptors and E-cadherin receptors, catalyze Rho guanine exchange factor (GEF)-mediated activation of Rho-GTPases (Rho, Rac and Cdc42). Activated Rho signaling induces actin polymerization by either ROCK-LIM kinase-mediated cofilin inhibition or activation of formins, the ARP2/3 complex or nucleation-promoting factors such as N-WASP or WAVE2 (Olson & Nordheim, 2010).

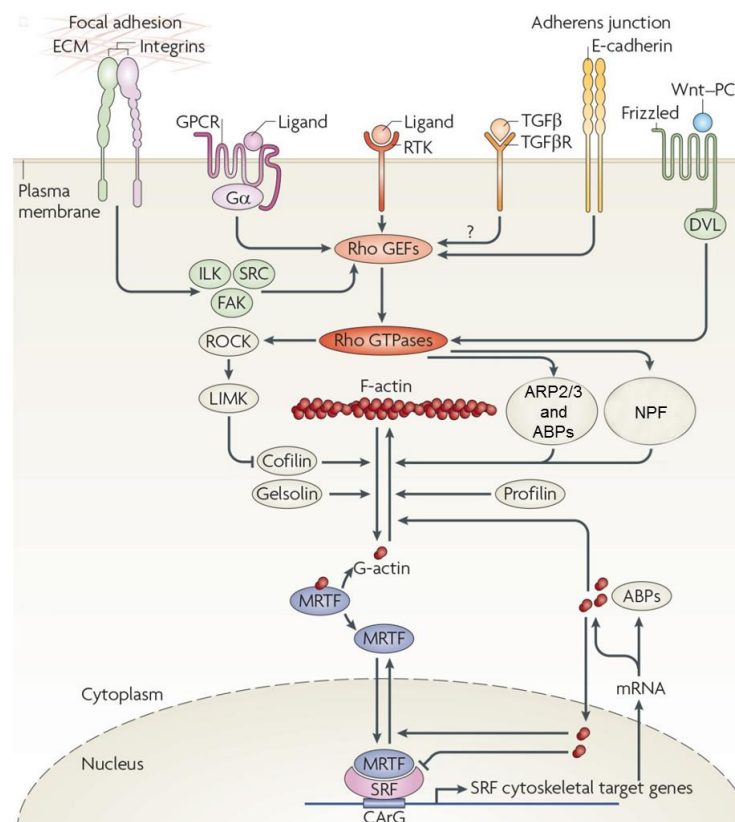


Figure II-2: Actin dynamics is controlled by numerous signaling pathways. Stimulation of Rho-GTPases mediated by GEFs, integrins, G protein-coupled receptors, protein tyrosine kinases and others, alters actin dynamics and MRTF-SRF activity. The SRF coactivator MRTF is restricted to the cytoplasm due to the repressive binding to G-actin. Cytoplasmic levels of G- and F-actin are controlled by numbers of actin-binding proteins such as members of the ARP2/3 complex, profilin or nucleation promoting factors (NPF). Modified from (Olson & Nordheim, 2010).

Branched actin networks are essential for the formation of protrusions like lamellipodia and filopodia during cell migration. Cross-linking of actin filaments with an existing mother filament is facilitated by the actin-related protein complex ARP2/3 (Pollard, 2007; Jockusch *et al*, 2006; Mullins *et al*, 1998). The ARP2/3 complex is a highly conserved component of the actin cytoskeleton in almost all eukaryotic cells. It consists of seven conserved proteins. The small subunits ARPC1-5 are responsible for positioning the complex at the daughter filament. The major subunits ARP2 and ARP3 represent a structure similar to actin monomers thereby serving as polymerization nucleation core (Goley & Welch, 2006; Veltman & Insall, 2010; Mullins *et al*, 1998; Rotty *et al*, 2013). ARP2/3 alone is not sufficient to induce nucleation. ARP2/3 activity requires co-activation by nucleation-promoting factors. NPF bind both G-actin and the ARP2/3 complex and contact a pre-existing mother filament through their F-actin-binding domain. Moreover, binding of NPF induces rearrangement of ARP2 and ARP3 into a nucleation-competent conformation (Ti *et al*, 2011; Padrick *et al*, 2011). Elongation of a new filament is promoted by NPF-mediated arrangement of further actin monomers along the growing filament. Starting from the core ARP2/3-mediated branching occurs in a 70 degree angle to the mother filament (Pollard & Cooper, 2009; Campellone & Welch, 2010; Rotty *et al*, 2013). Loss of ARP2/3 is lethal and ARP2/3 inhibition by small-molecule inhibitors like CK-666 results in asymmetric cell division or retrograde actin flow in neurons (Nolen *et al*, 2009; Sun *et al*, 2011).

II.4 Nucleation Promoting Factors – NPF

Nucleation-promoting factors (NPF) are efficient ARP2/3 co-activators for regulating dynamic actin remodeling in response to Rho-GTPase-mediated signaling. They are present in most eukaryotic organism and share conserved motifs to bind G- and F-actin as well as the ARP2/3 complex. According to this functional domains NPF are subdivided into three classes (Campellone & Welch, 2010).

Type I NPF include proteins like WASP (Wiskott-Aldrich syndrome protein) and its neuronal relative N-WASP, three isoforms of WAVE/SCAR (WASP family verprolin-homologous protein), WASH (WASP and SCAR homologue), WHAMM (WASP homologue associated with actin, membranes and microtubules) and JMY (junction-mediating and regulatory protein) (Rotty *et al*, 2013). They all possess a VCA

domain at their carboxyl terminus but differ in their amino terminus for different modes of regulatory functions (Stradal & Scita, 2006; Chereau *et al*, 2005; Dominguez, 2010). WH2 (V) (WASP homology 2/verprolin homology) domains are one of the most abundant G-actin-binding motifs (Symons *et al*, 1996). Beside class I NPF there are more than 60 actin-binding proteins known containing V domains like thymosin- β 4, verprolin and its mammalian homologue WIP (WASP-interacting protein), or CAP (adenylyl-cyclase-associated protein). WH2 (V) domains are 25 to 50 amino acids long, with a highly conserved LKKT motif and adopt an amphiphilic three-turn α -helical conformation. These helices bind to the hydrophobic cleft of an actin monomer (Paunola *et al*, 2002; Chereau *et al*, 2005). Recruitment and activation of the ARP2/3 complex is mediated by the central/connecting-acidic (CA) region (Chen *et al*, 2010; Kim *et al*, 2000; Renault *et al*, 2013). The CA region contacts multiple sites on the ARP2/3 complex inducing conformational changes into a nucleation-active form (Goley *et al*, 2004; Zencheck *et al*, 2009; Rodal *et al*, 2005).

Type II NPF are characterized by lacking the VCA domain. They interact with ARP2/3 through an N-terminal acidic motif thereby regulating F-actin stability at the branching points (Rotty *et al*, 2013). Mammalian cortactin and its hematopoietic relative HS1 (hematopoietic-specific protein 1) are representatives of this NPF class. They enhance interaction of N-WASP and ARP2/3 thereby playing a role on membrane dynamics and cell migration as well as vesicular trafficking (Kowalski *et al*, 2005; Ammer & Weed, 2008; Kirkbride *et al*, 2012).

Type III NPF like Spire and COBL (cordon-blue) are WH2 (V)-containing actin nucleators without ARP2/3 interaction. They mediate actin nucleation via a tandem cluster of WH2 (V) domains (Campellone & Welch, 2010). Spire was originally characterized as an actin nucleator during *Drosophila* development (Quinlan *et al*, 2005). The mammalian orthologues SPIRE1 and SPIRE2 harbor centrally located tandem repeats of four WH2 (V) domains in which the third and the fourth V domain exhibit the most efficient actin affinity to promote nucleation. In contrast, COBL contains three C-terminal WH2 (V) domains all required similarly for actin polymerization (Campellone & Welch, 2010). Spire-mediated F-actin is connected to microtubules, membrane transport and cytoskeletal interactions (Rosales-Nieves *et al*, 2006). COBL is essential in neuronal systems (Ahuja *et al*, 2007).

II.4.1 Neuronal Wiskott-Aldrich Syndrome Protein – N-WASP

Neuronal WASP (N-WASP) and its relative WASP both belong to the family of Wiskott-Aldrich syndrome proteins. The eponym WASP was initially described in context of the human Wiskott-Aldrich syndrome (WAS) (Aldrich *et al*, 1954; Derry *et al*, 1994). Mutations in the WAS gene are X-chromosomal recessive and result in a non-functional WAS protein which is an essential regulator of cytoskeletal reorganization and multiple signaling in the hematopoietic system (Stewart *et al*, 1996). Hence, WAS patients and also WASP deficient mice exhibit several defects in their immune system including thrombocytopenia, eczema, disordered blood coagulation and increased autoimmunity (Bosticardo *et al*, 2009; Fried *et al*, 2014).

In contrast to WASP, neuronal WASP is ubiquitously expressed in eukaryotic cells and responsible for ARP2/3-mediated regulation of actin dynamics at plasma membranes such as cell junction-related actin assembly, membrane ruffling and filopodia formation, formation of phagocytic structures, endocytosis and endosome movement (Campellone & Welch, 2010; Kovacs *et al*, 2011). The carboxyl terminus of N-WASP contains two G-actin-binding WH2 (V) domains and the ARP2/3 interacting CA region (Paunola *et al*, 2002). Adjacent to the VCA domain there is a proline-rich protein center acting as potent binding site for SH3-containing co-activators like Nck1,2 (non-catalytic kinase), TOCA1 (transducer of Cdc42-dependent actin assembly) and Abi1 (Abelson interactor) (Tomasevic *et al*, 2007; Ho *et al*, 2004; Innocenti *et al*, 2005). An N-terminal located WH1 domain and the basic motif CRIB (Cdc42 and Rac interactive binding) are responsible for N-WASP localization and function through interaction with filamentous actin, membrane lipids like phosphatidylinositol-4,5-phosphat (PI(4,5)P₂) or the co-activator WIP (Benesch *et al*, 2002; Stradal & Wehland, 2005). N-WASP-mediated actin remodeling has to be activated by Rho-GTPase signaling because unstimulated N-WASP adopts an auto-inhibited conformation. The GTPase-binding domain (GBD) within the CRIB is bound to the C-terminal VCA thereby inhibiting VCA-related ARP2/3 interaction and actin nucleation (Stradal & Wehland, 2005; Kim *et al*, 2000). Binding of WIP additionally stabilizes this auto-inhibitory conformation (Antón *et al*, 2007). Extracellular signals transduce activation and binding of Cdc42 to the GBD resulting in the dissociation of the inhibitory GBD-VCA bound and functional active N-WASP (Kim *et al*, 2000; Stradal & Wehland, 2005).

II.4.2 WASP Family Verprolin-homologous Protein 2 - WAVE2

WAVE2 is a member of the eukaryotic conserved WAVE family. It was initially found as a WASP-like molecule in a V domain-based sequence screen (Miki *et al*, 1998). The mammalian isoforms WAVE1 and WAVE3 are enriched in the nervous system whereas WAVE2 is ubiquitously expressed (Stradal & Wehland, 2005). As class I NPF also WAVE2 activates ARP2/3-dependent actin nucleation through the C-terminal VCA motif thereby regulating membrane-associated actin dynamics including membrane ruffling, lamellipodia formation and cell motility (Campellone & Welch, 2010). Binding to G-actin is mediated by a single WH2 (V) domain. Like N-WASP, WAVE2 harbors proline-rich sequences in the protein center responsible for SH3-protein interactions. WAVE2 activity is controlled by four associated proteins representing the WAVE regulatory complex (WRC). The WCR comprising WAVE, SRA1 (specifically Rac1-associated protein 1), NAP1 (NEF-associated protein 1), Abi2 (ABL interactor 2) and HSPC300 keeps WAVE in an inactive conformation (Eden *et al*, 2002; Bear *et al*, 1998; Rotty *et al*, 2013). Subunits of the WRC are bound to several WAVE2 motifs like the N-terminal located SCAR homology domain (SHD). SRA1 contacts the VCA thereby sequestering the V and the C domain (Chen *et al*, 2010). Activated Rac1 competes with SRA1 for VCA-binding leading to WRC disruption and functional WAVE2 (Innocenti *et al*, 2004; Steffen *et al*, 2004; Chen *et al*, 2010).

II.4.3 Junction-mediating and Regulatory Protein - JMY

The junction-mediating and regulatory protein JMY is a mammalian NPF expressed in many different cell types. It was initially described as an interactor of p300 and co-activator of p53-mediated gene transcription (Shikama *et al*, 1999). Although JMY is less characterized than other type I NPF, it is known to be involved in lamellipodia-related cell migration, regulation of cadherin expression and p53-mediated response to DNA damage (Cou tts *et al*, 2009; Zuchero *et al*, 2012; Zuchero & Cou tts, 2009). JMY is structurally related to WHAMM harboring an N-terminal coiled-coil domain followed by proline-rich motifs and the VCA region at the carboxyl terminus. In contrast to N-WASP or WAVE2, JMY is able to nucleate actin independently of an ARP2/3 interaction because it contains a tandem repeat of three (WH2) V domains. Tandem WH2 domains and the incorporated linkers enable JMY to bind a number of

actin monomers as responsible for a nucleation core. ARP2/3-independent nucleation by JMY results in unbranched actin filaments (Zuchero & Coutts, 2009). Interestingly, JMY seems to be regulated by actin in a way similar to MRTF-A. The JMY VCA domain harbors an atypical nuclear localization signal, which is blocked during actin-binding. Extracellular stimuli, in particular DNA damage signaling, alters actin dynamics thereby releasing JMY and uncovering the NLS resulting in nuclear accumulated and transcriptional active JMY (Zuchero *et al*, 2012).

II.5 Structure of MRTF:Actin Complexes and Aim of the Study

As already mentioned, a vast diversity of regulatory proteins and signaling pathways modulate actin dynamics which in turn control essential cellular processes including gene expression. Therefore, actin is the most important signaling node linking cytoskeleton dynamics to spatiotemporal regulation of transcription.

This study focus on the actin-mediated control of the transcription factors MRTF-A and SRF. As depicted in Figure II-1 and II-2, Rho-activated actin polymerization resulting in depletion of the cytoplasmic G-actin pool and dissociation of the inhibitory G-actin:MRTF-A complex is the current model for MRTF-SRF activation in mouse fibroblasts (Miralles *et al*, 2003; Sotiropoulos *et al*, 1999). However, it could be shown that actin-severing thymosin- β 4 as well as other barbed-end binders induce MRTF-SRF transcriptional activity without decreasing the pool of globular actin (Hinkel *et al*, 2014; Posern *et al*, 2004; Morita & Hayashi, 2013). Therefore, the critical regulatory step for actin:MRTF dissociation cannot be explained by a simple G-/F-actin ratio and the detailed molecular mechanism still has to be clarified. Structural data indicated an involvement of the WH2 (V) domain-containing nucleation-promoting factors. A computer-based alignment of X-ray structures revealed that the α -helix of a NPF WH2 domain and the α -helix of the MRTF-A RPEL motifs bind the same hydrophobic surface on an actin molecule (Fig. II-3) (Mouilleron *et al*, 2008). As simultaneous binding of WH2 domains and RPEL motifs is not possible, this study suggest a mutually exclusive binding of WH2 (V) domain-containing NPF and MRTF-A to actin.

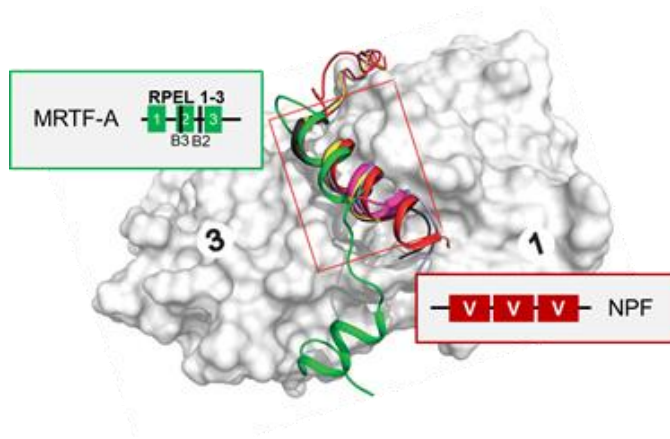


Figure II-3: Structure of a G-actin molecule and the formed complex with MRTF-A RPEL motifs or WH2 (V) domains. The helix $\alpha 1$ of each MRTF-A RPEL motif interacts with the hydrophobic cleft between subdomain 1 and 3 of an actin monomer. According to computer-based structural alignment, nucleation promoting factors (NPF) are able to bind to the same actin surface via the α -helix of their WH2 (V) domains. Modified from (Mouilleron *et al*, 2008).

To investigate whether a competitive mechanism is involved in activation of MRTF-A the WH2-containing NPF N-WASP, WAVE2 and JMY were analyzed using the well-characterized fibroblast cell line NIH 3T3 as a model system. *In vitro* complementation assays were performed for biochemical analysis of complex disruption. Moreover, functional analysis included luciferase-based SRF reporter activity, mRNA expression of known MRTF-SRF target genes by quantitative real-time PCR as well as nuclear accumulation of MRTF-A and quantitative assessment of cellular and nuclear F-actin by immunofluorescence studies and cell fractionation.

III Materials and Methods

III.1 Materials

III.1.1 Equipment

Agarose gel electrophoresis	Horizontal Elpho	Workshop of MPI of Biochemistry (Martinsried)
Balances	Kern ABS Kern 572	Kern & Sohn GmbH Kern & Sohn GmbH
Cell culture equipment	CASY cell counter HERAcell 150 HERAsafe Water bath	OMNI Life Science Thermo Scientific Thermo Scientific GFL
Centrifuges	Allegra 6KR Centrifuge Centrifuge 5417C Centrifuge 5417R Sprout Mini-Centrifuge Optima TL Ultracentrifuge	Beckman Coulter Beckman Coulter Eppendorf Biozym Beckman Coulter
Gel documentation	Gel Stick	Intas Science Imaging
Incubation	Duomax 1030 Mixing Block MB-102 Incubator RM 5 Rotamax 120 Thermomixer comfort WB 120 K	Heidolph BIOER Memmert CAT Heidolph Eppendorf mytron
Microplate readers	Clariostar Glomax Labsystem Multiskan RC	BMG Labtech Promega Thermo Scientific
Microscopes	Axio Imager.M1 Evos Core AMG SP5	Zeiss Jena Life Technologies Leica

Mixing	Lab dancer Magnetic Stirrer R 1000 MR Hei-Standard Vortex Genius 3	IKA Carl Roth GmbH Heidolph IKA
PAGE equipment	Mini-PROTEAN Tetra System	BIO-RAD
PCR equipment	LigthCycler 480 II real-time PCR system T 3000 Thermocycler	Roche Biometra
pH meter	LE409	Mettler Toledo
Power supplies	Consort EV261 peqPOWER	Peqlab Peqlab
Sonicator	UP200S	Hielscher Ultrasonics
Spectrophotometer	Nanodrop 2000c	Thermo Scientific
Western blotting	ODYSSEY CLx	LI-CORE

III.1.2 Chemicals and Reagents

General Laboratory Chemicals

Acrylamide/Bis solution.....	Carl Roth GmbH
Agar-Agar, bacteriological grade.....	Carl Roth GmbH
Agarose Standard.....	Carl Roth GmbH
Albumin fraction from bovine serum (BSA).....	Carl Roth GmbH
Ammonium persulfate (APS).....	Sigma-Aldrich
Boric acid (BH ₃ O ₃).....	Sigma-Aldrich
Bromophenol blue.....	Carl Roth GmbH
Coomassie Brilliant Blue R-250.....	Carl Roth GmbH
Dimethyl sulfoxide (DMSO).....	Sigma-Aldrich
Ethylene-diamine-tetra-acetic acid (EDTA).....	Carl Roth GmbH
Ethidium bromide, 1% solution.....	Promega
Ethyl alcohol, absolute.....	Sigma-Aldrich
Glycerol, 87%.....	Carl Roth GmbH
Glycine.....	Carl Roth GmbH
4-(2-hydroxyethyl)-1-piperazineethansulfonic acid (HEPES).....	Sigma-Aldrich
Hydrochloric acid (HCl), 37%.....	Sigma-Aldrich
Methyl alcohol, absolute.....	Sigma-Aldrich

Monopotassium phosphate (KH ₂ PO ₄)	Sigma-Aldrich
Non-fat milk powder	Carl Roth GmbH
Orange G	Carl Roth GmbH
Paraformaldehyde	Sigma-Aldrich
Potassium chloride (KCl)	Sigma-Aldrich
Prolong Gold Antifade	Life Technologies
Sodium acetate (NA)	Sigma-Aldrich
Sodium chloride (NaCl)	Carl Roth GmbH
Sodium hydroxide (NaOH)	Sigma-Aldrich
Sodium phosphate dibasic (Na ₂ HPO ₄)	Sigma-Aldrich
Tris-(2-carboxyethyl)-phosphine hydrochloride solution (TECEP)	Sigma-Aldrich
N,N,N,N-Tetra-methyl-ethylene-diamine (TEMED)	SERVA
2-amino-2-(hydroxymethyl) propane-1,3-diol (Tris)	Carl Roth GmbH
Tryptone	Carl Roth GmbH
Yeast Extract	Carl Roth GmbH
2-Mercaptoethanol	Sigma-Aldrich
2-Popanol	Sigma-Aldrich

Antibiotics

Ampicillin	Carl Roth GmbH
Geneticin (G418)	Calbiochem
Kanamycin	Sigma-Aldrich

Cell Culture Reagents

Antibiotic-Antimycotic (Penicillin/Streptomycin)	Life Technologies
Cholera toxin	Sigma-Aldrich
Dulbecco's modified Eagle medium (Gibco DMEM), high glucose	Invitrogen
Dulbecco's modified Eagle medium/F12 (Gibco DMEM/F12)	Invitrogen
Epithelial growth factor (EGF)	Peprotech
Fetal calf serum (FCS)	Life Technologies
Horse serum	Sigma-Aldrich
Hydrocortisone	Sigma-Aldrich
Insulin	Sigma-Aldrich
L-glutamine	Life Technologies
Opti-MEM reduced serum medium (Gibco)	Life Technologies
Trypsin	Life Technologies

Composite Reagents and Kits

ANTI-FLAG M2 magnetic beads	Sigma-Aldrich
Complete protease inhibitor cocktail	Carl Roth GmbH
Dual-Glo Luciferase Assay Kit	Promega
Fast SYBR Green Master Mix	Promega
Immobilon-FL PVDF membrane	Merck Millipore
μMACS HA Isolation Kit	Miltenyi Biotec
μMACS c-myc Isolation Kit	Miltenyi Biotec
MACS Inside Stain Kit	Miltenyi Biotec
Micro BCA Protein Assay Kit	Thermo Scientific

QIAGEN Plasmid Maxi Kit.....	Qiagen
QIAGEN Plasmid Mini Kit.....	Qiagen
QIAGEN RNeasy Mini Kit.....	Qiagen
QIAquick MinElute Gel Extraction Kit.....	Qiagen
QIAquick MinElute PCR Purification Kit.....	Qiagen
Verso cDNA Kit.....	Thermo Scientific

Detergents

Sodium dodecyl sulfate (SDS), 20%.....	Carl Roth GmbH
Triton X-100.....	Carl Roth GmbH
Tween 20.....	Carl Roth GmbH

Enzymes and Reagents used in Molecular Cloning

Adenosine triphosphate.....	Sigma-Aldrich
CutSmart Buffer.....	New England Biolabs
Deoxy nucleotides, Solution Mix.....	New England Biolabs
DNase I.....	Molecular Probes
λ -Phosphatase.....	New England Biolabs
Nicotinamide adenine dinucleotide (NAD ⁺).....	Sigma-Aldrich
Phusion High-Fidelity DNA Polymerase.....	New England Biolabs
Q5 High-Fidelity DNA Polymerase.....	New England Biolabs
Q5 High-Fidelity Reaction Buffer (10x).....	New England Biolabs
Q5 High GC Enhancer (10x).....	New England Biolabs
Restriction Endonucleases.....	New England Biolabs
Shrimp Alkaline Phosphatase.....	Fermentas
T4 DNA Ligase.....	New England Biolabs
T4 DNA Ligase buffer.....	New England Biolabs
T4 Polynucleotide Kinase.....	New England Biolabs
Taq DNA Polymerase.....	New England Biolabs
Thermo Pol Reaction Buffer (10x).....	New England Biolabs

Inhibitors and Inducer

CK-548.....	Sigma-Aldrich
CK-666.....	Sigma-Aldrich
Cytochalasin D.....	Calbiochem
Latrunculin B.....	Calbiochem
Wiskostatin.....	Sigma-Aldrich

Standards

GeneRuler 100 bp DNA ladder.....	Thermo Scientific
GeneRuler 100 bp Plus DNA ladder.....	Thermo Scientific
GeneRuler 1 kb DNA ladder.....	Thermo Scientific
Precision Plus Protein Standards.....	BIO-RAD

Transfection Reagents

Lipofectamine Reagent.....	Invitrogen
Lipofectamine 2000 Reagent.....	Invitrogen
Lipofectamine RNAiMAX Reagent.....	Invitrogen
X-tremeGENE 9 DNA Transfection Reagent.....	Roche

III.1.3 Common Buffers and Solutions

PBS pH 7.4		TBE Buffer (1x) pH 8.0		TBS Buffer (1x) pH 7.5	
2.7 mM	KCl	90 mM	Tris-HCl	20 mM	Tris-HCl
137 mM	NaCl	90 mM	BH ₃ O ₃	150 mM	NaCl
10 mM	Na ₂ HPO ₄	3 mM	EDTA		
1.8 mM	KH ₂ PO ₄				

TBS-T Buffer (1x) pH 7.5		TE Buffer (1x) pH 8.0		Blocking Solution (IF)	
20 mM	Tris-HCl	10 mM	Tris-HCl	10% (v/v)	FCS
150 mM	NaCl	1 mM	EDTA	1% (w/v)	BSA
0.1% (v/v)	Tween 20			0.05% (v/v)	Triton X-100 in PBS

Blocking Solution (PAGE)		Loading Buffer (DNA) pH 8.0		Loading Buffer (PAGE) pH 6.8	
5% (w/v)	non-fat milk in TBS-T	85% (v/v)	Glycerol	40% (v/v)	Glycerol
		0.5 M	EDTA	12% (v/v)	SDS
		1x	TE-Buffer	1 M	Tris-HCl
			Bromophenol blue	10% (v/v)	Mercaptoethanol Bromophenol blue

Lysis Buffer (G-/F-actin fractionation) pH 7.7		Lysis Buffer (anti-Flag magnetic beads) pH 7.4		RIPA Buffer pH 7.4	
20 mM	HEPES	50 mM	Tris-HCl	50 mM	Tris-HCl
50 mM	NaCl	150 mM	NaCl	150 mM	NaCl
1 mM	EDTA	1 mM	EDTA	2 mM	EDTA
0.5% (v/v)	Triton X-100	1% (v/v)	Triton X-100	1% (v/v)	Triton X-100
				0.1% (v/v)	SDS

Running Buffer (PAGE)	Running Gel (PAGE) pH 8.8	Stacking Gel (PAGE) pH 6.8
25 mM Tris base 192 mM Glycine 0.1% (v/v) SDS	8-14% Acrylamide/Bis 375 mM Tris-HCl 0.1% (v/v) SDS 0.1% (v/v) APS 0.1% (v/v) TEMED	5% Acrylamide/Bis 127 mM Tris-HCl 4.5% (v/v) Glycerol 0.1% (v/v) SDS 0.1% (v/v) APS 0.1% (v/v) TEMED
Inside Staining Buffer pH 7.2	Transfer Buffer (PAGE)	
0.5% (w/v) BSA 2 mM EDTA in PBS	25 mM Tris base 192 mM Glycine 20% (v/v) Methanol 0.05% (v/v) SDS	

III.1.4 Antibodies and Staining Reagents

Primary Reagents

Reagent	Description	Source	used in
anti-ARP3	Rabbit polyclonal	Proteintech Cat. 13822-1-AP	IF 1:100 WB 1:1000
anti- α -tubulin	Mouse monoclonal IgG ₁ , clone DM1A	Sigma-Aldrich Cat. T9026	WB 1:2000
anti- β -actin	Mouse monoclonal, IgG ₁ , clone AC-15	Sigma-Aldrich Cat. A5441	WB 1:2000
anti-FLAG	Rabbit polyclonal	Sigma-Aldrich Cat. F7425	WB 1:2000
anti-FLAG M2	Mouse monoclonal, clone M2	Sigma-Aldrich Cat. F3165	IF 1:100
anti-GFP	Rabbit polyclonal	Sigma-Aldrich Cat. G1544	IF 1:200 WB 1:1000

anti-HA.11	Mouse monoclonal IgG ₁ , clone 16B12	Convance Cat. MMS-101R	IF 1:100
anti-JMY	Mouse monoclonal, clone G-11	Santa Cruz Cat. sc-166030	IF 1:100 WB 1:1000
anti-MRTF-A	Goat polyclonal, clone C-19	Santa Cruz Cat. sc-21558	IF 1:100 WB 1:100
anti-MRTF-A/B	Rabbit polyclonal serum	Homemade (Sina Pleiner)	IF 1:1000 WB 1:1000
anti-C-MYC	Mouse monoclonal	Invitrogen Cat. 13-2500	IF 1:500 WB 1:1000
anti-MYC-tag	Rabbit monoclonal	Cell signaling Cat. 2278S	IF 1:100 WB 1:1000
anti-N-WASP	Rabbit polyclonal, clone H100	Santa Cruz Cat. sc-20770	IF 1:100 WB 1:1000
anti-p44/p42	Rabbit polyclonal	Cell signaling Cat. 9101	WB: 1:1000
anti-WAVE2	Rabbit polyclonal, clone H110	Santa Cruz Cat. sc-33548	IF 1:100 WB 1:1000
DAPI	4',6-Diamidino-2- Phenylindole, Di-hydro-chloride	Sigma-Aldrich Cat. D9542	IF 1:50000
DNase I-Alexa 488	Marker for G-actin	Molecular Probes Cat. 12371	FACS 1:500
Phalloidin-Alexa 546	Marker for F-actin	Invitrogen Cat. A22283	IF 1:200
Phalloidin-Alexa 647	Marker for F-actin	Invitrogen Cat. A22287	IF 1:200
Phalloidin-Atto-488	Marker for F-actin	Sigma-Aldrich Cat. 49409	IF 1:200

Secondary Reagents

Reagent	Source	used in
Alexa 350-goat anti-rabbit IgG	Molecular Probes Cat. A11046	IF 1:200
Alexa 488-goat anti-mouse IgG	Molecular Probes Cat. A11001	IF 1:200
Alexa 488-donkey anti-rabbit IgG	Invitrogen Cat. A21206	IF 1:200
Alexa 488-donkey anti-goat IgG	dianova Cat. 705-546-147	IF 1:200
Alexa 546-goat anti-mouse IgG	Molecular Probes Cat. A11030	IF 1:200
Alexa 546-goat anti-rabbit IgG	Invitrogen Cat. 11010	IF 1:200
Alexa 546-donkey anti-rabbit IgG	Invitrogen Cat. A10040	IF 1:200
Alexa Flour 680-donkey anti-goat IgG	dianova Cat. 705-625-147	WB 1:15000
IRDye680RD-goat anti-mouse IgG	LI-COR Cat. 926-68070	WB 1:15000
IRDye680RD-goat anti-rabbit IgG	LI-COR Cat. 926-68071	WB 1:15000
IRDye800CW-goat anti-mouse IgG	LI-COR Cat. 926-32210	WB 1:15000
IRDye800CW-goat anti-rabbit IgG	LI-COR Cat. 926-32211	WB 1:15000

III.1.5 Oligonucleotides

Cloning Primers

Amplicon	Name	Sequence
JMY	EcoRI-JMY-forward	<u>GAATTCTCGTTCGCGCTGGAGGAGACA</u>
	XbaI-JMY-reverse	<u>TCTAGACTAGTTCTCCCAGTCTGTGCACGG</u>
JMY-ΔC	JMY-ΔC	TTGAGAGAATCCTTCACACTTGGTCAGAG GATGAGGAAG
JMY-ΔA	EcoRI-JMY-forward	<u>GAATTCTCGTTCGCGCTGGAGGAGACA</u>
	XbaI-JMY-ΔA-reverse	<u>TCTAGATTATGACTCTGGGGAC</u> GCTTCTTTGATTCTT
JMY-ΔCA	EcoRI-JMY-forward	<u>GAATTCTCGTTCGCGCTGGAGGAGACA</u>
	XbaI-JMY-ΔCA-reverse	<u>TCTAGATTAAAGTGTGAAGGATTCTCTCAA</u>
JMY-ΔVCA	EcoRI-JMY-forward	<u>GAATTCTCGTTCGCGCTGGAGGAGACA</u>
	XbaI-JMY-ΔVCA-reverse	<u>TCTAGACTACTGTTCAACCTTTTTTCAGAT</u>
JMY-R961E	JMY-R961E	AGTATCCACGAAGCTCTAAGAGAAATCAAG AAGCGTCCCCAGAG
JMY-Δ960-963	JMY-Δ960-963	CGGAGTATCCACGAAGCTCTAGAAGCGTC CCCAGAGTCAGAG
N-WASP	EcoRI-N-WASP-forward	<u>GAA TTCAGCTCGGGCCAGCAGCCCCCG</u>
	XbaI-N-WASP-reverse	<u>TCTAGATCAGTCTTCCCACATCATCATC</u>
N-WASP-ΔC	N-WASP-ΔC	TCCACACCACCAACCCCGCAGATGAAGA TGAAGACGATGA

N-WASP- Δ A	EcoRI-N-WASP-forward	<u>GAATTCAGCTCGGGCCAGCAGCCCCCG</u>
	XbaI-N-WASP- Δ A-reverse	<u>TCTAGATTAATCTTCATCTGAGGAAT</u>
N-WASP- Δ CA	EcoRI-N-WASP-forward	<u>GAATTCAGCTCGGGCCAGCAGCCCCCG</u>
	XbaI-N-WASP- Δ CA-reverse	<u>TCTAGATTATGCGGGTGTGGTGGTGTGGA</u>
N-WASP-R474E	N-WASP-R474E	GAAGTGATGCAGAAAGAGAGCAAAGCCA TTCATTCTCA
N-WASP- Δ 473-476	N-WASP- Δ 473-476	GCGCTGATGGAAGTGATGCAGGCCATTCAT TCCTCAGATGAA
WAVE2	NcoI-WAVE2-forward	<u>CCATGGCGCCGTTAGTAACCAGGAAC</u> ATC
	XbaI-WAVE2-reverse	<u>TCTAGATTA</u> ATCCGACCAGTCGTCTTCATC
WAVE2- Δ C	WAVE2- Δ C	GAGCAAGAGAAGCGTGATGTGGACTCGGA AGATGATTCTTCT
WAVE2- Δ A	NcoI-WAVE2-forward	<u>CCATGGCGCCGTTAGTAACCAGGAAC</u> ATC
	XbaI-WAVE2- Δ A-reverse	<u>TCTAGATTAT</u> CCGAGTCGCTGTAC
WAVE2- Δ CA	NcoI-WAVE2-forward	<u>CCATGGCGCCGTTAGTAACCAGGAAC</u> ATC
	XbaI-WAVE2- Δ CA-reverse	<u>TCTAGATTACACATCACGCTTCTCTTGCTC</u>
WAVE2-R474E	WAVE2-R474E	GATGTGGCCACCATCCTGTCCGAGCGGATC GCTGTTGAGTACAGC
WAVE2- Δ 473-476	WAVE2- Δ 473-476	AATGATGTGGCCACCATCCTGGCTGTTGA GTACAGCGACTCG

Detection Primers

Amplicon	Name	Sequence	Source
Acta2	ADM1 SMA2 forward	GGGAGTAATGGTTGGAATGG	A. Descot
	ADM1 SMA2 reverse	CAGTGTCGGATGCTCTTCAG	
ALAS	ADM1 ALAS forward	CTCCTCGAACCTGTCCAC	A. Descot
	ADM1 ALAS reverse	GCCATCTGGGACTCGTCAG	
HPRT	ADM1 HPRT1 forward	TCAGTCAACGGGGGACATAAA	A. Descot
	ADM1 HPRT1 reverse	GGGGCTGTACTGCTTAACCAG	
Integrin α 5	ADM1 Itg α 5 F2836	GGTGACAGGACTCAGCAACTG	A. Descot
	ADM1 Itg α 5 R3053	GCAGACTACGGCTCTCTTGG	
Plakophilin	ADM1 Pkp2 F2293	CTGTCCTCCTTTACTCTCTGTGG	A. Descot
	ADM1 Pkp2 R2402	GTGGTAGGCTTTGGCAGTCC	
SRF	ADM1 SRF forward	GGCCGCGTGAAGATCAAGAT	A. Descot
	ADM1 SRF reverse	CACATGGCCTGTCTCACTGG	
Vinculin	ADM2 Vcl forward	GGCCGGACCAACATCAGTG	A. Descot
	ADM2 Vcl reverse	ATGTACCAGCCAGATTTGACG	

Small Interfering RNA

Name	Sequence	Source
ARP3	ON-TARGETplus Actr3 GAGUCAACGCCAUCUCAAA; GCUGACGGGUACAGUAAUA; AAGCAGUGAAGGAACGCUA; GAAGAGAGCUAAGACGAUU	GE Healthcare
silencer negative control (ARP3)	ON-Non-targeting Pool UGGUUUACAUGUCGACUAA; UGGUUUACAUGUUGUGUGA; UGGUUUACAUGUUUUCUGA; UGGUUUACAUGUUUCCUA	GE Healthcare
N-WASP	AJ318416_stealth_1373 GACCAGAUACGACAG GGCAUUCAAU	Thermo Scientific
silencer negative control (N-WASP)	AJ318416_stealth_control_1373 GACAUAGCAGCGGGA UUACCACAAU	Thermo Scientific
WAVE2	AY135643_stealth_927 CAGAAUUCAGCUACCC UGCAGACAA	Thermo Scientific
silencer negative control (WAVE2)	AY135643_stealth_control_927 CAGACUUAUCGUCCCGA CGAAACAA	Thermo Scientific

III.1.6 Plasmids

Pre-Existing

Plasmid Name	Description	Source
p ^{CMV} LifeAct-TagGFP2	LifeAct is a 17 amino acid fragment of <i>Saccharomyces cerevisiae</i> actin-binding domain, marker for F-actin fused to TagGFP2 (Riedl et al. 2008)	R. Wedlich-Soldner

p ^{CMV} LifeAct-TagRFP	similar to p ^{CMV} LifeAct-TagGFP2 labeled with TagRFP (Riedl et al. 2008)	ibidi
p3D.A-Luc	firefly luciferase expression is controlled by triple cfos-derived SRF binding sites, in front of a TATA-box of cytoskeletal actin in pGL3 (Geneste <i>et al</i> , 2002; Sotiropoulos <i>et al</i> , 1999)	G. Posern
pEF-MAL-f.l.-HA	murine MRTF-A with C-terminal HA-tag, ATG codon introduced before Leu -92	D. Shaposhnikov
pEF plink	also called pEF-Tplink, pEFplink-TAG and pEF-E910, from Richard Marais EFplink from MLV plink (Dalton & Treisman, 1992; Mizushima & Nagata, 1990)	G. Posern
pEF-Flag plink	from Richard Marais EFplink from MLV plink (Dalton & Treisman, 1992; Mizushima & Nagata, 1990)	G. Posern
pEF-Flag-actin-WT	human β -actin inserted into pEF-Flag plink (Sotiropoulos <i>et al</i> , 1999)	G. Posern
pEF-Flag-actin-R62D	human β -actin R62D inserted into pEF-Flag plink (Posern <i>et al</i> , 2002)	G. Posern
pEF-Flag-NLS-actin-WT	pEF-Flag-actin-WT (Sotiropoulos <i>et al</i> , 1999) with NLS	G. Posern
pEF-Flag-NLS-actin-S14C	human β -actin S14C in pEF-Flag plink (Posern <i>et al</i> , 2004) with NLS	G. Posern
pEF-Flag-NLS-actin-G15S	human β -actin G15S in pEF-Flag plink (Posern <i>et al</i> , 2004) with NLS	G. Posern
pEF-Flag-NLS-actin-R62D	human β -actin R62D in pEF-Flag plink (Posern <i>et al</i> , 2002) with NLS	G. Posern

pEF-Flag-NLS-actin-V159S	human β -actin V159S in pEF-Flag plink (Posern <i>et al</i> , 2004) with NLS	G. Posern
pEF-myc plink	myc-tag (myc (9E10) epitope) N-terminal of the multiple cloning site into pEF plink (Dalton & Treisman, 1992; Mizushima & Nagata, 1990)	G. Posern
pEGFP-C1-N-WASP	murine N-WASP-f.l. in pEGFP-C1 with BsrG1 and EcoRI (Lommel <i>et al</i> , 2001)	T. Stradal
pEGFP-C1-WAVE2	murine WAVE2-f.l. in pEGFP-C1 with HindIII and Sal1 (Benesch <i>et al</i> , 2002)	T. Stradal
pEGFP-C2	EGFP inserted	Clontech
pEGFP-C1-JMY	murine JMY-f.l. in pEGFP-C (Schlüter <i>et al</i> , 2014)	T. Stradal
pET41a 3CA MRTF-A (2-261)	bacterial expression vector for GST-tagged MRTF-A (2-261) (Posern <i>et al</i> , 2004)	G. Posern
ptkRL	<i>Renilla</i> luciferase expression as internal control, thymidine kinase promoter from herpes simplex virus	Promega

Created

Plasmid Name	Description
pEF-myc-N-WASP	N-WASP (aa 1-501) was amplified using EcoRI-N-WASP-forward/XbaI-N-WASP-reverse on pEGFP-C1-N-WASP and was subcloned into pEF-myc plink
pEF-myc-N-WASP- Δ C	N-WASP- Δ C (Δ aa 459-481) was generated by performing Single Oligonucleotide Mutagenesis and Cloning Approach (SOMA) (Pfirschmann <i>et al</i> , 2013) using N-WASP- Δ C on pEGFP-C1-N-WASP and was

	subcloned into pEF-myc plink
pEF-myc-N-WASP- Δ A	N-WASP- Δ A (aa 1-484) was amplified by inserting a premature STOP codon using EcoRI-N-WASP-forward/XbaI-N-WASP- Δ A-reverse on pEGFP-C1-N-WASP and was subcloned into pEF-myc plink
pEF-myc-N-WASP- Δ CA	N-WASP- Δ CA (aa 1-458) was amplified by inserting a premature STOP codon using EcoRI-N-WASP-forward/XbaI-N-WASP- Δ CA-reverse on pEGFP-C1-N-WASP and was subcloned into pEF-myc plink
pEF-myc-N-WASP-R474E	N-WASP-R474E (aa 1-501) was generated by performing SOMA (Pfirrman <i>et al</i> , 2013) using N-WASP-R474E on pEGFP-C1-N-WASP and was subcloned into pEF-myc plink
pEF-myc-N-WASP- Δ 473-476	N-WASP- Δ 473-476 (Δ aa 473-476) was generated by performing SOMA (Pfirrman <i>et al</i> , 2013) using N-WASP- Δ 473-476 on pEGFP-C1-N-WASP and was subcloned into pEF-myc plink
pEF-myc-WAVE2	WAVE2 (aa 1-497) was amplified using NcoI WAVE2-forward/XbaI-WAVE2-reverse on pEGFP-C1-WAVE2 and was subcloned into pEF-myc plink
pEF-myc-WAVE2- Δ C	WAVE2- Δ C (Δ aa 465-481) was generated by performing SOMA (Pfirrman <i>et al</i> , 2013) using WAVE2- Δ C on pEGFP-C1-WAVE2 and was subcloned into pEF-myc plink
pEF-myc-WAVE2- Δ A	WAVE2- Δ A (aa 1-484) was amplified by inserting a premature STOP codon using NcoI-WAVE2-forward/XbaI-WAVE2- Δ A-reverse on pEGFP-C1-WAVE2 and was subcloned into pEF-myc plink
pEF-myc-WAVE2- Δ CA	WAVE2- Δ CA (aa 1-463) was amplified by inserting a premature STOP codon using NcoI-WAVE2-forward/XbaI-WAVE2- Δ CA-reverse on pEGFP-C1-WAVE2 and was subcloned into pEF-myc plink

pEF-myc-WAVE2-R474E	WAVE2-R474E (aa 1-497) was generated by performing SOMA (Pfirschmann <i>et al</i> , 2013) using WAVE2-R474E on pEGFP-C1-WAVE2 and was subcloned into pEF-myc plink
pEF-myc-WAVE2- Δ 473-776	WAVE2- Δ 473-476 (Δ aa 473-476) was generated by performing SOMA (Pfirschmann <i>et al</i> , 2013) using WAVE2- Δ 473-476 on pEGFP-C1-WAVE2 and was subcloned into pEF-myc plink
pEF-myc-JMY	JMY (aa 1-983) was amplified using EcoRI-JMY-forward/XbaI-JMY-reverse on pEGFP-C1-JMY and was subcloned into pEF-myc plink
pEF-myc-JMY- Δ C	JMY- Δ C (Δ aa 945-967) was generated by performing SOMA (Pfirschmann <i>et al</i> , 2013) using JMY- Δ C on pEGFP-C1-JMY and was subcloned into pEF-myc plink
pEF-myc-JMY- Δ A	JMY- Δ A (aa 1-967) was amplified by inserting a premature STOP codon using EcoRI-JMY-forward/XbaI-JMY- Δ A-reverse on pEGFP-C1-JMY and was subcloned into pEF-myc plink
pEF-myc-JMY- Δ CA	JMY- Δ CA (aa 1-944) was amplified by inserting a premature STOP codon using EcoRI-JMY-forward/XbaI-JMY- Δ CA-reverse on pEGFP-C1-JMY and was subcloned into pEF-myc plink
pEF-myc-JMY- Δ VCA	JMY- Δ VCA (aa 1-905) was amplified by inserting a premature STOP codon using EcoRI-JMY-forward/XbaI-JMY- Δ VCA-reverse on pEGFP-C1-JMY and was subcloned into pEF-myc plink
pEF-myc-JMY-R961E	JMY-R961E (aa 1-983) was generated by performing SOMA (Pfirschmann <i>et al</i> , 2013) using JMY-R961E on pEGFP-C1-JMY and was subcloned into pEF-myc plink

pEF-myc-JMY-Δ960-963	JMY-Δ960-963 (Δaa 960-963) was generated by performing SOMA (Pfaffmann <i>et al</i> , 2013) using JMY-Δ960-963 on pEGFP-C1-JMY and was subcloned into pEF-myc plink
pEF-NLS-MRTF-A-HA	NLS-MRTF-A was generated using ClaI-NLS-MAL-forward/ XbaI-HA-MAL-reverse on pEF-MAL-f.l.-HA and subcloned into pEF plink

III.1.7 Cells and Culture Media

Bacterial Strains and Media

Name	Description	Source
<i>E. coli</i> DH5α	F- φ80/lacZ ΔM15 Δ (lacZYA-argF) U169 deoR recA1 endA1 endA1 hsdR17(rK-, mK+) phoA supE44 thi-1 gyrA96 relA1 λ-, chemically competent	Invitrogen

Culture medium.....	Lysogeny broth (LB) with	5 g yeast extract 10 g tryptone/peptone 10 g NaCl per 1 l 100 μg/ml ampicillin or 30 μg/ml kanamycin
Solid medium.....	Culture medium with	1.5% agar-agar

Mammalian Cells and Cell Culture Media

Cell line	Description	Source
NIH 3T3	National Institutes of Health, Swiss embryonic mouse fibroblasts, spontaneously immortalized (Todaro & Green, 1963)	R. Treisman, Cancer Research UK (London)

Culture medium.....	DMEM supplemented with	10% (v/v) FCS 2 mM L-glutamine 100 U/ml penicillin 100 μg/ml streptomycin
---------------------	------------------------	--

Freezing medium	90% (v/v) FCS, 10% DMSO
Starvation medium	DMEM supplemented with 0.5% (v/v) FCS 2 mM L-glutamine 100 U/ml penicillin 100 µg/ml streptomycin
Selection medium	DMEM supplemented with 10% (v/v) FCS 2 mM L-glutamine 100 U/ml penicillin 100 µg/ml streptomycin 1 mg/ml G418

III.2 Methods

III.2.1 Molecular Cloning and DNA Manipulation Methods

High-Fidelity PCR

For molecular cloning and exponential amplification of DNA fragments Q5 High-Fidelity DNA Polymerase (New England Biolabs) was used to perform polymerase chain reaction (PCR) (Saiki *et al*, 1988). According to the manufacturer's instructions each reaction setup was composed as follows:

x µl	plasmid DNA (final concentration 0.3-1 µg)
10 µl	5 x Q5 High-Fidelity Reaction Buffer (final concentration 1 x)
10 µl	1 x Q5 High GC Enhancer (final concentration 1 x)
1 µl	10 mM dNTPs (final concentration 200 µM)
2.5 µl	10 µM primers each (final concentration 0.5 µM)
0.5 µl	Q5 High-Fidelity DNA Polymerase (0.02 U/µl)
<hr/>	
add x µl	<u>H₂O to a final volume of 50 µl</u>

The PCR was performed using the T 3000 Thermocycler and set up as follows:

Step	Temperature	Time
initial denaturation	98°C	30 seconds
denaturation	98°C	10 seconds
primer annealing	3°C lower than primer melting temperature	30 seconds
synthesis	72°C	30 seconds/kb
end synthesis	72°C	2 minutes
<hr/>		30 cycles

PCR products were analyzed by agarose gel electrophoresis and purified using either QIAquick MinElute Gel Extraction Kit or QIAquick MinElute PCR Purification Kit.

Single Oligonucleotide Mutagenesis and Cloning Approach

For restriction site-independent deletions or nucleotide substitutions the Single Oligonucleotide Mutagenesis and Cloning Approach (SOMA) was performed according to Pfirrmann (Pfirrmann *et al*, 2013). A single mutagenic and phosphorylated oligonucleotide was used to synthesize a circular mutant strand followed by isolation from template DNA by DpnI digestion. Modified DNA was purified using QIAquick MinElute PCR Purification Kit and transformed in chemically competent *E. coli DH5a*.

DNA Manipulation – Digestion and Ligation

Restriction site-directed digestion of plasmid DNA or amplified DNA fragments was performed using restriction endonucleases (NEB). According to the manufacturer's instructions each reaction setup was composed as follows:

x μ l	DNA (1 μ g plasmid DNA or 10 μ l from PCR)
1 μ l	restriction enzyme I
1 μ l	restriction enzyme II
3 μ l	CutSmart Buffer
<hr/>	
add x μ l	<u>H₂O to a final volume of 30 μl</u>

Incubation was for 2 hours at 37°C. Re-circularization of digested DNA was prevented by de-phosphorylation of the 5'ends using 1 μ l shrimp alkaline phosphatase (NEB) for 30 minutes at 37°C. DNA was analyzed by agarose gel electrophoresis and purified using QIAquick MinElute Gel Extraction Kit.

Ligation of purified digested insert DNA with digested vector DNA was performed in a molar ratio of 1:3 (vector:insert) using T4 DNA ligase (NEB). According to the manufacturer's instructions each ligation setup was composed as follows:

x μ l	vector DNA
x μ l	insert DNA
1 μ l	10 x T4 DNA Ligase Buffer
0.5 μ l	T4 DNA Ligase
<hr/>	
add x μ l	<u>H₂O to a final volume of 10 μl</u>

Ligation was carried out overnight at 16°C or 2 hours at room temperature. The ligation approach was used to transform chemically competent cells.

Transforming Chemically Competent *DH5α* Cells

For non-viral transfer of plasmid DNA into bacterial cells chemically competent *E. coli DH5α* were used. Cells were transformed using 100 ng plasmid DNA or 1-5 µl of a ligation approach. DNA together with 50 µl competent cells were incubated for 30 minutes on ice followed by a thermal shock (45 seconds at 42°C) and 5 minutes re-incubation on ice. Afterwards, cells were kept in 500 µl pre-warmed LB-medium without antibiotics for 1 hour under constant shaking (550 rpm at 37°C). 100 µl of transformed cells were plated on LB-agar plates containing appropriated antibiotics and incubated overnight at 37°C to cultivate positive transformed *DH5α* cells.

Colony PCR

Bacterial clones were insert-specifically analyzed performing colony PCR (Hofmann & Brian, 1991). Well separated colonies were picked from LB-agar plates, dipped into PCR tubes, provided with 5 µl water for PCR reaction, and finally kept in 3 ml pre-warmed LB-medium supplemented with antibiotics for bacterial cultures. Colony PCR was performed using Taq DNA Polymerase (NEB) according to the manufacturer's instructions. Each reaction setup was composed as follows:

5 µl	H ₂ O (provided in PCR tube, supplemented with bacterial DNA)
1.5 µl	10 x Thermo Pol Reaction Buffer (final concentration 1 x)
0.3 µl	10 mM dNTPs (final concentration 200 µM)
0.3 µl	10 µM primers each (final concentration 0.5 µM)
0.075 µl	Taq DNA Polymerase (1.25 U/50 µl)
<hr/>	
add x µl	<u>H₂O to a final volume of 20 µl</u>

The PCR was performed using the T 3000 Thermocycler and set up as follows:

Step	Temperature	Time
initial denaturation	95°C	30 seconds
denaturation	95°C	25 seconds
primer annealing	3°C lower than the primer-specific melting temperature	30 seconds
synthesis	68°C	1 minute/kb
end synthesis	68°C	5 minutes

30 cycles

PCR products were analyzed by agarose gel electrophoresis.

Agarose Gel Electrophoresis

DNA fragments from PCR or digestion were electrophoretically separated depending on their size using agarose gel electrophoresis according to Rickwood & Hames (Rickwood & Hames, 1990). For electrophoretic separation 1% agarose gels (1 g agarose per 100 ml 1 x TBE buffer) were used and supplemented with 0.01% (v/v) of DNA-intercalating ethidium bromide for visualization of nucleic acids by UV light. Gel polymerization was at room temperature. DNA samples were mixed with 5 x loading dye, loaded into gel wells and separated at 90-120V and 400 mA. Intas Science Imaging system was used at 312 nm for UV light-mediated DNA visualization and documentation. Fragment size could be determined using GeneRuler DNA ladders (Thermo Scientific) as controls. Separated fragments were isolated from the agarose gel using QIAquick MinElute Gel Extraction Kit.

Purification of DNA

DNA fragments from PCR or digestion were purified from agarose gel using QIAquick MinElute Gel Extraction Kit or from PCR using QIAquick MinElute PCR Purification Kit according to the manufacturer's instructions. Both purification methods are based on the binding of nucleic acids on silica membrane under high-salt buffer conditions. Elution was under low-salt conditions using 10 µl water. For spectrophotometric analysis of DNA purity and concentration the Nanodrop 2000c was used to measure absorption at 260 nm and 280 nm.

Preparation of Plasmid DNA

For preparation and purification of plasmid DNA from bacterial cultures QIAGEN Plasmid Mini or Maxi Kit were used according to manufacturer's instructions. Plasmid purification by these kits are based on gravity-flow anion-exchange tips. Elution of plasmid DNA was performed using 40 µl water. For spectrophotometric analysis of DNA purity and concentration the Nanodrop 2000c was used to measure absorption at 260 nm and 280 nm.

Sequencing of DNA Fragments

Sequencing of DNA fragments was performed by Eurofins MWG Operons according to the Sangers chain-terminating method and according to the manufacturer's recommendations (Sanger *et al*, 1992).

III.2.2 Cell Culture Methods

General Procedures

Cell culture work was performed using sterile laminar flow cabinets under biosafety level S1 conditions. NIH 3T3 mouse fibroblasts were cultured at 37°C and 5% CO₂ in 75 cm² cell culture flasks. Cell passaging was done every two or three days by washing cells with warmed PBS followed by detaching cell-cell- and cell-surface-contacts using 1.5 µl warmed 1 x trypsin (5 ml 10 x trypsin per 45 ml PBS). New passages were seeded in a 1:7.5 dilutions to a final volume of 15 ml with DMEM culture medium in 75 cm² culture flasks.

Cell numbers and size were measured using a CASY cell counter (OMNI Life Science) according to the manufacturer's instructions. This cell counting system is based on the varying electrical resistance of cells during their passage through a measurement pore. Long term cell storage was at -150°C. Therefore, 1 x 10⁶ cells were re-suspended in freezing medium and stored at -80°C in CryoTube™ vials and isopropanol chambers for 48 hours followed by long term storage at -150°C. For re-use, cells were thawed at 37°C in water bath for 1-2 minutes.

Introduction of Nucleic Acids into the Cells

Transient Transfection of DNA

Transient transfection of plasmid DNA was performed using X-tremeGENE 9 (Roche) according to the manufacturer's instructions which is based on the lipofection method (Felgner *et al*, 1987). For luciferase reporter assay, 7×10^4 NIH 3T3 cells were cultured overnight in 12-well plates followed by medium change to starvation medium and transfection of 500 ng plasmid DNA in total. For each well, 50 μ l complex was prepared using OPTI-MEM medium, 1.5 μ l X-tremeGENE 9, 50 ng p3D.A-Luc firefly luciferase reporter plasmid, 5 ng pRL-TK *Renilla* luciferase control plasmid, 300 ng NPF constructs and 145 ng empty vector. Incubation was for 15 minutes at room temperature followed by dropwise addition of transfection mixtures to the cells. 7 hours prior the experiment, cells were serum stimulated with 15% (v/v) FCS or treated with 100 μ M CK-666, 30 μ M CK-548 or 1 μ M Latrunculin B where indicated.

Transient Transfection of siRNA

Transient transfection of siRNA was performed using Lipofectamine RNAiMAX reagent (Invitrogen) according to the manufacturer's instructions which based on the lipofection method (Felgner *et al*, 1987). 7×10^4 NIH 3T3 cells were cultured overnight in 12-well plates followed by medium change and transfection of 30 pmol siRNA in total. Where indicated, 24 hours later siRNA transfection was followed by transient transfection of plasmid DNA using X-tremeGENE 9 (Roche).

Reverse Transfection

In contrast to a conventional transient transfection, reverse transfection is an improved transfection method where cell seeding and incubation with the transfection reagents were done at the same time. Where indicated, reverse transfection of siRNA was performed using Lipofectamine RNAiMAX (Invitrogen) according to the manufacturer's instructions.

Generation of Stable Cell Lines

For generating stably expressing NIH 3T3 cell lines 1×10^6 cells were cultured overnight in 10 cm dishes followed by transfection of 5 μ g plasmid DNA in total using X-tremeGENE 9 (Roche) according to the manufacturer's instructions. 48 hours post transfection the medium was changed to selection medium. Antibiotic-based selection of positive transfected cells was maintained over two weeks followed by cell dilution

and re-seeding into 96-well plates to produce single-cell-clones. Single-cell-clones were maintained on selection medium over four weeks followed by expansion to 10 cm dish-scales.

III.2.3 Protein Analytical Methods

Cell lysis for Immunoblotting

For protein analysis 3×10^5 NIH 3T3 cells were cultured in 6-well plates and transfected with 1 μ g plasmid DNA in total. Cells were washed with pre-chilled PBS and incubated with 200 μ l pre-chilled RIPA buffer supplemented with 1 x Complete protease inhibitor cocktail for a minimum of 20 minutes at -20°C . Following freeze lysis, cells were harvested using cell scrapers, transferred into Eppendorf tubes and centrifuged at 4°C and $20\ 817 \times g$ for 20 minutes. Supernatants were transferred into fresh Eppendorf tubes. Protein concentration was measured using the Micro BCA Protein Assay Kit (Thermo Scientific) according to the manufacturer's instructions. Protein lysates were supplemented with 1 x loading buffer, denatured (5 minutes at 95°C) and loaded on SDS gel or stored at -20°C .

Cell Fractionation by Ultracentrifugation (G-/F-actin)

To prepare cell fractions of G- and F-actin 3×10^5 NIH 3T3 cells were cultured in 6-well plates and transfected with 1 μ g plasmid DNA in total. Cells were washed with pre-chilled PBS and incubated with 750 μ l fractionation lysis buffer supplemented with 1 x Complete™ protease inhibitor cocktail for 10 minutes on ice. Cells were harvested using cell scrapers and transferred into suitable polycarbonate tubes. Ultracentrifugation of cells was performed using Optima TL Ultracentrifuge (1.5 hours at $100\ 000 \times g$ and 4°C). Following centrifugation, 700 μ l of the supernatants (soluble G-actin fraction) were transferred into fresh Eppendorf tubes. Before denaturation (5 minutes at 95°C) 1 x loading buffer was added. After careful remove of remaining G-actin fraction, cell pellets (cytoskeletal/F-actin fraction) were supplemented with 700 μ l fractionation lysis buffer and 1 x loading buffer and sonicated until the F-actin pellet was sheared. Samples were denatured (5 minutes at 95°C) and loaded on SDS gels or stored at -20°C .

Determination of Protein Concentration

Quantitative measurement of protein concentration was performed in 96-well plates using the Micro BCA Protein Assay Kit (Thermo Fisher) according to the bicinchoninic acid method (Smith *et al*, 1985). As control, a standard curve with 0 mg/ml up to 2 mg/ml BSA was prepared using the appropriated BSA solution. For sample measurement, 10 μ l of protein lysates were mixed with 100 μ l of BCA reagent mixture and incubated for 30 minutes at 37°C. Absorption at 560 nm was analyzed using the Multiskan microplate reader. Protein concentrations were calculated using the standard curve and quadratic equation.

Co-Immunoprecipitation

To analyze protein complexes and protein binding partners an antibody-mediated co-immunoprecipitation assay was performed (Firestone & Winguth, 1990). Antibodies for precipitation are coupled to magnetic beads whereby separation occurred by magnet. In 10 cm dishes 1×10^6 NIH 3T3 cells were cultured and transfected with 5 μ g plasmid DNA in total. The total amount of DNA was composed of 1.5 μ g pEF-Flag-actin-WT or -R62D and 3.5 μ g pEF-myc-NPF, according to the experiment. After overnight incubation medium was changed to starvation medium for 24 hours followed by co-immunoprecipitation.

Flag-immunoprecipitation was performed using anti-Flag M2 magnetic beads (Sigma) according to the manufacturer's instructions. Cells were scraped and harvested in anti-Flag magnetic beads lysis buffer and incubated with anti-Flag magnetic beads and 4.8 μ g pET41a 3C Δ MRTF-A (2-261) where indicated. Immunoprecipitation was under constant rotation (2 hours at for 4°C). Precipitates were washed with 1 x TBS, re-suspended in 1 x loading buffer and denatured (5 minutes at 95°C) before loading on SDS gel.

Myc-immunoprecipitation was performed using the μ MACS c-myc Isolation Kit (Miltenyi Biotec) according to the manufacturer's instructions. Cells were lysed using the recommended lysate buffer. Where indicated, ultra-centrifuged supernatants (100 000 x g) were prepared following cell lysis in G-actin fraction lysis buffer. Incubation of lysates with anti-myc MicroBeads and 4.8 μ g MRTF-a (2-261) was on ice for 1 hour. Precipitates were washed and eluted with 95°C pre-heated elution buffer before loading on SDS gel.

SDS-Polyacrylamide Gel Electrophoresis

Proteins were analyzed using SDS-polyacrylamide gel electrophoresis for electrophoretic size separation according to Laemmli (Laemmli, 1970). Running- and stacking-gels were prepared as listed above, TEMED was used for polymerization. Equal amounts of total protein (20-40 μ g) were loaded. Separation on SDS gel was performed at 130-150V for 1-1.5 hours, according to the experiment. Protein size could be determined using Precision Plus Protein™ Standards (BIO-RAD). SDS gels with size separated proteins were either stained with Coomassie using Coomassie Brilliant Blue R-250 or used for immunoblotting.

Immunoblotting

SDS-PAGE separated proteins could be visualized by immunoblotting according to Harlow and Lane (Harlow & Lane, 1988). Electrophoretic transfer of negatively charged proteins onto PVDF membrane was performed using Mini-PROTEAN Tetra System (BIO-RAD) according to the manufacturer's instructions. Transfer was at 100V for 1-1.3 hours onto a PVDF membrane specific for the use of fluorescence-labeled antibodies (PVDF-FL). Membrane blotting was followed by washing (5 minutes in 1 x TBS-T) and blocking (1 hour in 5% milk in 1 x TBS-T at room temperature). Incubation with primary antibodies (diluted 1:500 to 1:2000 in 5% milk in 1 x TBS-T) was overnight at 4°C followed by washing (3 x 5 minutes in 1 x TBS-T) and incubation with fluorophore-labelled secondary antibodies (diluted 1:15000 in 5% milk in 1 x TBS-T) for 1 hour at room temperature. Fluorescence signals were detected using ODYSSEY CLx (LI-COR) and quantified using the associated LI-COR Image Studio software according to the manufacturer's recommendations. Signal detection via two near-infrared lasers decreased auto-fluorescence and increased signal intensity. For quantification of band intensity signals are given as fluorescence intensity over area and were calculated as relative to the loading control.

III.2.4 Immunofluorescence Staining and Microscopy

For fluorescence microscopy-based analysis of cytoskeletal structures and protein localization cells were immune-stained using fluorophore-labeled antibodies. In 12-well plates 7×10^4 NIH 3T3 cells were cultured overnight on coverslips followed by medium change to starvation medium and transfection with 500 μg plasmid DNA in total. 24 hours post transfection cells were fixed (3.7% formaldehyde in PBS for 15 minutes), extracted (0.2% (v/v) Triton X-100 in PBS for 10 minutes) and unspecific binding sites were blocked (10% FCS/1% BSA/0.05% Triton X-100 (v/v) in PBS for 30 minutes). Incubation with primary antibodies (diluted 1:100 to 1:1000 in blocking solution, for 1 hour at room temperature) was followed by washing (3 x with PBS) and incubation with Alexa-conjugated secondary antibodies (diluted 1:200 in blocking solution, for 1 hour at room temperature). Stained cells were (3 x with PBS) and covered with the mounting ProLong Gold antifade reagent to decrease photo bleaching. For imaging the Leica TCS SP2 AOBS confocal microscope (63 x oil objective) and the Zeiss Axio Imager M (63 x oil objective) equipped with a monochrome Axiocam MRm camera were used. For image adaption Adobe Photoshop CS6 software was used. For quantification 50 positive transfected cells each of three independent biological experiments were analyzed for their localization of endogenous MRTF-A. Relative nuclear and cytoplasmic distribution of MRTF-A were calculated as mean values and are shown in percentage.

III.2.5 Luciferase Reporter Assay

To analyze the activity of transcription factors a luciferase-based reporter system was used. Luciferase expression is controlled by the transcription factor-specific binding site (Geneste *et al*, 2002; Sotiropoulos *et al*, 1999). Luciferase-mediated bioluminescence is detected using Glomax (Promega) according to the manufacturer's instructions. For luciferase reporter assay, 7×10^4 NIH 3T3 cells were cultured overnight in 12-well plates followed by medium change to starvation medium and co-transfection with 50 ng p3D.A-Luc firefly luciferase reporter plasmid, 5 ng pRL-TK *Renilla* luciferase control plasmid and 300 ng pEF-myc-NPF in a total of 500 ng plasmid DNA. Cell harvest was 24 hours post transfection in pre-chilled 1 x passive lysis buffer followed by centrifugation (15 minutes at 20 817 x g and 4°C). The reporter assay was performed in white 96-well plates using 20 μl of cell extract and with 50 μl each of the Dual-Glo

Luciferase Assay Kit corresponding luciferase substrates. Firefly luciferase was normalized to *Renilla* luciferase readings and are expressed as fold induction.

III.2.6 Isolation of total RNA

Isolation of total RNA from cell cultures was performed according the single-step method by guanidine-thiocyanate (Chomczynski & Sacchi, 1987; Chirgwin *et al*, 1979). For isolation the QIAGEN RNeasy Mini Kit was used which combines the principle of guanidine-thiocyanate-mediated RNA extraction and silica membrane-mediated RNA isolation. 3×10^5 NIH 3T3 cells were cultured overnight in 6-well plates followed by transient transfection of 1 μ g plasmid DNA in total. Overnight incubation was followed by cell harvest and RNA isolation according to the manufacturer's instructions. For spectrophotometric analysis of RNA purity and concentration the Nanodrop 2000c was used to measure absorption at 260 nm and 280 nm. Isolated RNA was used for cDNA syntheses or stored at -20°C .

III.2.7 cDNA Synthesis and Quantitative real-time PCR

For quantitative analysis of gene expression single stranded complementary DNA (cDNA) was synthesized from total RNA via reverse transcription and used as template for real-time qPCR. First-strand cDNA synthesis was performed using 500 ng RNA, random hexamers and the Verso cDNA Synthesis Kit (Thermo Scientific) according to the manufacturer's instructions. The qRT-PCR reaction was performed using the DyNAmo ColorFlash SYBR Green qPCR Kit (Promega) according to the manufacturer's instructions and was composed as follows:

1.5 μ l	cDNA (1:5 diluted with water)
5 μ l	DyNAmo ColorFlash SYBR Green qPCR Kit
0.25 μ l	10 μ M gene-specific primers each
<hr/>	
add 3 μ l	<u>H₂O to a final volume of 10 μl</u>

The qPCR was performed using the LightCycler 480 II instrument. The amount of amplified DNA correlated with the fluorescence intensity of the SYBER Green fluorophore and was given as CT value. ALAS and HPRT expression levels were analyzed as reference (housekeeping genes). To access the specificity of the PCR,

melting curves were generated from each reaction. Relative gene expression levels were calculated according to the $2^{-\Delta\Delta CT}$ method (Livak & Schmittgen, 2001). Thereby the differences of target gene CT value to housekeeping gene CT value (ΔCT) were calculated and compared as fold inductions between samples ($\Delta\Delta CT$).

III.2.8 Calculation and Statistics

Calculations and statistics were performed using Microsoft-Office Excel 2010. Significances were calculated from at least three independent biological replicates using the T-test according to Gossets *Student's T Distribution* (Student, 1908). By an unpaired one sample student's t-test the mean value of one data set was compared to a relative control value, which was set to one. For comparison the mean values of two different data sets an unpaired two sample student's t-test was used.

IV Results

IV.1 Actin Polymerization inside the Nucleus

Previous findings underlined an important role of actin dynamics in regulating gene transcription activity mediated by the actin-MRTF-SRF pathway. The critical step to activate MRTF-A/SRF is the dissociation of inhibitory G-actin:MRTF complexes which are known to exist both in the cytoplasm and inside the nucleus (Miralles *et al*, 2003; Posern & Treisman, 2006; Vartiainen *et al*, 2007). An approved model described complex disruption as response to increased F-actin formation and depletion of available G-actin (Sotiropoulos *et al*, 1999; Posern *et al*, 2004). But, actin filament formation in the interphase nucleus was rarely shown and very controversial.

To answer the question whether F-actin polymerization is present also inside the nucleus already established actin mutants fused to a nuclear localization signal (NLS) were transiently expressed in mouse fibroblasts and analyzed for filamentous actin via immunofluorescence (Fig. IV-1, VIII-1) (Posern *et al*, 2004, 2002). The mutants are known to either enhance actin filament stability, like actin G15S, S14C and V159N, or they are polymerization-deficient, like actin R62D. Actin filaments were visualized by co-transfection of LifeAct-GFP, a 17 amino acid fragment of the yeast actin-binding protein Abp140 (Riedl *et al*, 2008). Expression of NLS-actin-wildtype (WT), -G15S, -S14C and -V159N together with LifeAct showed actin filaments inside the nucleus (Fig. IV-1, first to fourth line). Whereas WT and G15S induced formation of long thin actin filaments expression of NLS-actin-S14C and -V159N displayed filament-like actin rods which are more short and dense. In contrast, polymerization-deficient actin R62D failed to form LifeAct-positive actin filaments and is uniformly distributed all over the nucleoplasm (Fig. IV-1, last line). These results clearly demonstrated that F-actin structures can form inside the nucleus which are positive for LifeAct-staining. In addition, nuclear actin filament formation could be confirmed using the F-actin marker phalloidin (Fig. VIII-1).

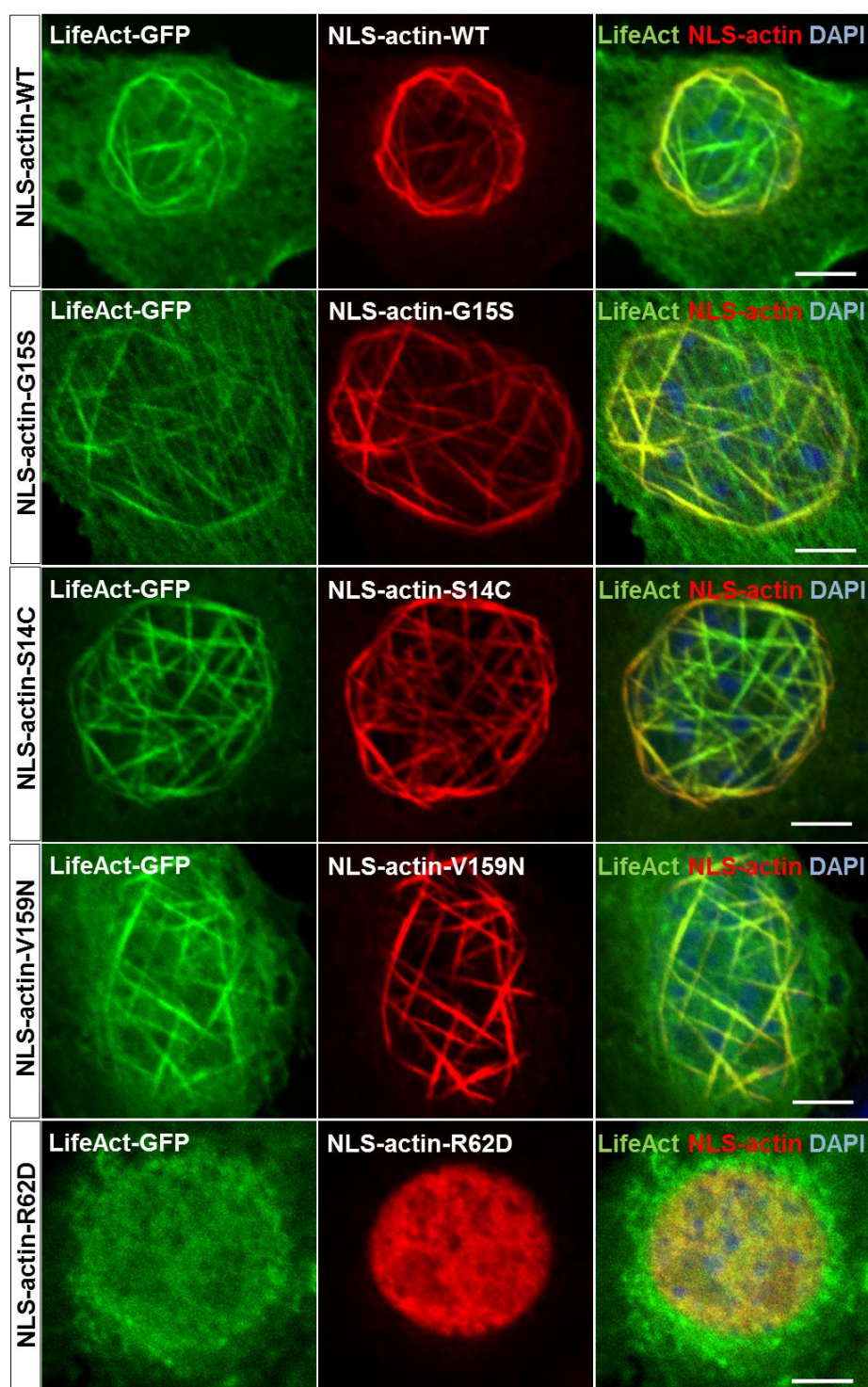


Figure IV-1: Analysis of nuclear actin networks through LifeAct-GFP staining. NIH 3T3 fibroblasts were co-transfected with LifeAct-GFP (green) and the indicated actin mutants, fixed, counterstained with DAPI (blue), immune-stained against Flag-tag for the localization of the expressed actins (red) and analyzed by confocal microscopy. Cells expressing NLS-actin-WT/-G15S/-S14C/-V159N show LifeAct- and Flag-positive nuclear F-actin bundles. Bundle thickness is increased from actin-WT to actin-V159N whereas bundle length is decreased. Polymerization-deficient NLS-actin-R62D is negative for LifeAct- or Flag-positive actin bundles and shows a uniform distribution over the nucleoplasm. *Scale bars, 5 μ m.*

IV.2 WH2 (V) Domain-containing N-WASP and WAVE2

IV.2.1 N-WASP and WAVE2 activate MRTF-SRF-dependent Target Gene Transcription

Although MRTF-A activity is associated with increased actin dynamics, a crucial yet unsolved issue is the detailed explanation for complex dissociation in view of only slight changes on the cellular G-actin pool and the massive excess of G-actin compared to MRTF-A. Previous findings gave evidence for nucleation promoting factors (NPF) to be involved. Therefore, a possible competition model was investigated in which MRTF-A is released from repressive G-actin by mutually exclusive binding of WH2 (V) domain-containing NPF. As representative NPF murine N-WASP and WAVE2 were selected to test this hypothesis.

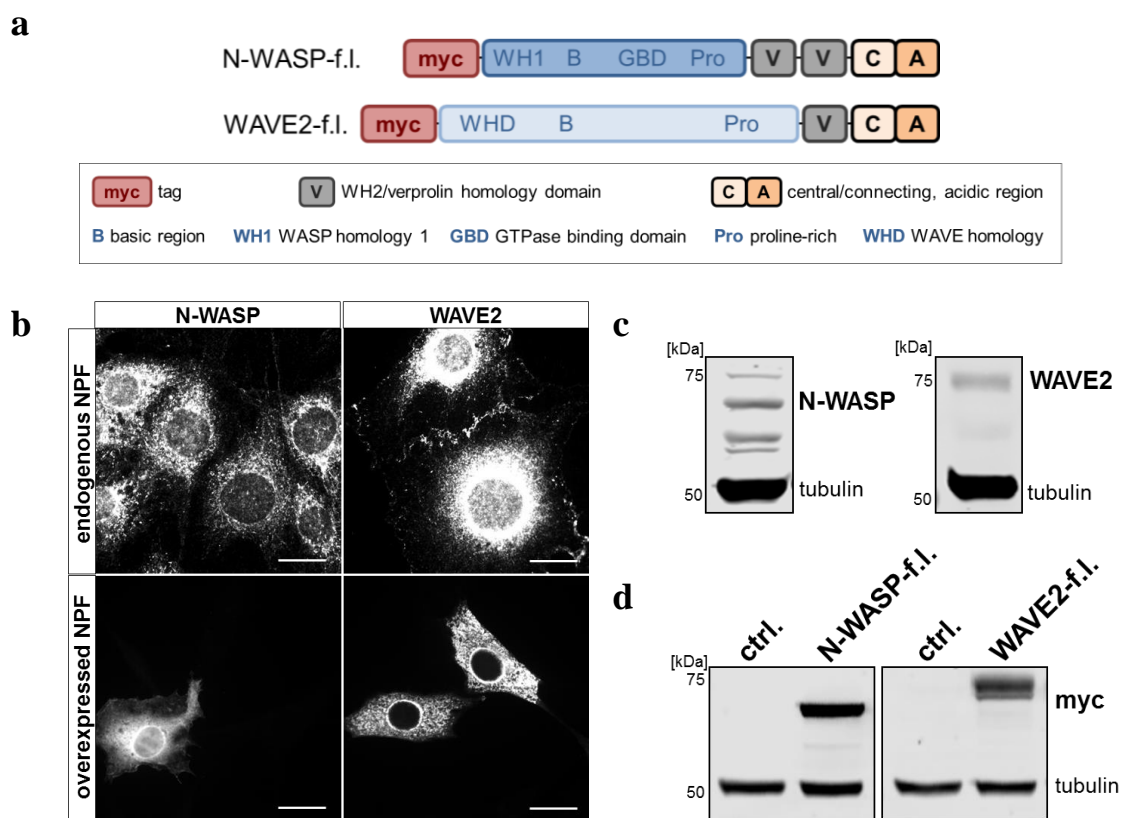


Figure IV-2: Expression and localization of murine N-WASP and WAVE2 in mouse fibroblasts. NIH 3T3 cells were analyzed for expression and localization of endogenous N-WASP and WAVE2 and of overexpressed myc-tagged N-WASP and WAVE2 following transient transfection. **a** Schematics of myc-tagged N-WASP- and WAVE2-full length constructs and domain topology. **b** Non-transfected cells (endogenous NPF) and cells transiently transfected with myc-tagged N-WASP and WAVE2 (overexpressed NPF) were fixed and immune-stained with anti-N-WASP, -WAVE2 or -myc antibody and analyzed by epifluorescence microscopy. **c-d** Western blot analysis of endogenous and overexpressed N-WASP and WAVE2. Equal loading was controlled by tubulin. **c** Endogenous expression in NIH 3T3 cells using anti-N-WASP and anti-WAVE2 antibody. **d** Overexpression of myc-tagged NPF using tag-specific antibody. *Scale bars, 20 μm.*

N-WASP and WAVE2 are endogenously present in mouse fibroblasts (Fig. IV-2 b, c). However, all assays were performed as overexpression analysis. Therefore constructs of N-WASP and WAVE2 fused to a myc-tag were generated and transiently expressed in NIH 3T3 fibroblasts. Their correct subcellular localization, protein size and expression level was verified by immunofluorescence and western blot analysis (Fig. IV-2). Transient transfection showed WAVE2 to be largely excluded from the nucleus whereas N-WASP was located in the cytoplasm and inside the nucleus. In contrast, endogenous N-WASP and WAVE2 both were restricted to the cytoplasm (Fig. IV-2 b).

Activity of MRTF-A and the MRTF-SRF transcription module mediated by WH2-containing NPF was investigated performing a luciferase-based SRF reporter assay and quantitative RT-PCR of target genes (Fig. IV-3). The SRF reporter plasmid contains multiple SRF binding sites which promote luciferase expression upon binding of transcriptional active MRTF-A:SRF. Similar to serum-stimulation (FCS), N-WASP and WAVE2 both significantly activated the SRF reporter compared with the starved control (ctrl.) (Fig. IV-3 a). Their impact on MRTF-SRF target gene transcription was analyzed for the main target *smooth muscle actin* (*Acta2*). Upon transient transfection N-WASP and WAVE2 induced increased *Acta2* mRNA expression compared with the level of starved control cells (ctrl.) (Fig. IV-3 b).

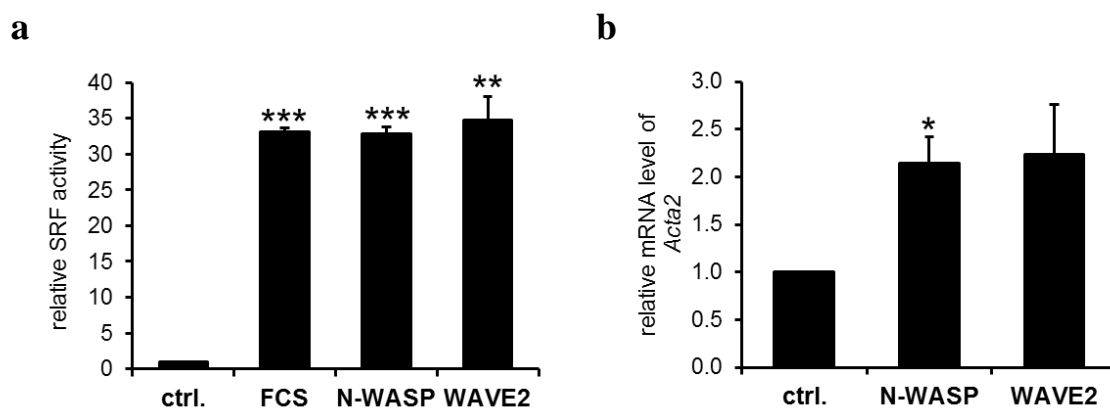
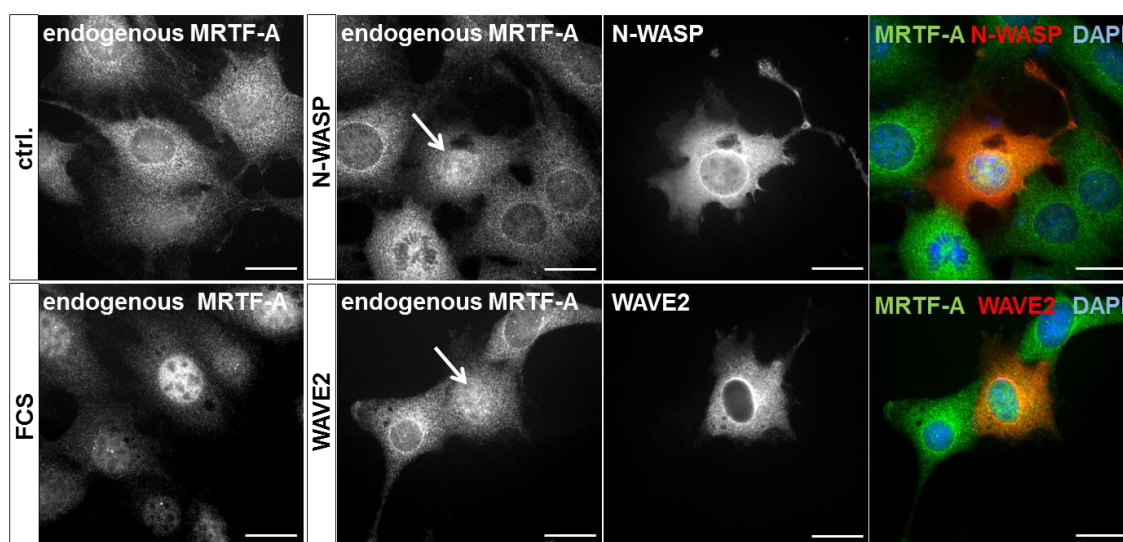


Figure IV-3: WH2 (V) domain-containing N-WASP and WAVE2 activate MRTF-SRF-dependent target gene transcription. NIH 3T3 cells were transiently transfected with full length N-WASP and WAVE2, serum-starved for 24 hours and analyzed for SRF target gene expression. **a** Relative MRTF-SRF luciferase reporter activity was increased upon co-transfection with the indicated constructs. As a control, cells transfected with vector control (ctrl.) were stimulated for 7 hours with 15% serum (FCS). **b** Endogenous mRNA expression of smooth muscle α -actin (*Acta2*) upon transient transfection of full length N-WASP and WAVE2 in comparison to the serum-starved control (ctrl.). All data were normalized to the starvation control which was set to 1. Error bars, s.e.m., n = 3 (* $p \leq 0.05$, ** $p \leq 0.01$, *** $p \leq 0.001$ according to an unpaired one sample student's t-test).

IV.2.2 N-WASP and WAVE2 induce Nuclear Accumulation of MRTF-A

Transcriptional activity of MRTF-A correlates with its nuclear translocation. Thus, subcellular localization of MRTF-A in response to NPF expression was investigated by immunofluorescence (Fig. IV-4). Following transient transfection of myc-tagged N-WASP and WAVE2, cells were immune-stained for endogenous MRTF-A (Fig. IV-4 a). In non-stimulated cells (ctrl.) MRTF-A was predominantly located in the cytoplasm. Translocation into the nucleus was induced by serum-stimulation (FCS). Expression of myc-tagged N-WASP and WAVE2 both led to nuclear accumulation of endogenous MRTF-A under serum-starved conditions.

a



b

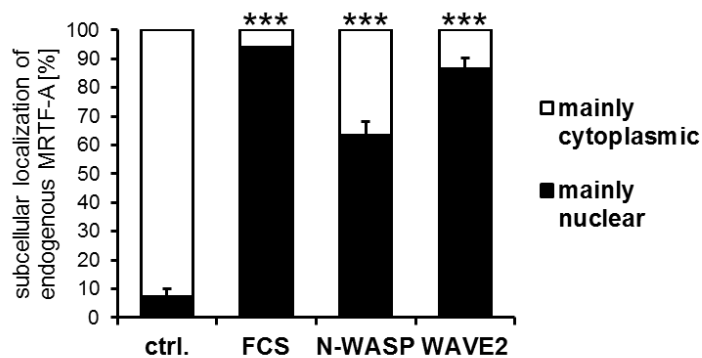


Figure IV-4: Nuclear accumulation of MRTF-A upon overexpression of N-WASP and WAVE2. **a** Serum-starved NIH 3T3 cells were transiently transfected with the indicated myc-tagged constructs, fixed, counterstained with DAPI (blue), immune-stained with anti-myc (red) and anti-MRTF-A antibody for localization of endogenous MRTF-A (green) and analyzed by epifluorescence microscopy. Starved conditions (ctrl.) and serum-stimulation for 1 hour (FCS) were as controls. **b** Quantification of MRTF-A localization by counting 50 myc-positive cells each. Arrows indicate myc-expressing cells. Scale bars, 20 μ m. Error bars, s.e.m., n = 3 (* $p \leq 0.05$, ** $p \leq 0.01$, *** $p \leq 0.001$ according to an unpaired two sample student's t-test).

Quantification of MRTF translocation revealed less cells with nuclear accumulated MRTF-A upon N-WASP or WAVE2 expression compared with serum-stimulation which could be for reasons of transient transfection (Fig. IV-4 b). Nevertheless, both WH2-containing NPF significantly induced nuclear translocation of MRTF-A in 65-85% of transfected cells.

IV.2.3 N-WASP and WAVE2 compete with MRTF-A for Actin-Binding independently of ARP2/3 Interaction

Mutually exclusive binding of NPF WH2 (V) domains and MRTF-A RPEL motifs was hypothesized because of their predicted ability to bind to the same surface on G-actin molecules. Therefore NPF-mediated MRTF activation by direct competition independently of altered actin dynamics was speculated. N-WASP and WAVE2 both modulate actin polymerization via the ARP2/3 complex. To exclude ARP2/3 interaction and ARP2/3-mediated changes of the G-/F-actin ratio in the following analysis N-WASP and WAVE2 constructs with deficient ARP2/3 binding sites were required. ARP2/3 recruitment and activation is mediated by the C-terminal central acidic (CA) region of NPF. Thus, constructs with deletions of either the C- or the A-region or the complete CA-region were generated (Fig. IV-5 a). Additionally, a critical role on ARP2/3 activation was described for arginine 474 (R474) within a KRSK motif of murine N-WASP (Kim *et al*, 2000; Banzai *et al*, 2000). This arginine is conserved in numerous NPF and was therefore mutated (R474E), as well as the adjacent amino acids (Δ 473-476) (Fig. IV-5 a, VIII-2). All constructs were fused to myc-tag, expressed in mouse fibroblasts and initially analyzed for correct protein size and expression level (Fig. IV-5 a-b). As being representative for impaired ARP2/3 interaction, the following assays focused on the constructs N-WASP- and WAVE2- Δ A, -R474E and - Δ CA.

The direct impact of N-WASP and WAVE2 on actin:MRTF-A complexes was investigated in a co-immunoprecipitation assay. Precipitated Flag-tagged actin and the purified MRTF-A were analyzed for complex formation in presence of full length and ARP2/3 deficient N-WASP and WAVE2 (Fig. IV-6). Lysates from cells overexpressing Flag-actin and myc-tagged N-WASP- or WAVE2-f.l., - Δ A, -R474E or - Δ CA were combined, supplemented with the purified RPEL domain of MRTF-A (MRTF-A 2-261) and incubated with anti-Flag beads (Fig. IV-6).

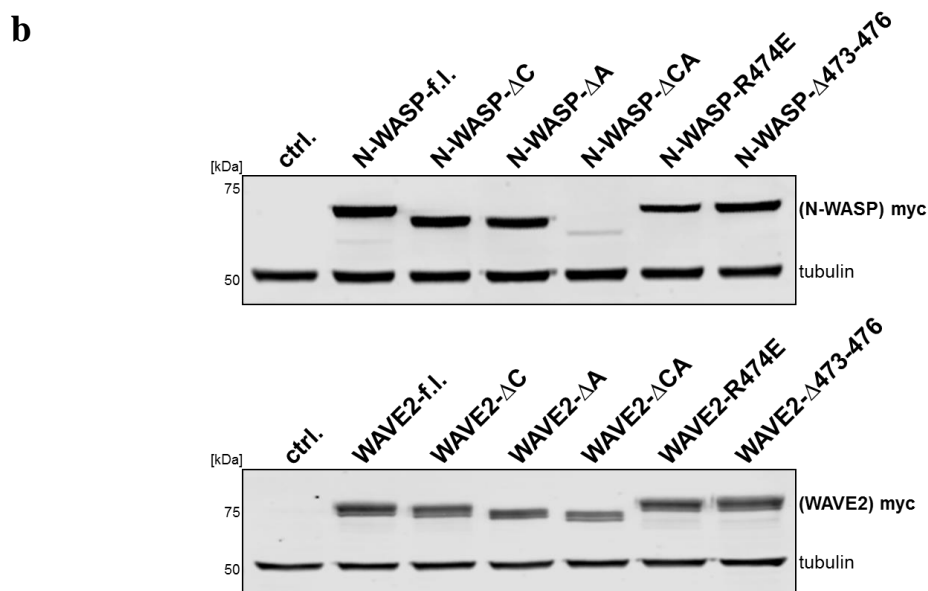
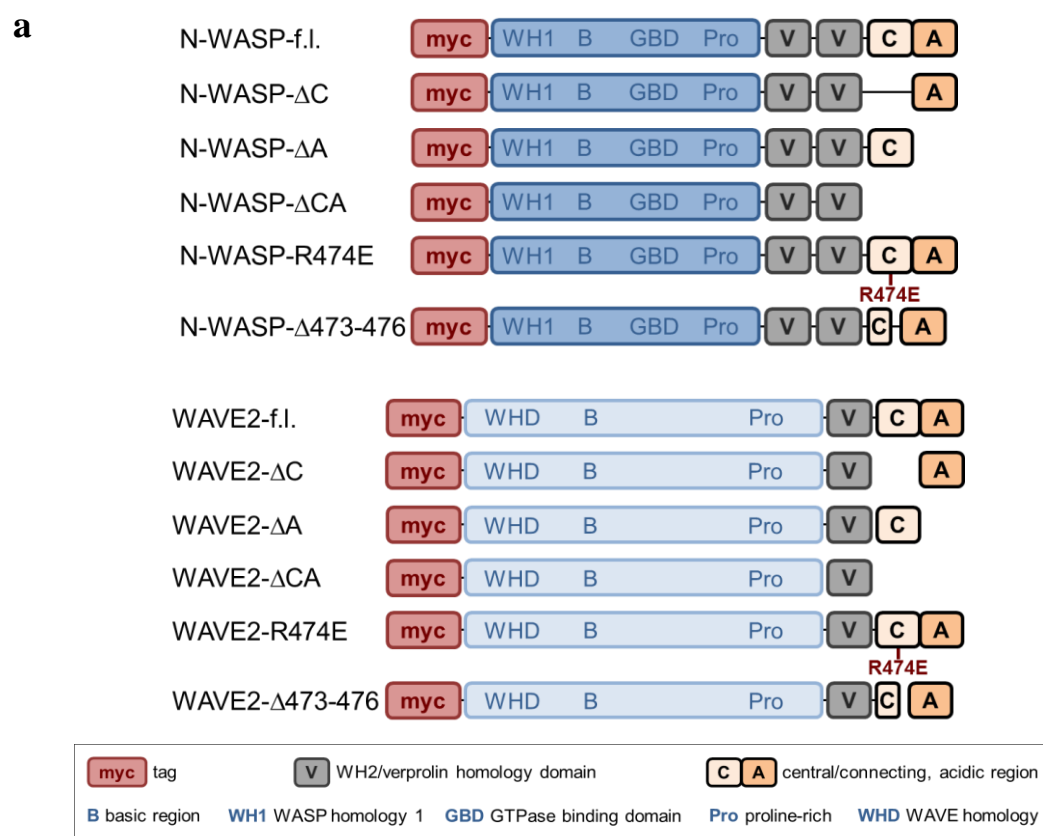


Figure IV-5: Domain topology and protein expression of truncated, myc-tagged N-WASP and WAVE2 constructs. NIH 3T3 cells were transiently transfected with the indicated constructs and analyzed for the expression level. **a** Schematics of myc-tagged N-WASP and WAVE2 constructs and domain topology. **b** Analysis of protein expression levels and protein size of the indicated constructs using tag-specific antibody. Equal loading was controlled by tubulin.

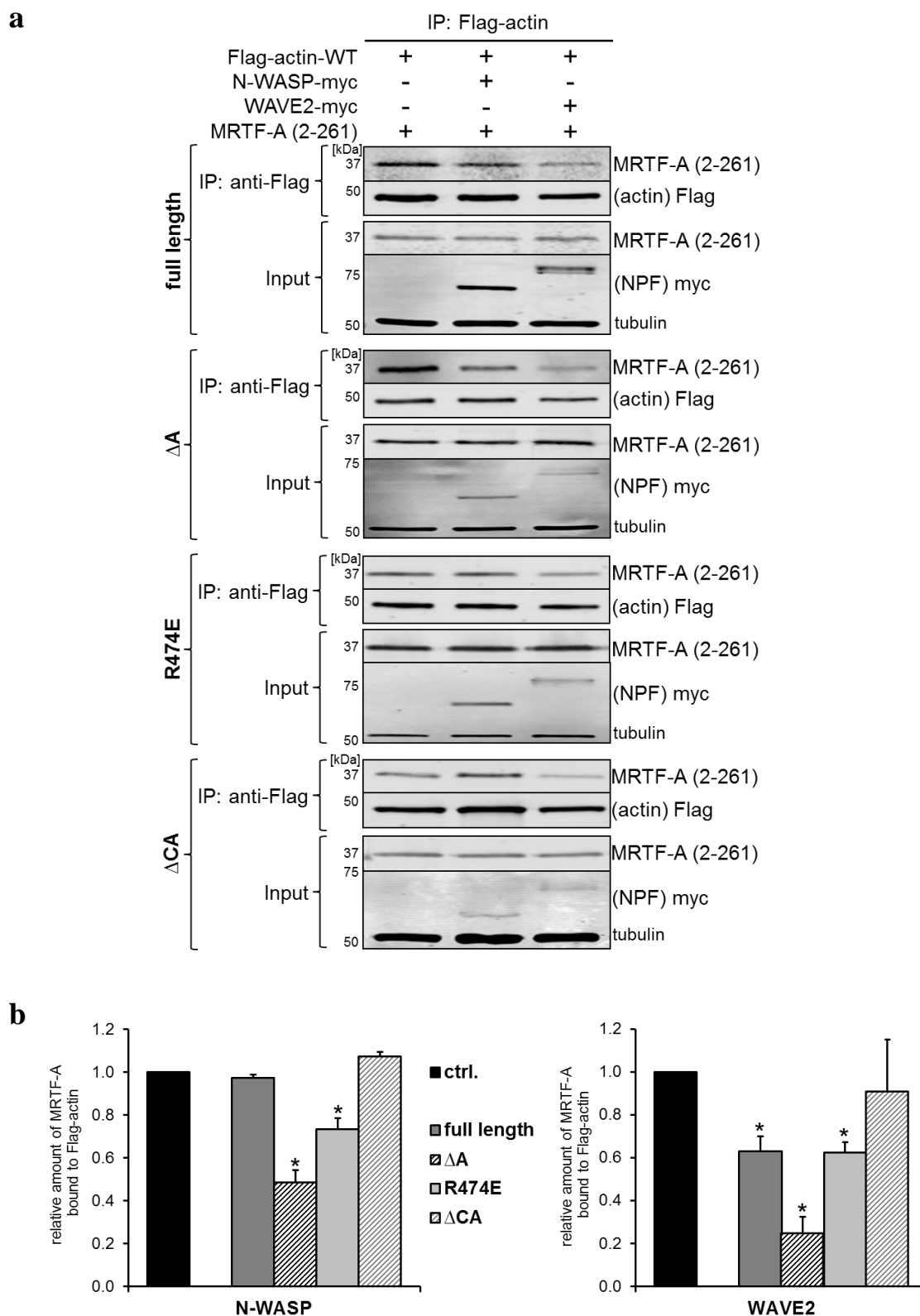


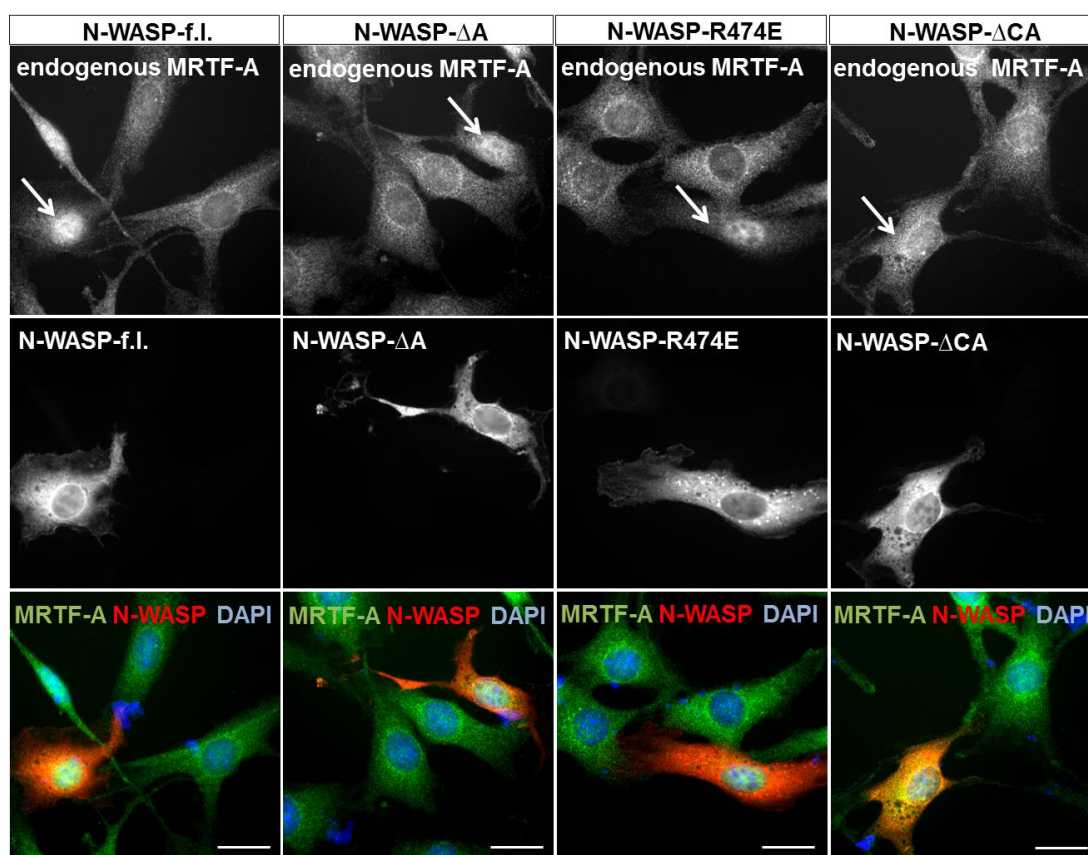
Figure IV-6: WH2 (V)-containing N-WASP and WAVE2 compete with MRTF-A for actin-binding independently of the CA region. **a** Flag-actin-WT together with full length N-WASP, WAVE2 or their indicated mutants was transiently co-expressed in serum-starved NIH 3T3 cells. For anti-Flag co-immunoprecipitation lysates were mixed with purified MRTF-A (2-261). Precipitated proteins were analyzed using anti-MRTF-A and anti-Flag antibody. **b** Quantification of the amount of MRTF-A (2-261) bound to precipitated Flag-actin in presence of N-WASP or WAVE2 constructs. Data were normalized to the control without NPF co-expression (ctrl.) which was set to 1. Error bars, s.e.m., n = 3 (* $p \leq 0.05$, ** $p \leq 0.01$, *** $p \leq 0.001$ according to an unpaired one sample student's t-test).

By western blot analysis, it could be demonstrated that the presence of full length N-WASP and WAVE2 both reduced the amount of MRTF-A (2-261) bound to precipitated actin in comparison to the control without NPF (Fig. IV-6 a). Quantification of three independent experiments showed that full length WAVE2 significantly reduced actin-MRTF-A binding whereas full length N-WASP did not (Fig. IV-6 b). Expression of ARP2/3-deficient N-WASP- or WAVE2- Δ A and -R474E efficiently reduced MRTF-A binding to Flag-actin. In contrast, N-WASP- Δ CA and WAVE2- Δ CA both failed to dissociate actin:MRTF complexes (Fig. IV-6 a, b). Because of that, the major effects of full length NPF in this experimental context seemed to be mediated by the central acidic (CA) region.

IV.2.4 N-WASP and WAVE2 induce MRTF-A Nuclear Accumulation and Target Gene Expression independently of ARP2/3-mediated Actin Polymerization

The dissociation of inhibitory actin:MRTF complexes leads to the translocation of MRTF-A into the nucleus which induces MRTF-SRF-mediated transcriptional activity. Therefore, WH2-containing full length and ARP2/3-deficient N-WASP and WAVE2 should be analyzed for nuclear accumulated MRTF-A via immunofluorescence. Following transient transfection cells were fixed and immuno-stained for subcellular localization of endogenous MRTF-A and myc-tagged NPF (Fig. IV-7, -8). Overexpression of N-WASP-f.l., - Δ A and -R474E significantly induced nuclear translocation of endogenous MRTF-A under serum-starved conditions (Fig. IV-7, first to third column). In contrast, expression of N-WASP- Δ CA displayed MRTF-A in the cytoplasm which is similar to serum-starved non-transfected control cells (ctrl.) (Fig. IV-4 a, -7, last column). However, quantification of three independent experiments offered 20% more cells with nuclear accumulated MRTF-A upon N-WASP- Δ CA expression compared with the control (Fig. IV-7 b). Expression of WAVE2-f.l., - Δ A or -R474E also significantly induced nuclear accumulation of endogenous MRTF-A (Fig. IV-8, first to third column). Whereas just slightly depicted by the immunofluorescence, quantification of WAVE2- Δ CA expressing cells of three independent experiments showed 30% more cells with nuclear accumulated MRTF-A in comparison to serum-starved non-transfected control cells (ctrl.) (Fig. IV-9 b).

a



b

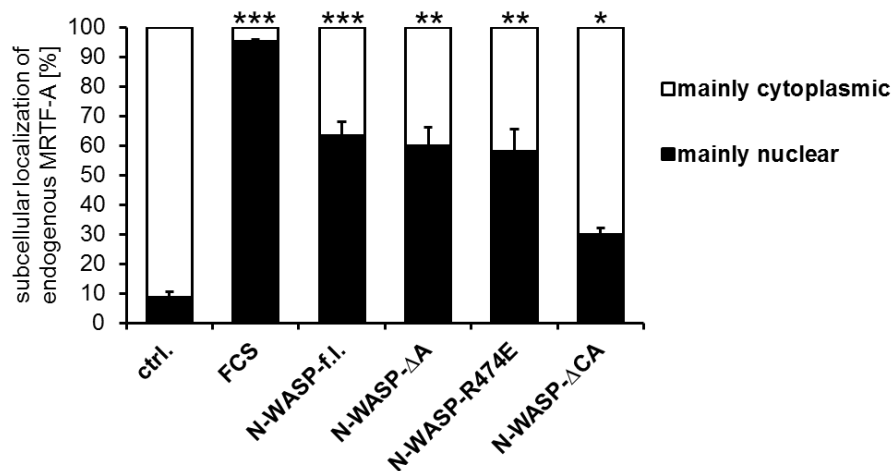
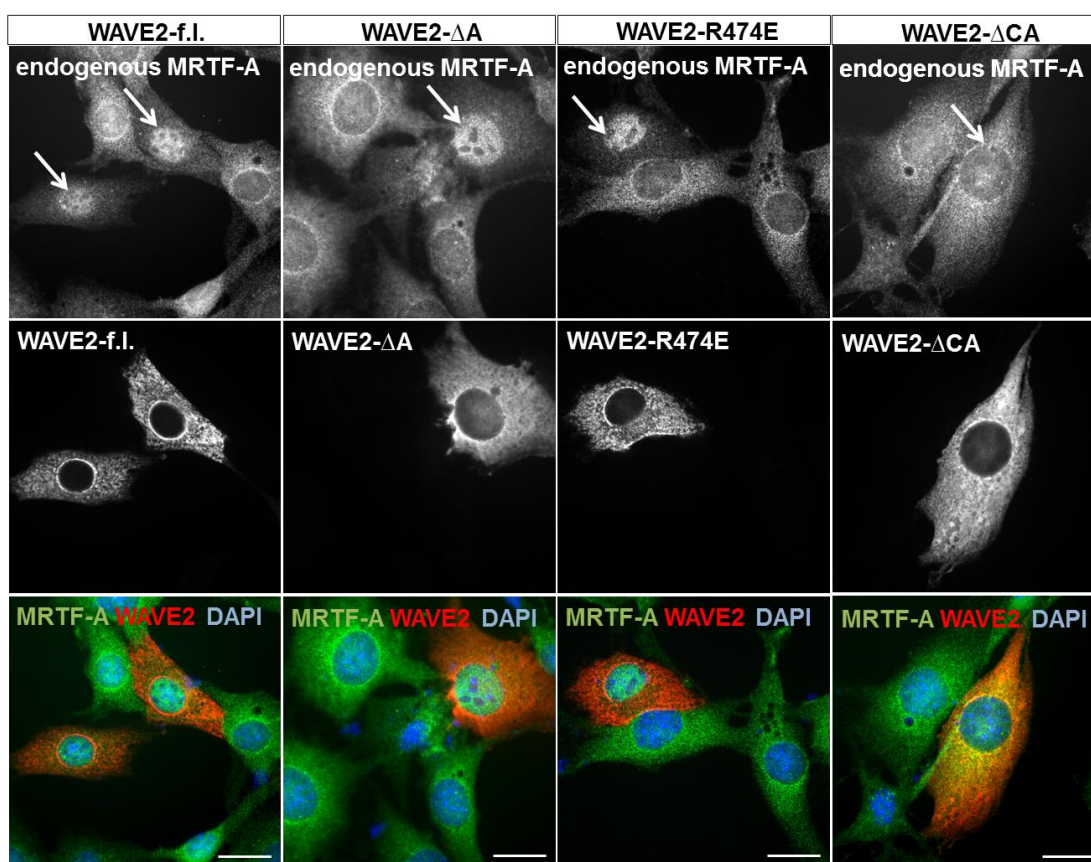


Figure IV-7: N-WASP induces nuclear accumulation of MRTF-A independently of the CA region.

a Serum-starved NIH 3T3 cells were transiently transfected with the indicated myc-tagged N-WASP constructs, fixed, counterstained with DAPI (blue) and stained with anti-myc and anti-MRTF-A antibody. Localization of myc-expressing cells (red) and subcellular localization of endogenous MRTF-A (green) were analyzed by epifluorescence microscopy. **b** Quantification of MRTF-A localization by counting 50 myc-positive cells each. Cells expressing the vector control (ctrl.) and serum-stimulation for 1 hour (FCS) were as control. Arrows indicate myc-expressing cells. Scale bars, 20 μ m. Error bars, s.e.m., $n = 3$ (* $p \leq 0.05$, ** $p \leq 0.01$, *** $p \leq 0.001$ according to an unpaired two sample student's t-test).

a



b

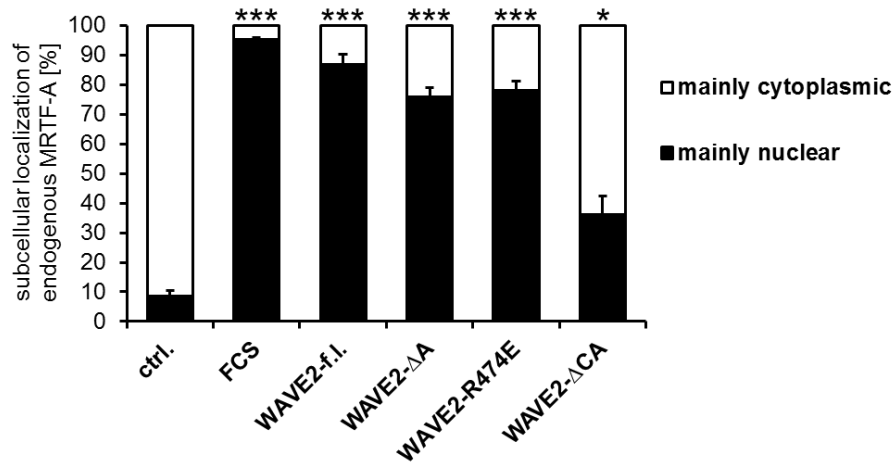


Figure IV-8: WAVE2 induces nuclear accumulation of MRTF-A independently of the CA region.
a Serum-starved NIH 3T3 cells were transiently transfected with the indicated myc-tagged WAVE2 constructs, fixed, counterstained with DAPI (blue) and stained with anti-myc and anti-MRTF-A antibody. Localization of myc-expressing cells (red) and subcellular localization of endogenous MRTF-A (green) were analyzed by epifluorescence microscopy. **b** Quantification of MRTF-A localization by counting 50 myc-positive cells each. Cells expressing the vector control (ctrl.) and serum-stimulation for 1 hour (FCS) were as control. Arrows indicate myc-expressing cells. Scale bars, 20 μ m. Error bars, s.e.m., n = 3 (* $p \leq 0.05$, ** $p \leq 0.01$, *** $p \leq 0.001$ according to an unpaired two sample student's t-test).

The ability of N-WASP and WAVE2 to efficiently induce translocation of MRTF-A into the nucleus directly through their WH2 domains was confirmed by the absence of induced actin polymerization (Fig. IV-10, -11). Transiently transfected NIH 3T3 cells were analyzed for phalloidin-positive actin filaments via immunofluorescence (Fig. IV-10 a, -11 a) and for the level of total cellular F-actin via cell fractionation (Fig. IV-10 b, -11 b). Expression of full length N-WASP as well as ARP2/3 deficient ΔA , -R474E and ΔCA did not induce increased formation of actin stress fibers compared to serum-starved non-transfected control cells (ctrl.) (Fig. IV-9, -10 a). However, measuring the amount of cellular G- and F-actin revealed comparable F-actin levels when cells are either stimulated with serum (FCS) or transfected with the indicated N-WASP constructs. But, the total amount of G-actin was still higher than the F-actin level and the results were not significant (Fig. IV-10 b). WAVE2-f.l., ΔA , -R474E and ΔCA also showed no altered phalloidin-staining (Fig. IV-11 a). The amount of cellular F-actin was higher in response to WAVE2 overexpression compared to serum-stimulation (FCS), but the stimulation itself was not sufficient due to a higher F-actin amount in non-treated control cells (ctrl.) (Fig. IV-11 b). In general, the experimental setup of cell fractionation did not deliver significant results and did not correlate with the immunofluorescence studies. However, the absence of any obvious alteration of the actin cytoskeleton, especially upon expression of N-WASP- ΔA and WAVE2- ΔA , together with the efficient MRTF-A nuclear translocation (Fig. IV-7, -8) indicates a direct impact of WH2-containing NPF on actin:MRTF-A complexes independently of ARP2/3-NPF-mediated actin polymerization.

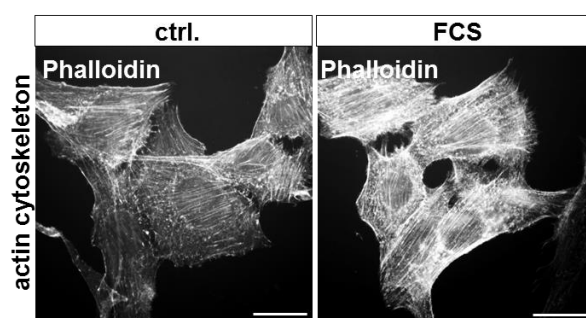
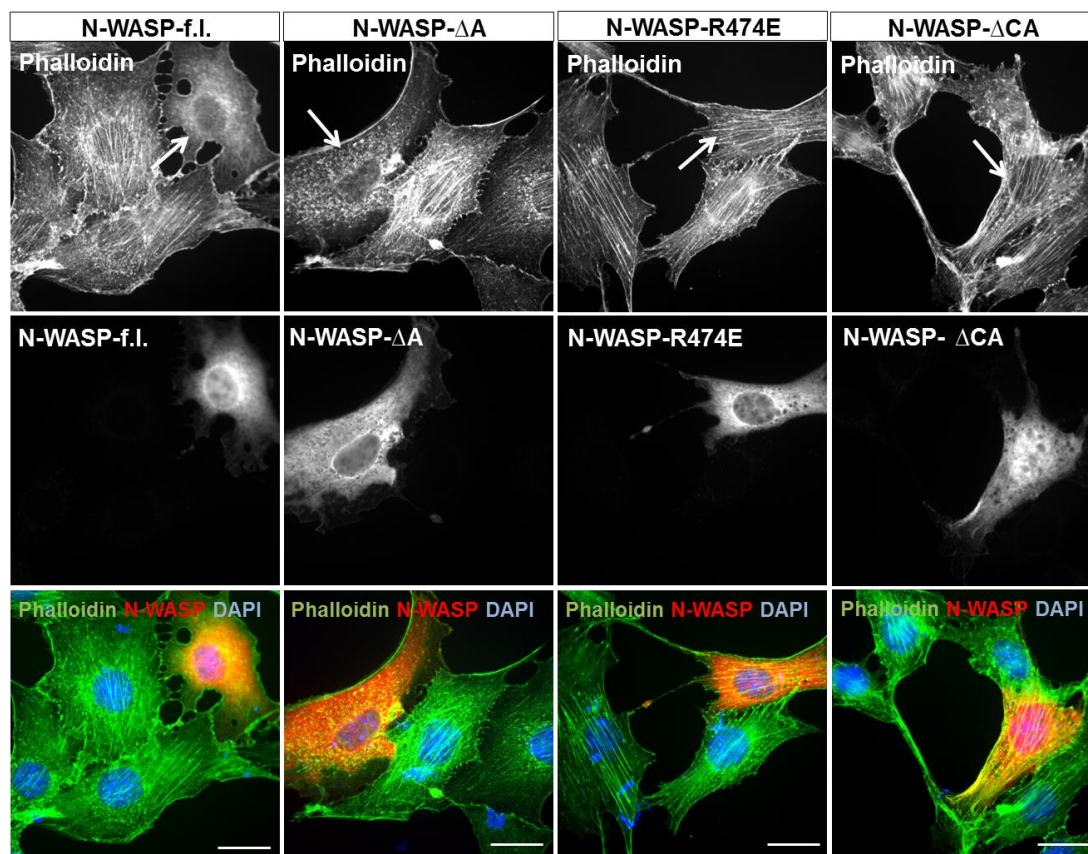


Figure IV-9: Actin stress fiber formation in NIH 3T3 mouse fibroblasts. NIH 3T3 cells were cultivated under starved conditions (ctrl.) or serum stimulated for 1 hour (FCS), fixed and stained with phalloidin to visualize the F-actin cytoskeleton. Serum-stimulation induced enhanced stress fiber formation in comparison to the starved control.

a



b

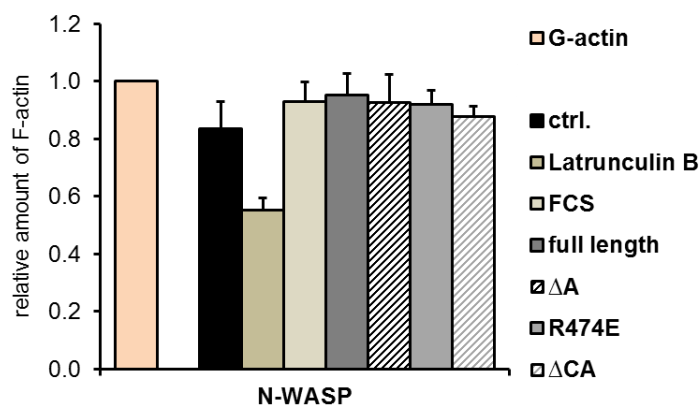


Figure IV-10: N-WASP does not induce enhanced polymerization of the actin cytoskeleton. Serum-starved NIH 3T3 cells were transiently transfected with the indicated myc-tagged N-WASP constructs and analyzed for the actin cytoskeleton by epifluorescence microscopy. **a** Transfected cells were fixed, counterstained with DAPI (blue) and immune-stained with anti-myc antibody for the localization of myc-expressing cells (red) and phalloidin (green) to visualize F-actin. **b** Quantification of G-/F-actin fractionations via ultracentrifugation. F-actin levels were normalized to G-actin which was set to 1. Non-transfected, non-treated cells (ctrl.) and treatment with 1 μ M Latrunculin B or 15% serum (FCS) for 1 hour were as controls. *Arrows* indicate myc-expressing cells. *Scale bars*, 20 μ m. *Error bars*, s.e.m., n = 3 (* $p \leq 0.05$, ** $p \leq 0.01$, *** $p \leq 0.001$ according to an unpaired two sample student's t-test).

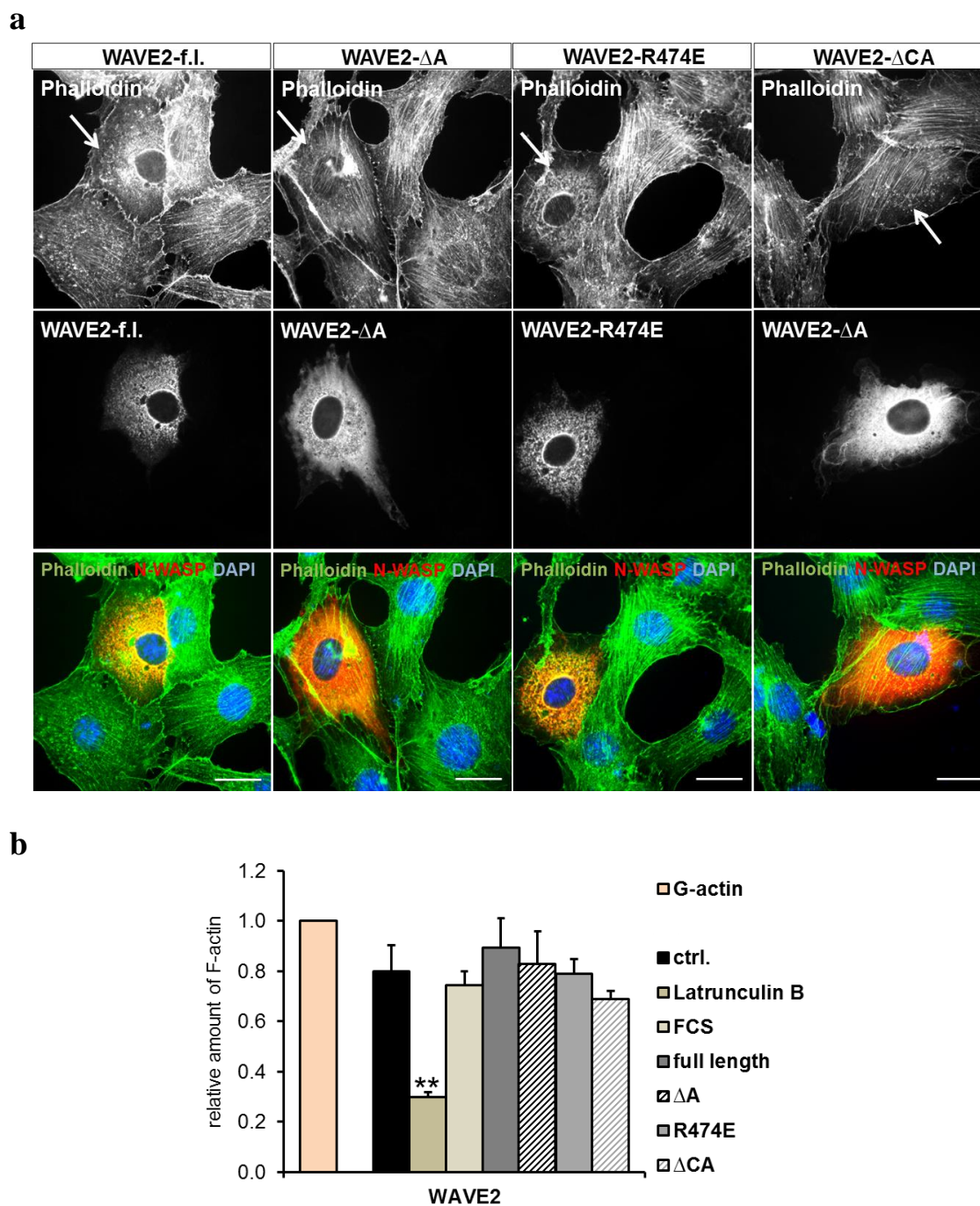


Figure IV-11: WAVE2 does not induce enhanced polymerization of the actin cytoskeleton. Serum-starved NIH 3T3 cells were transiently transfected with the indicated myc-tagged WAVE2 constructs and analyzed for the actin cytoskeleton by epifluorescence microscopy. **a** Transfected cells were fixed, counterstained with DAPI (blue) and immune-stained with anti-myc antibody for the localization of myc-expressing cells (red) and phalloidin (green) to visualize F-actin. **b** Quantification of G-/F-actin fractionations via ultracentrifugation. F-actin levels were normalized to G-actin which was set to 1. Non-transfected, non-treated cells (ctrl.) and treatment with 1 μ M Latrunculin B or 15% serum (FCS) for 1 hour were as controls. *Arrows* indicate myc-expressing cells. *Scale bars*, 20 μ m. *Error bars*, s.e.m., n = 3 (* $p \leq 0.05$, ** $p \leq 0.01$, *** $p \leq 0.001$ according to an unpaired two sample student's t-test).

Beside disruption of inhibitory actin:MRTF complexes and nuclear accumulation of MRTF-A, activation of the MRTF-SRF transcription module by ARP2/3 deficient WH2-containing NPF was investigated performing SRF reporter assay and quantitative RT-PCR (Fig. IV-12). Expression of N-WASP and WAVE2 significantly activated the MRTF-SRF reporter plasmid and SRF target gene transcription despite impaired ARP2/3 interaction. N-WASP- Δ A and -R474E (Fig. IV-12 a) as well as WAVE2- Δ A and -R474E (Fig. IV-12 b) considerably induced SRF activity. Induction by WAVE2- Δ A and -R474E was as sufficient as induction by full length WAVE2. In contrast, SRF activation by N-WASP- Δ A or -R474E are generally low. According to previous results, N-WASP- Δ CA and WAVE2- Δ CA both failed to considerably activate the MRTF-SRF reporter. Analysis of the mRNA expression of the main SRF target genes *smooth muscle actin (Acta2)*, *vinculin (Vcl)* and *integrin α 5 (Itga5)* showed increased induction of *Acta2* mRNA level upon expression of full length N-WASP or WAVE2 compared with serum-starved non-transfected control cells (dotted line) (Fig. IV-12 c, d). Expression of the ARP2/3 deficient mutants did not sufficiently induce target gene transcription. However, SRF reporter activity was considerably induced by N-WASP- Δ A and WAVE2- Δ A which reveals a capability of N-WASP and WAVE2 to trigger MRTF-SRF activity despite lacking a functional ARP2/3 activating central acidic region.

To further distinguish a WH2 domain-mediated and an ARP2/3-mediated impact on MRTF-A activation, the SRF reporter assay was performed under ARP2/3-inhibiting conditions using ARP3-specific siRNA, the chemical ARP2/3 inhibitor CK-666 or the cytoskeletal drug Latrunculin B (Fig. IV-13, -15, -16). Transient transfection of NIH 3T3 cells with ARP3 siRNA reduced the endogenous ARP3 protein level to 40% (Fig. IV-13 b). Immunofluorescence analysis showed that treatment with the ARP2/3 inhibitor CK-666 efficiently blocked ARP3 distribution on cell edges which was also observed upon ARP3 siRNA transfection (Fig. IV-14). N-WASP and WAVE2 still induced the SRF reporter plasmid more than 10-fold compared with serum-starved control cells (ctrl.) despite siRNA-mediated ARP3 depletion (Fig. IV-13 a) or inhibition by CK-666 (Fig. IV-15). Interestingly, serum-induced (FCS) MRTF-SRF activity was also marginal decreased by ARP3 knockdown or inhibition (Fig. IV-13, -15).

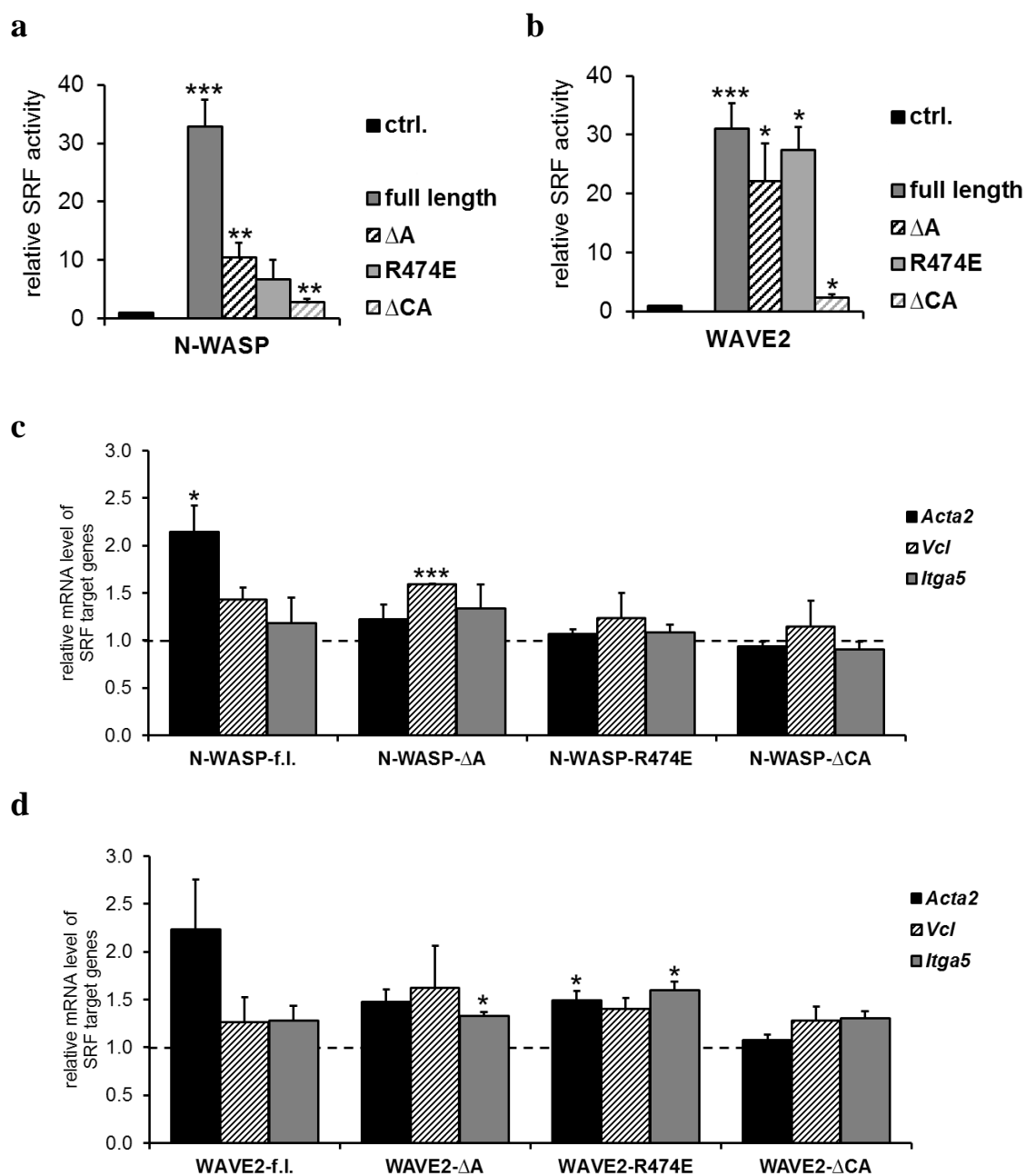


Figure IV-12: N-WASP and WAVE2 activate MRTF-SRF-dependent gene expression independently of the CA region. Serum-starved NIH 3T3 cells were transiently transfected with the indicated constructs and analyzed for SRF target gene expression. **a-b** Relative MRTF-SRF luciferase reporter activity upon co-transfection with truncated NPF constructs. All data were normalized to the non-transfected, serum-starved control (ctrl.), which was set to 1. **a** Expression of myc-tagged N-WASP variants increased SRF reporter activity in comparison to the control. **b** Cells, expressing myc-tagged WAVE2 variants, showed strong induction of SRF reporter activity. **c-d** Endogenous mRNA expression of the SRF target genes smooth muscle α -actin (*Acta2*), vinculin (*Vcl*) and integrin $\alpha 5$ (*Itga5*) upon transient transfection of the indicated constructs. All data were normalized to the non-transfected, serum-starved control (dotted line), which was set to 1. **c** Endogenous expression of *Acta2*, *Vcl* and *Itga5* upon expression of myc-tagged N-WASP variants. **d** Endogenous expression of *Acta2*, *Vcl* and *Itga5* upon expression of myc-tagged WAVE2 variants. Error bars, s.e.m., n = 3 (* p \leq 0.05, ** p \leq 0.01, *** p \leq 0.001 according to an unpaired one sample student's t-test).

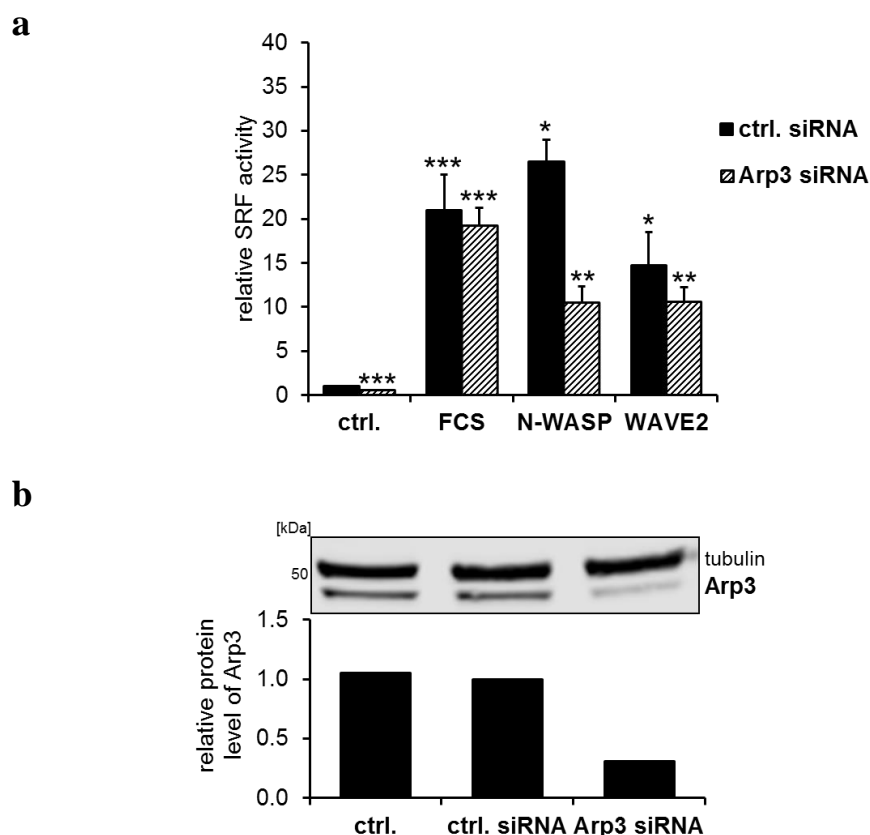


Figure IV-13: N-WASP and WAVE2 induce MRTF-SRF activity despite siRNA-mediated ARP3 knockdown. **a** NIH 3T3 cells were transiently transfected with the indicated siRNAs for 24 hours following starvation and co-transfection with reporter plasmids and the indicated NPF. Transfection without NPF (ctrl.) and serum-stimulation for 7 hours (FCS) were as controls. Overexpression of full length N-WASP and WAVE2 induce SRF activity independently of the ARP2/3 complex. **b** Validation of ARP3 knockdown efficiency by western blot analysis. Cells were transiently transfected with the indicated siRNA and analyzed for endogenous ARP3 protein level by anti-ARP3 antibody. Equal loading was controlled by tubulin. Non-transfected cells (ctrl.) were as control. All data were normalized to the control which was set to 1. *Error bars*, s.e.m., $n = 3$ (* $p \leq 0.05$, ** $p \leq 0.01$, *** $p \leq 0.001$ according to an unpaired one sample student's t-test).

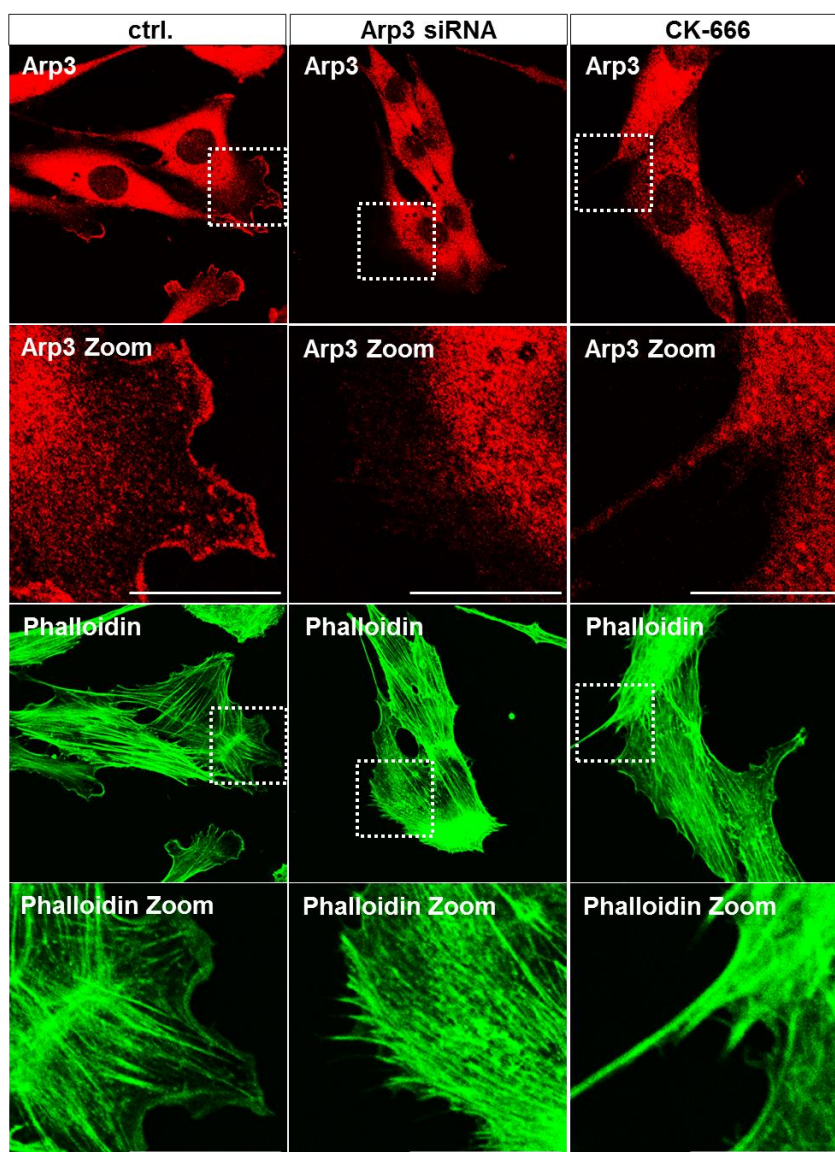


Figure IV-14: Validation of siRNA-mediated ARP3 knockdown efficiency and CK-666-mediated ARP2/3 inhibition by immunofluorescence. NIH 3T3 cells were either transfected with ARP3-specific siRNA or treated with 100 μ M CK-666 for 7 hours, fixed, immune-stained with anti-ARP3 antibody and phalloidin and analyzed by confocal microscopy. Anti-ARP3 (red) was for localization of endogenous ARP3 and phalloidin (green) to visualize F-actin cytoskeleton. ARP3 siRNA and CK-666 reduced localization of endogenous ARP3 at the cell edges. Untreated cells (ctrl.) were as control. *Scale bars*, 20 μ m.

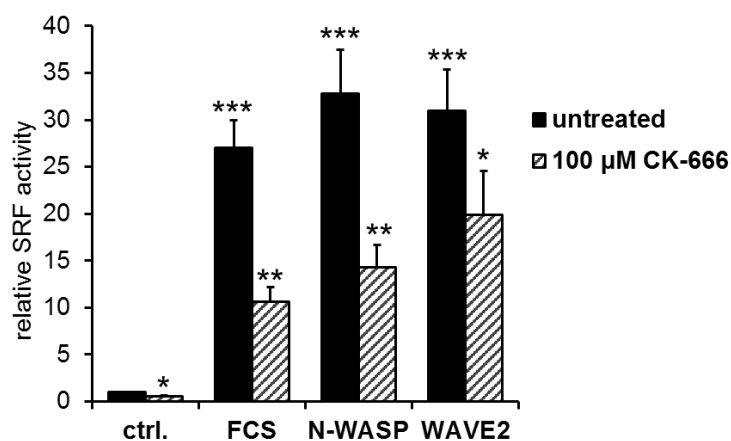


Figure IV-15: N-WASP and WAVE2 induce MRTF-SRF activity despite CK-666-mediated ARP2/3 inhibition. Serum-starved NIH 3T3 cells were co-transfection with reporter plasmids and the indicated NPF following treatment with 100 μ M CK-666 for 7 hours. Transfection with vector control (ctrl.) and serum-stimulation for 7 hours (FCS) were as controls. Overexpression of full length N-WASP and WAVE2 induced SRF activity independently of the ARP2/3 complex. All data were normalized to the control which was set to 1. Error bars, s.e.m., n = 3 (* $p \leq 0.05$, ** $p \leq 0.01$, *** $p \leq 0.001$ according to an unpaired one sample student's t-test).

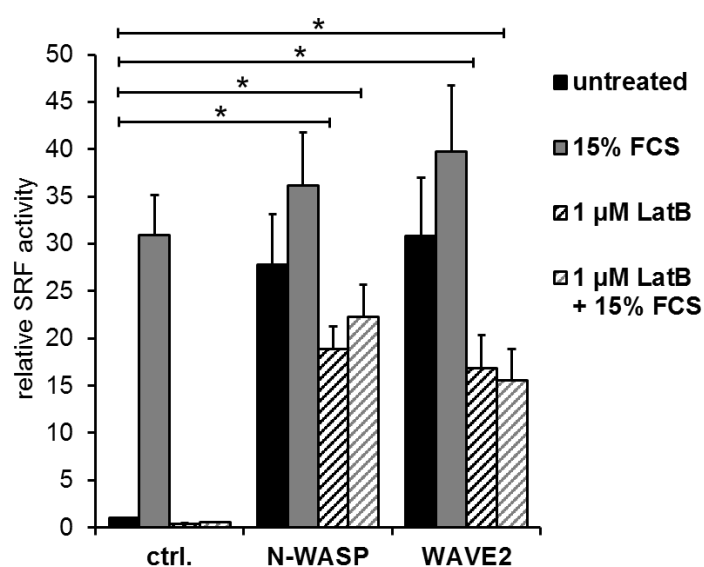


Figure IV-16: N-WASP and WAVE2 induce MRTF-SRF activity despite Latrunculin B treatment. Serum-starved NIH 3T3 cells were co-transfected with reporter plasmids and the indicated NPF following serum-stimulation, treatment with 1 μ M Latrunculin B or both for 7 hours. Overexpression of full length N-WASP and WAVE2 induced SRF activity despite Latrunculin B treatment. All data were normalized to the untreated control which was set to 1. Error bars, s.e.m., n = 3 (* $p \leq 0.05$, ** $p \leq 0.01$, *** $p \leq 0.001$ according to an unpaired one sample student's t-test).

Thus, the results demonstrated MRTF-SRF activation by serum or WH2-containing N-WASP or WAVE2 which is partially independent of ARP2/3 and ARP2/3-mediated actin polymerization.

The cytoskeleton drug Latrunculin B de-polymerizes actin filaments thereby strongly increasing the cellular G-actin pool. Hence, Latrunculin B treatment completely blocked serum-induced SRF reporter activation (FCS) (Fig. IV-16). In contrast, Latrunculin failed to abolish MRTF-SRF induction upon overexpression of N-WASP or WAVE2. NPF-mediated SRF activation was rather decreased to a remaining level of 15- to 20-fold in presence of the cytoskeleton drug. These results, together with the data from ARP3 knockdown and inhibition by CK-666, confirmed the hypothesis that N-WASP and WAVE2 are able to induce MRTF-A transcriptional activity directly by their WH2 domains and independently of ARP2/3-mediated actin nucleation.

IV.2.5 Serum-stimulated Actin:MRTF-A Complex Disruption is mediated by a *Trans-Acting* Factor

Stimulation of mouse fibroblasts with serum induces dissociation of actin:MRTF-A complexes. The detailed molecular mechanism of complex disruption is still unclear and should be analyzed in an *in vitro* co-immunoprecipitation approach. Thus, the recombinant RPEL domain of MRTF-A, MRTF-A (2-261), was added to the G-actin fractions of either serum-starved (w/o FCS) or serum-stimulated (with FCS), Flag-actin expressing cells. Precipitated Flag-actin was analyzed for the amount of bound MRTF-A (2-261) (Fig. VIII-4). Western blot analysis showed that the binding of MRTF-A to actin from serum-stimulated cells was reduced by 50% compared with binding to actin from serum-starved cells (Fig. IV-17). Therefore, complex dissociation was rather due to an event on the actin molecule than on MRTF because the MRTF-A RPEL domain could not be affected by the serum under this experimental setup (Fig. VIII-4). Moreover, the MRTF-A RPEL motifs seemed to be sufficient for binding to and regulation by actin.

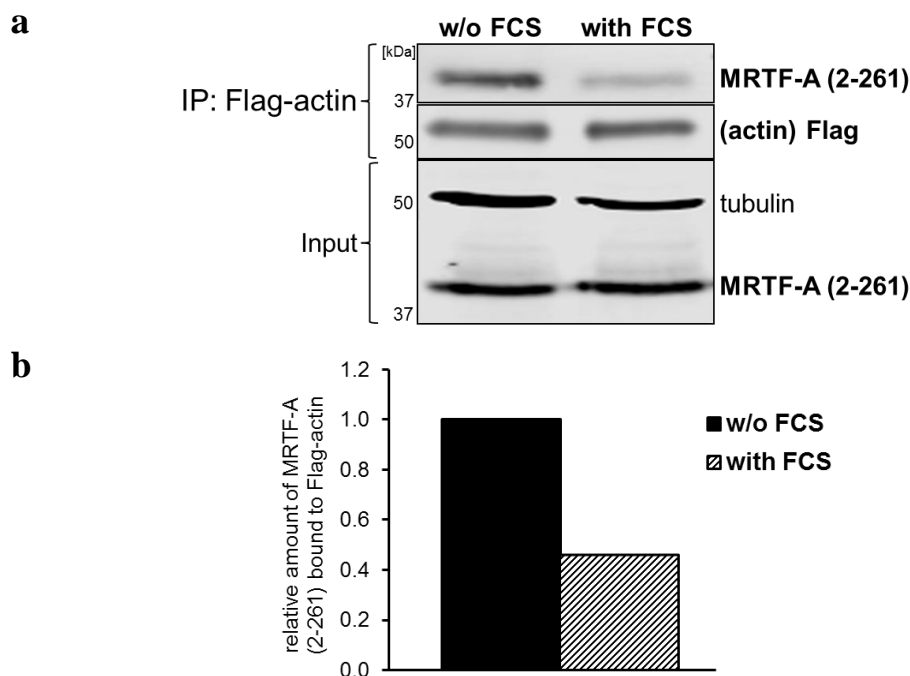


Figure IV-17: Serum-mediated complex dissociation takes effect on actin and not on MRTF-A. **a** Flag-actin-WT was transiently expressed in serum-starved NIH 3T3 cells. As control, cells were serum-stimulated (with FCS) for 1 hour. For anti-Flag co-immunoprecipitation, lysates were mixed with purified MRTF-A (2-261). Precipitated proteins were analyzed using anti-MRTF-A and anti-Flag antibody. **b** Quantification of the amount of MRTF-A (2-261) bound to precipitated Flag-actin. Data were normalized to the control without FCS (w/o FCS) which was set to 1.

To further investigate possible events on the actin molecule leading to reduced MRTF-A association the activity of a transferable factor in response to serum-stimulation was hypothesized. Therefore, recombinant MRTF-A (2-261) was added to ultra-centrifuged lysates from serum-starved Flag-actin expressing cells. Precipitated Flag-actin was analyzed for the amount of bound MRTF-A (2-261) according to the presence of ectopic lysates from either serum-starved or serum-stimulated, non-transfected cells (Fig. VIII-5). Western blot analysis showed that the binding of MRTF-A to actin was reduced by 40% following addition of serum-stimulated cell extract (Fig. IV-18). This pointed towards an inducible factor, present in the lysate of serum-stimulated cells, which affected actin:MRTF-A complexes in trans. The following experiments were performed to identify the predicted *trans*-acting factor in cell extracts.

That dissociation of actin:MRTF-A complexes results from subsequent actin polymerization during the precipitation approach could be excluded using polymerization-deficient Flag-actin-R62D (Fig. IV-19 a). MRTF-A binding to actin R62D was still reduced by 20% following addition of serum-stimulated cell extracts.

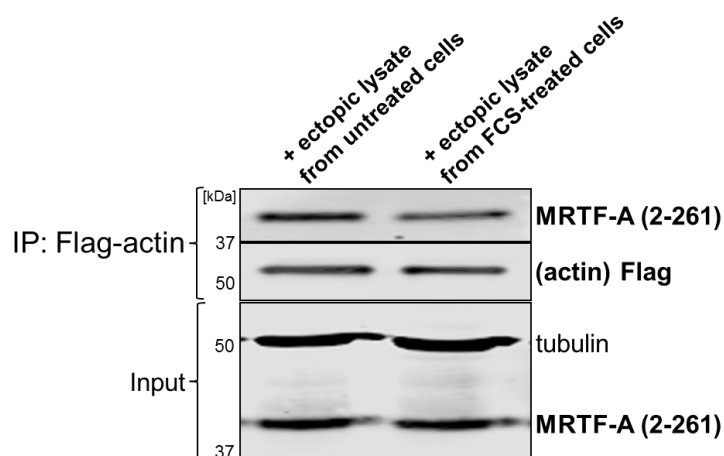
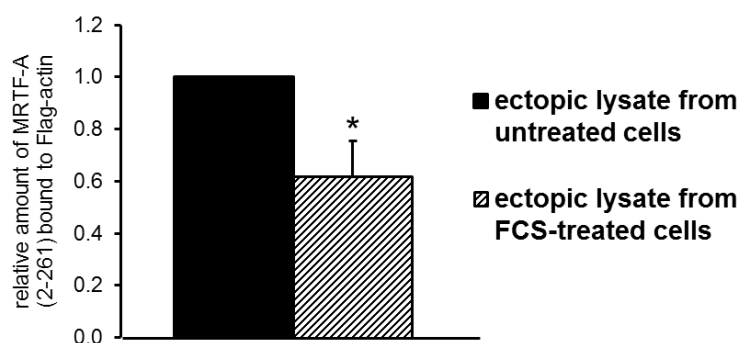
a**b**

Figure IV-18: Complex dissociation in response to serum-stimulation is mediated by a *trans*-acting factor. **a** Flag-actin-WT was transiently expressed in serum-starved NIH 3T3 cells. As control, non-transfected cells were serum-stimulated (with FCS) for 1 hour. Lysates were prepared in G-actin buffer (soluble fraction buffer) following ultracentrifugation. For anti-Flag co-immunoprecipitation, lysates of Flag-actin expressing cells and non-transfected, FCS treated cells were mixed and supplemented with purified MRTF-A (2-261). Precipitated proteins were analyzed using anti-MRTF-A and anti-Flag antibody. **b** Quantification of the amount of MRTF-A (2-261) bound to precipitated Flag-actin. Data were normalized to the non-transfected, untreated control (ectopic lysate from untreated cells) which was set to 1. *Error bars*, s.e.m., $n = 3$ (* $p \leq 0.05$, ** $p \leq 0.01$, *** $p \leq 0.001$ according to an unpaired one sample student's *t*-test).

To define the biochemical character of the predicted *trans*-acting factor a co-immunoprecipitation assay was performed using differentially treated ectopic lysates from serum-stimulated, non-transfected cells. According to the previous experiment (Fig. IV-18), MRTF-A (2-261) was added to ultra-centrifuged lysates from serum-starved Flag-actin expressing cells. Precipitated Flag-actin was analyzed for the amount of bound MRTF-A (2-261) according to the presence of ectopic lysates from serum-stimulated, non-transfected cells which were before boiled for 5 minutes or pre-treated with λ -phosphatase (Fig. IV-19 b). Boiling at 95°C induces denaturation and loss of the biological function of proteins, especially enzymes. Pre-treatment with the λ -phosphatase induces protein de-phosphorylation. The impaired complex formation of

Flag-actin and MRTF-A (2-261) in response to serum-stimulation was not considerably effected by either boiling or de-phosphorylation (Fig. IV-19 b). This refuted the predicted serum-induced factor as phosphatase or phosphorylation-dependent as well as a heat-sensitive protein with enzymatic activity. However, the nature of the *trans*-acting factor could not be demonstrated by these results because complex disruption following serum-stimulation was low and not significant for Flag-actin-R62D as well as pre-treated ectopic lysates (Fig. IV-19 a, b).

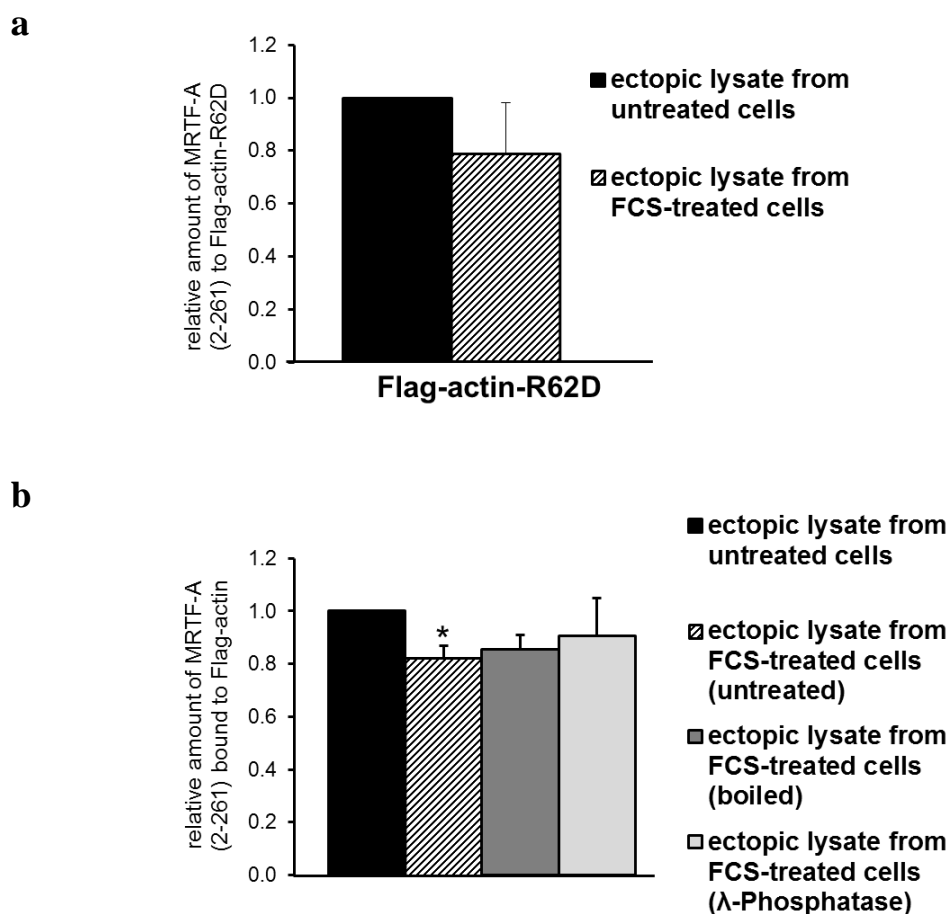


Figure IV-19: Identification of the serum-mediated *trans*-acting factor. a-b Quantification of the amount of MRTF-A (2-261) bound to precipitated Flag-actin. Ultra-centrifuged supernatants (100.000 x g) were prepared in G-actin buffer (soluble fraction buffer) following supplementation of purified MRTF-A (2-261) and anti-Flag co-immunoprecipitation. Precipitated proteins were analyzed using anti-MRTF-A and anti-Flag antibody. **a** Flag-actin-R62D was expressed in serum-starved NIH 3T3 cells. As control, cells were serum-stimulated (with FCS) for 1 hour. **b** Flag-actin-WT was expressed in serum-starved NIH 3T3 cells (ctrl.). 24 hours post transfection cells were serum-stimulated (FCS) for 1 hour. Following ultracentrifugation, lysates of FCS treated cells were either boiled for 5 minutes (boiled) or supplemented with protein phosphatase (λ -Phosphatase) for 1 hour. All data were normalized to the control (w/o FCS/ctrl.) which was set to 1. Error bars, s.e.m., n = 3 (* p \leq 0.05, ** p \leq 0.01, *** p \leq 0.001 according to an unpaired one sample student's t-test).

IV.3 WH2 (V) Domain-containing JMY

IV.3.1 Full length JMY has a slight Impact on MRTF Activation and Nuclear Translocation

MRTF-A activation upon actin:MRTF-A complex disruption cannot be explained by a simple alteration of available G-actin. Much more likely, MRTF-SRF transcriptional activity can be induced by mutually exclusive actin-binding of WH2 (V) domain-containing nucleation promoting factors (NPF) with MRTF-A. Beside N-WASP and WAVE2, JMY is another representative WH2 domain NPF and therefore an attractive candidate to play a role on actin:MRTF complexes.

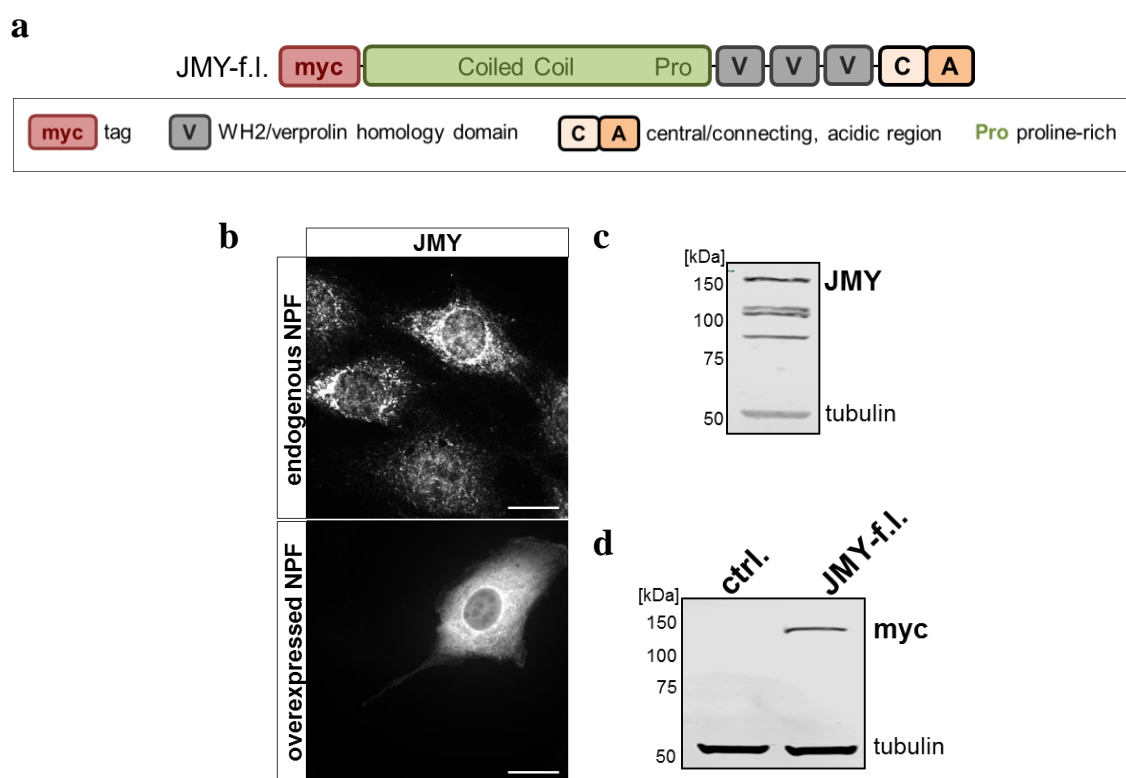


Figure IV-20: Expression and localization of murine JMY in NIH 3T3 mouse fibroblasts. NIH 3T3 cells were analyzed for expression and localization of endogenous JMY and overexpressed myc-tagged JMY following transient transfection. **a** Schematics of myc-tagged JMY-full length and domain topology. **b** Non-transfected cells (endogenous NPF) and cells transiently transfected with myc-tagged JMY (overexpressed NPF) were fixed and immune-stained with JMY- or myc-antibody and analyzed by epifluorescence microscopy. **c-d** Western blot analysis of endogenous and overexpressed JMY. Equal loading was controlled by tubulin. **c** Endogenous expression in NIH 3T3 cells using JMY-specific antibody. **d** Expression of myc-tagged JMY using tag-specific antibody. Scale bars, 20 μ m.

JMY is endogenously present in mouse fibroblasts (Fig. IV-20 b, c). However, all assays were performed as overexpression analysis. Therefore, full length JMY was fused to myc-tag and transiently expressed in NIH 3T3 cells. The correct subcellular localization, protein size and expression level was verified by immunofluorescence and western blot analysis (Fig. IV-20). Transient transfection showed JMY predominantly located to the cytoplasm and to some extent inside the nucleus, which was similar to the distribution of endogenous JMY (Fig. IV-20 b).

Activity of MRTF-A and the MRTF-SRF transcription module mediated by WH2-containing JMY was investigated performing a luciferase-based SRF reporter assay and quantitative RT-PCR of the main SRF target gene *smooth muscle actin* (*Acta2*) (Fig. IV-21). Overexpression of myc-tagged JMY slightly activated the MRTF-SRF reporter compared with serum-starved control cells (ctrl.) (Fig. IV-21 a). In addition, endogenous mRNA expression of *Acta2* was increased around 1.6-fold (Fig. IV-21 b). Thus, the results revealed just a minor impact of WH2-containing JMY on MRTF-SRF-dependent gene expression.

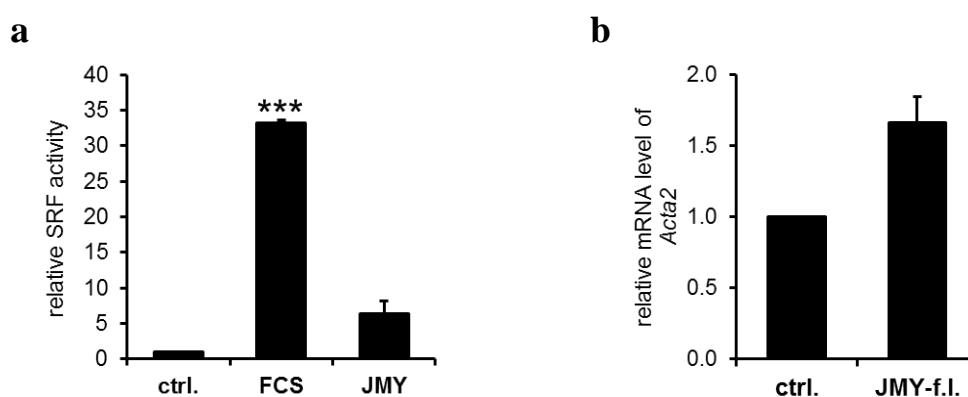
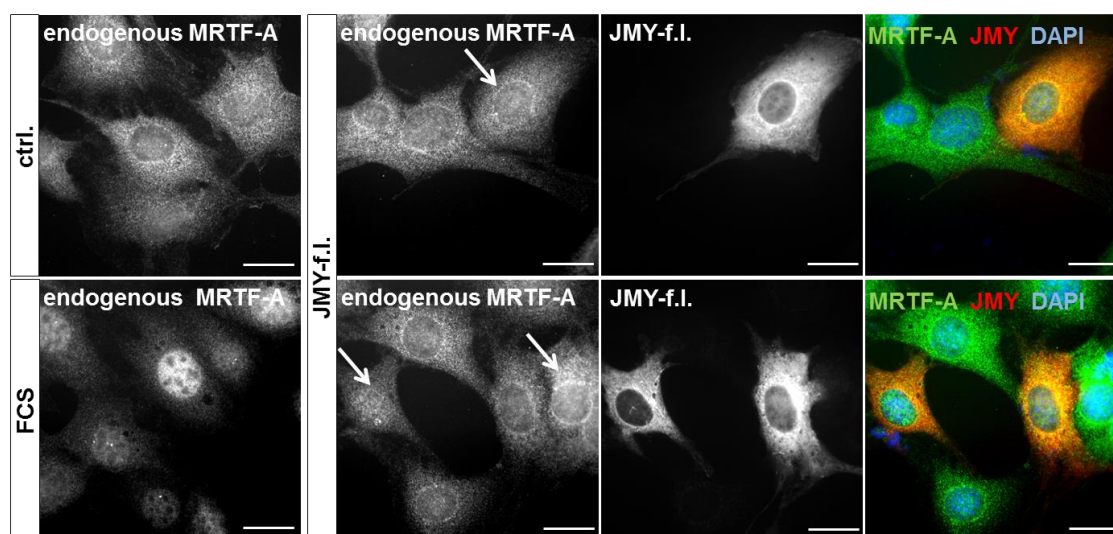


Figure IV-21: WH2 (V) domain-containing JMY activates MRTF-SRF-dependent target gene transcription. NIH 3T3 cells were transiently transfected with full length JMY, serum-starved for 24 hours and analyzed for SRF target gene expression. **a** Relative MRTF-SRF luciferase reporter activity was slightly increased upon co-transfection with full length JMY. As control, cells transfected with vector control (ctrl.) were stimulated for 7 hours with 15% serum (FCS). **b** Endogenous mRNA expression of smooth muscle α -actin (*Acta2*) upon transient transfection of full length JMY in comparison to the serum-starved control (ctrl.). All data were normalized to the starvation control which was set to 1. *Error bars*, s.e.m., n = 3 (* $p \leq 0.05$, ** $p \leq 0.01$, *** $p \leq 0.001$ according to an unpaired one sample student's t-test).

Transcriptional activity of MRTF-A correlates with its nuclear translocation. Thus, subcellular localization of MRTF-A in response to JMY expression was investigated by immunofluorescence (Fig. IV-22). Following transient transfection of myc-tagged JMY cells were immune-stained for endogenous MRTF-A (Fig. IV-22 a). In non-stimulated cells (ctrl.) MRTF-A was predominantly located in the cytoplasm. Translocation into the nucleus was induced by serum-stimulation (FCS). Under serum-starved conditions, overexpression of JMY led to nuclear accumulation of endogenous MRTF-A in 30% of transfected cells (Fig. IV-22 a, b) which is comparable to the induction of the MRTF-SRF reporter plasmid (Fig. IV-21 a).

a



b

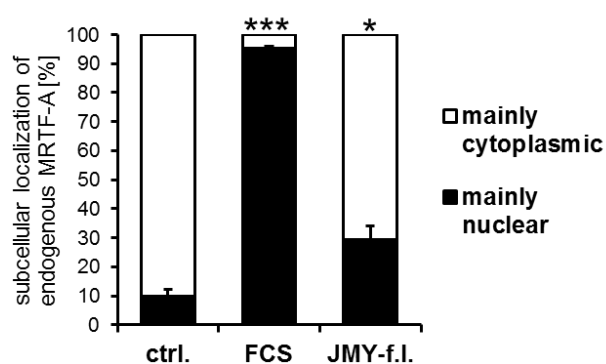


Figure IV-22: Overexpression of full length JMY has a weak impact on nuclear accumulation of MRTF-A. **a** Serum-starved NIH 3T3 cells were transiently transfected with myc-tagged JMY, fixed, counterstained with DAPI (blue), immune-stained with anti-myc (red) and anti-MRTF-A antibody for localization of endogenous MRTF-A (green) and analyzed by epifluorescence microscopy. Starved conditions (ctrl.) and serum-stimulation for 1 hour (FCS) were as controls. **b** Quantification of MRTF-A localization by counting 50 myc-positive cells each. *Arrows* indicate myc-expressing cells. *Scale bars*, 20 μ m. *Error bars*, s.e.m., n = 3 (* $p \leq 0.05$, ** $p \leq 0.01$, *** $p \leq 0.001$ according to an unpaired two sample student's t-test).

IV.3.2 C-Terminal truncated JMY competes with MRTF-A for Actin-Binding

Mutually exclusive binding of NPF WH2 (V) domains and MRTF-A RPEL motifs was hypothesized because of their predicted ability to bind to the same surface on G-actin molecules. MRTF activation therefore is supposed to be induced independently of altered actin dynamics. Like N-WASP and WAVE2, JMY mediates actin polymerization via interaction with the ARP2/3 complex but is also able to nucleate actin independently of ARP2/3. However, to exclude ARP2/3-mediated polymerization JMY constructs with deficient ARP2/3 binding sites were required. Similar to other NPF, ARP2/3 interaction by JMY is mediated by the C-terminal central acidic (CA) region. Thus, constructs with deletions of either the C- or the A-region, the complete CA-region or the CA-region plus one WH2 domain (Δ VCA) were generated (Fig. IV-23 a). As described previously, arginine 474 as well as surrounding amino acids of murine N-WASP are known to have a critical role in ARP2/3 activation (Kim *et al*, 2000; Banzai *et al*, 2000).

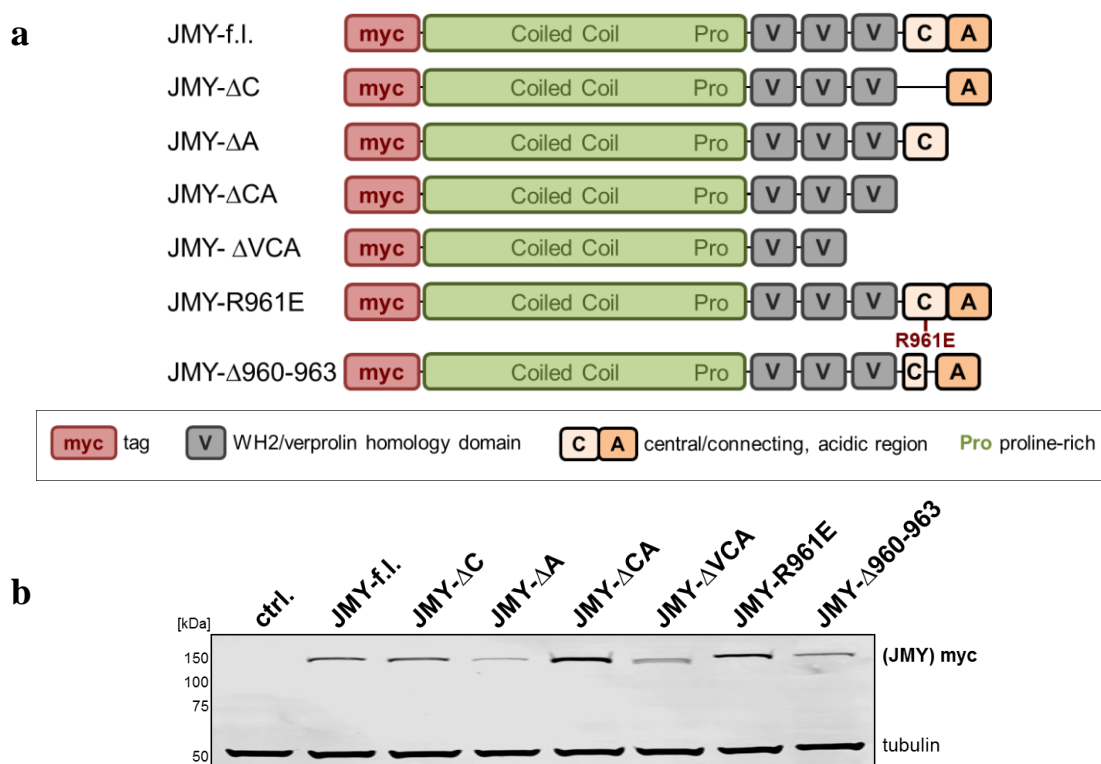


Figure IV-23: Domain topology and protein expression of truncated, myc-tagged JMY constructs. NIH 3T3 cells were transiently transfected with the indicated constructs and analyzed for the expression level. **a** Schematics of myc-tagged JMY constructs and domain topology. **b** Analysis of the protein expression level and protein size of the indicated constructs using tag-specific antibody. Equal loading was controlled by tubulin.

Thus, the corresponding amino acids on the JMY protein (R961E and Δ 960-963) were mutated (Fig. IV-23 a, VIII-2). All constructs were fused to myc-tag, expressed in mouse fibroblasts and initially analyzed for correct protein size and expression level (Fig. IV-23 a, b).

The direct impact of WH2 (V)-containing JMY on actin:MRTF-A complexes was investigated in a co-immunoprecipitation assay. Precipitated Flag-tagged actin and the purified MRTF-A were analyzed for complex formation in presence of full length and ARP2/3 deficient JMY (Fig. IV-24, VIII-3). Lysates from cells overexpressing Flag-actin and myc-tagged JMY variants were combined, supplemented with recombinant MRTF-A (2-261) and incubated with anti-Flag beads. By western blot analysis, it seemed at first that the presence of full length JMY reduced the amount of MRTF-A (2-261) bound to precipitated actin in comparison to the control without JMY (Fig. IV-24). However, quantification of three independent experiments showed that full length JMY did not reduce actin-MRTF-A binding (Fig. IV-25). In contrast, expression of JMY- Δ C, - Δ A, -R961E and - Δ 960-963 considerably reduced MRTF-A binding to Flag-actin. JMY- Δ CA failed to prevent complex association (Fig. IV-24, -25). These results confirmed an effect on actin-MRTF-A complexes by the ARP2/3 deficient mutant JMY, maybe due to altered conformational conditions.

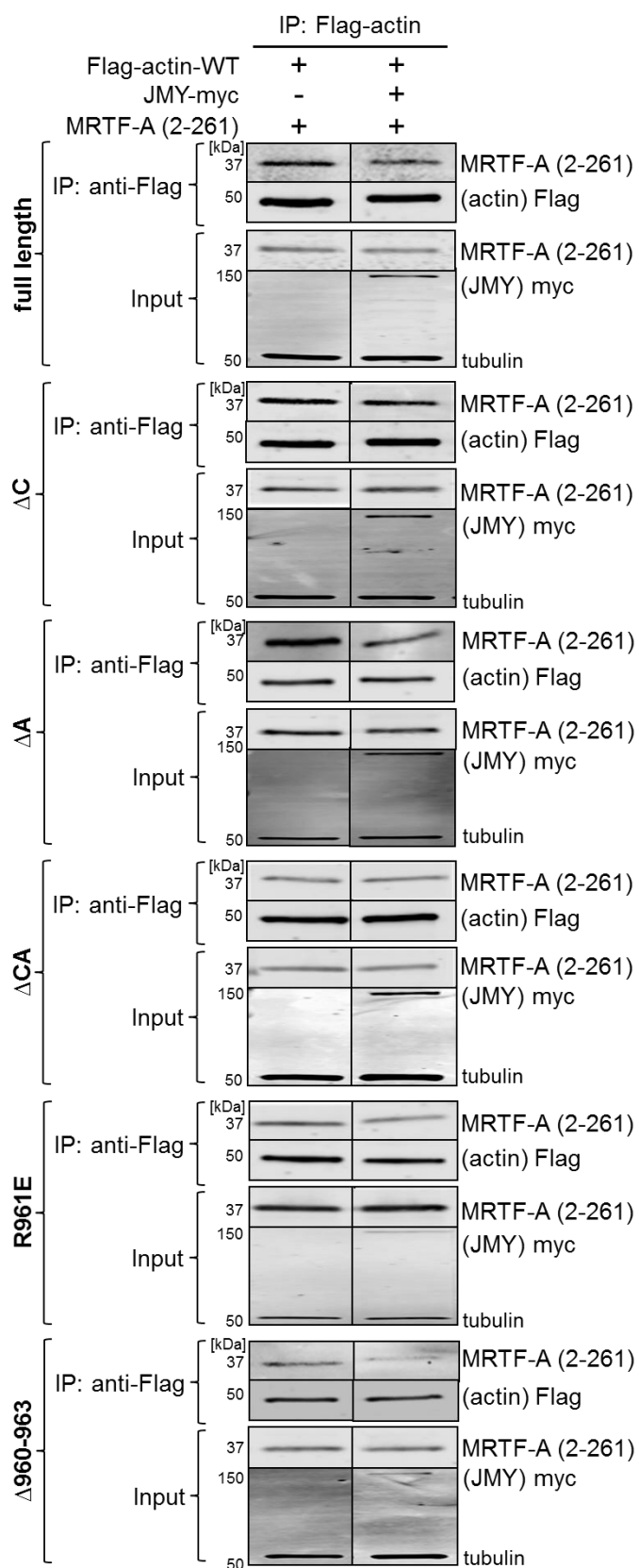


Figure IV-24: C-terminal truncated JMY competes with MRTF-A for actin-binding. Flag-actin-WT together with full length JMY or the indicated mutants were transiently co-expressed in serum-starved NIH 3T3 cells. For anti-Flag co-immunoprecipitation, cell lysates were mixed with purified MRTF-A (2-261). Precipitated proteins were analyzed using anti-MRTF-A and anti-Flag antibody.

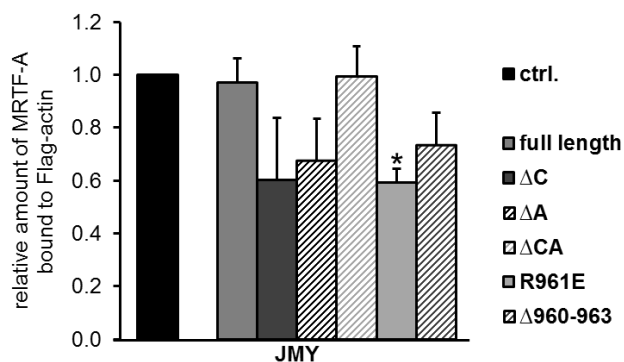


Figure IV-25: Impaired association of actin and MRTF-A upon overexpression of truncated JMY. Quantification of the amount of MRTF-A (2-261) bound to precipitated Flag-actin in presence of the indicated JMY constructs. Data were normalized to the control without JMY co-expression (ctrl.) which was set to 1. Error bars, s.e.m., n = 3 (* $p \leq 0.05$, ** $p \leq 0.01$, *** $p \leq 0.001$ according to an unpaired one sample student's t-test).

IV.3.3 C-Terminal truncated JMY induces Nuclear MRTF-A Accumulation

The dissociation of inhibitory actin:MRTF complexes leads to nuclear accumulation of MRTF-A and transcriptional activation of MRTF-SRF. Therefore, JMY truncations with impaired ARP2/3 interaction should be analyzed for nuclear translocation of MRTF-A via immunofluorescence (Fig. IV-26). Following transient transfection cells were fixed and immuno-stained for subcellular localization of endogenous MRTF-A and myc-tagged JMY constructs under serum-starved conditions. Expression of full length JMY displayed MRTF-A in the cytoplasm which is similar to serum-starved non-transfected control cells (ctrl.) (Fig. IV-4 a, -26, first line). However, quantification of three independent experiments revealed 30% of JMY-f.l. expressing cells with nuclear accumulated MRTF-A (Fig. IV-27). In contrast, transiently expressed JMY-ΔC, -ΔA, -ΔCA, -R961E and -Δ960-963 significantly induced nuclear translocation of MRTF-A (Fig. IV-26, -27). JMY-ΔVCA expression showed a subcellular localization of MRTF-A in the cytoplasm, similar to the effect of full length JMY. However, compared with JMY-f.l., quantification offered less cells with nuclear MRTF-A upon JMY-ΔVCA expression. This suggested an essential functional role for the presence of all three WH2 domains. The induction of nuclear translocated MRTF-A by JMY truncation constructs partially correlated with their ability to dissociate actin:MRTF-A complexes. This effect is independent of enhanced actin polymerization which was verified performing immunofluorescence assay and cell fractionation (Fig. VIII-6, -7).

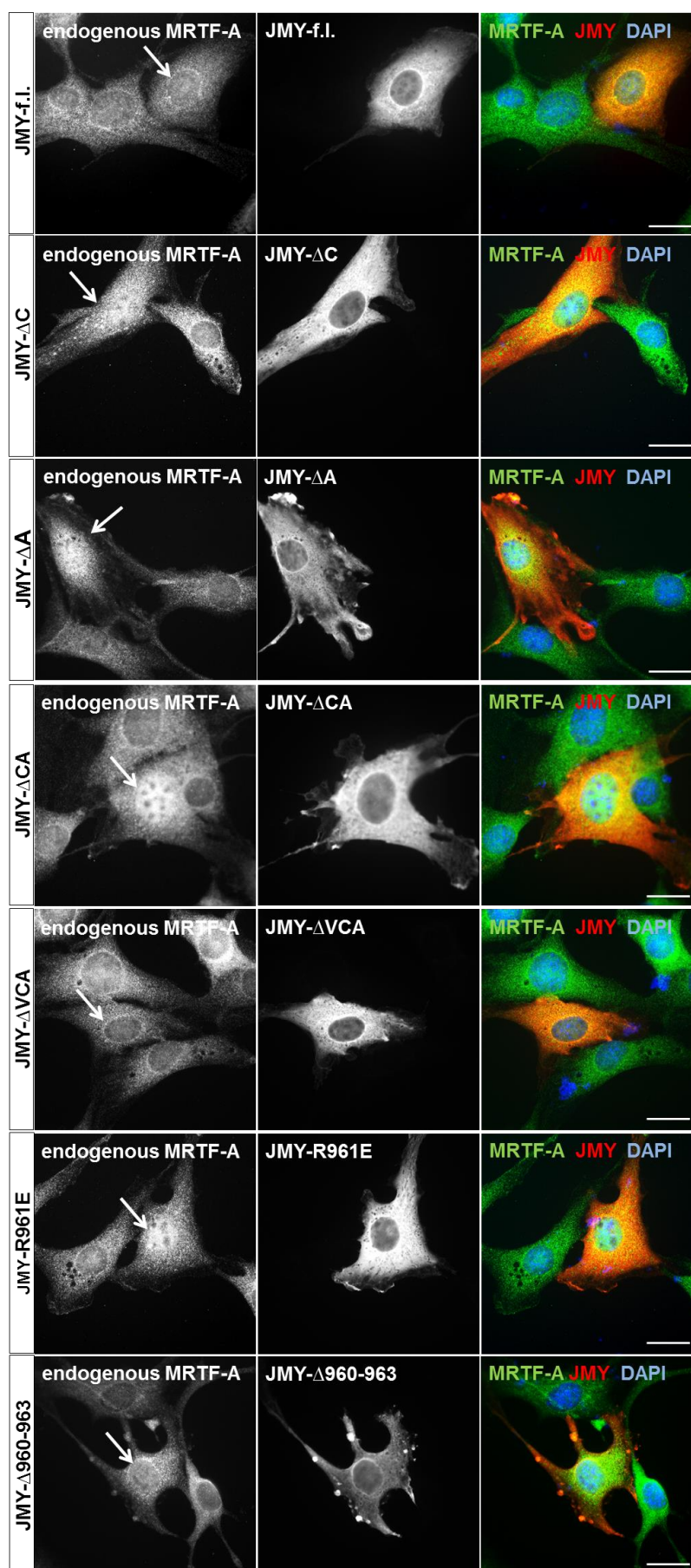


Figure IV-26: C-terminal truncated JMY induces nuclear accumulation of endogenous MRTF-A in NIH 3T3 mouse fibroblasts. Serum-starved NIH 3T3 cells were transiently transfected with the indicated myc-tagged JMY constructs, fixed, counterstained with DAPI (blue) and immune-stained with anti-myc and anti-MRTF-A antibody. Localization of myc-expressing cells (red) and subcellular localization of endogenous MRTF-A (green) was analyzed by epifluorescence microscopy. Arrows indicate myc-expressing cells. Scale bars, 20 μ m.

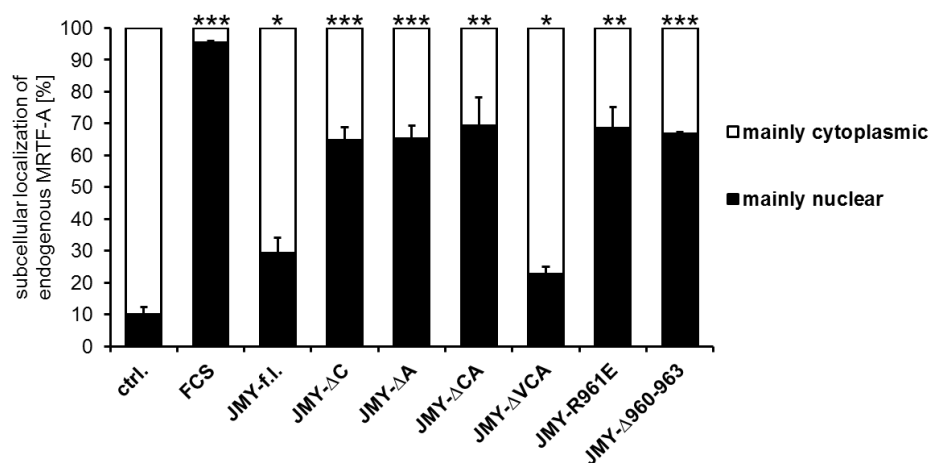


Figure IV-27: Quantification nuclear accumulation of endogenous MRTF-A upon overexpression of C-terminal truncated JMY. NIH 3T3 cells were transiently transfected with the indicated constructs and analyzed via immunofluorescence. Cells expressing the vector control (ctrl.) and serum-stimulation for 1 hour (FCS) were as controls. Quantification of MRTF-A localization by counting 50 myc-positive cells each. Error bars, s.e.m., n = 3 (* p ≤ 0.05, ** p ≤ 0.01, *** p ≤ 0.001 according to an unpaired two sample student's t-test).

IV.3.4 C-Terminal truncated JMY activates MRTF-SRF-dependent Gene Expression

Whereas full length JMY slightly induced MRTF-SRF activity and nuclear MRTF-A accumulation (Fig. IV-21, -22), expression of C-terminal truncated JMY led to efficient disruption of actin:MRTF complexes and nuclear accumulated MRTF-A (Fig. IV-25, -26, -27). Thus, activation of the MRTF-SRF transcription module by truncated WH2-containing JMY was investigated performing SRF reporter assay and quantitative RT-PCR (Fig. IV-28). Expression of CA-truncated JMY significantly activated the MRTF-SRF reporter plasmid and transcription of the SRF target *smooth muscle actin* (*Acta2*). With exception of JMY-ΔVCA, all JMY mutants were able to considerably induce MRTF-SRF activity around 8- to 15-fold compared with the serum-starved control (ctrl.) (Fig. IV-28 a). Thereby, the strongest effect was observable for JMY-ΔCA. Moreover, the induction levels by the mutants were significantly higher compared to full length JMY. JMY-ΔVCA did not induce SRF activity at all, highlighting a requirement of all three WH2 domains. In line with this, *Acta2* mRNA expression and SRF reporter activation were induced to comparable levels by JMY truncations, with the strongest impact for JMY-ΔCA (Fig. IV-28 b). JMY-ΔVCA did not increase *Acta2* mRNA level, according to the starvation control (dotted line). Analysis of the MRTF-SRF target genes vinculin (*Vcl*) and integrin- $\alpha 5$ (*Itga5*) revealed no altered mRNA expression in response to overexpressed JMY constructs.

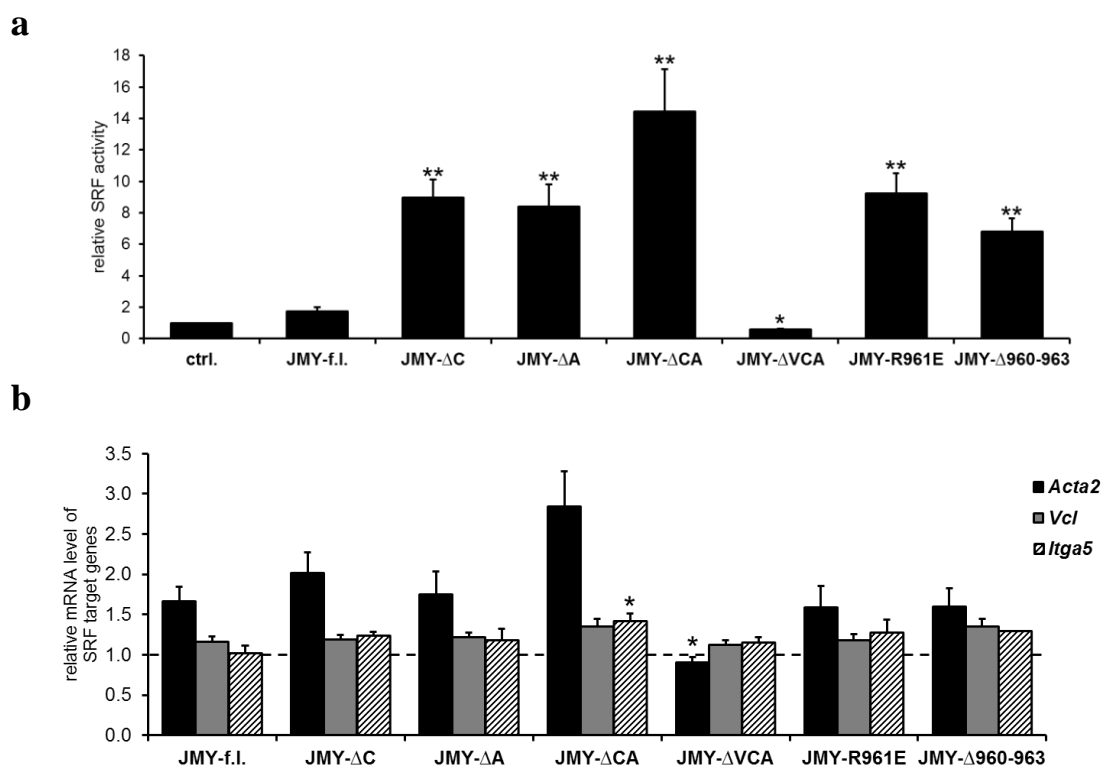


Figure IV-28: C-terminal truncated JMY activates MRTF-SRF-dependent gene expression. Serum-starved NIH 3T3 cells were transiently transfected with the indicated myc-tagged constructs and analyzed for SRF target gene expression. **a** Relative MRTF-SRF luciferase reporter activity upon co-transfection with truncated JMY constructs. Overexpression of myc-tagged, truncated JMY variants increased SRF reporter activity in comparison to the control and to full length JMY. All data were normalized to the non-transfected, serum-starved control (ctrl.) which was set to 1. Significance was related to full length JMY. **b** Endogenous mRNA expression of the SRF target genes smooth muscle α -actin (*Acta2*), vinculin (*Vcl*) and integrin $\alpha 5$ (*Itga5*) upon expression of the indicated constructs. All data were normalized to the non-transfected, serum-starved control (dotted line) which was set to 1. Significance for each gene was related to full length JMY, respectively. Error bars, s.e.m., n = 3 (* p \leq 0.05, ** p \leq 0.01, *** p \leq 0.001 according to an unpaired two sample student's t-test).

IV.3.5 C-Terminal truncated JMY activates MRTF-SRF-dependent Gene Expression independently of ARP2/3-mediated Actin Polymerization

The results given by the different CA-truncated mutants indicated a role for JMY WH2 (V) domains on actin:MRTF-A complex disruption and activation of the MRTF-SRF transcription module which is independent of the ARP2/3 complex. An exception was presented by JMY-ΔVCA which failed to activate MRTF-SRF despite availability of two WH2 domains. Moreover, the data pointed towards an intramolecular auto-inhibition of full length JMY mediated by the central acidic (CA) region because JMY truncations were more active compared with the full length protein.

To further distinguish WH2-mediated and ARP2/3-mediated effects on MRTF-A activation, the SRF reporter assay was performed under ARP2/3-inhibiting

conditions using ARP3-specific siRNA, the chemical ARP2/3 inhibitors CK-666 and CK-548 or the cytoskeletal drug Latrunculin B (Fig. IV-29, -30, -31). Efficient ARP3 depletion and ARP2/3 inhibition were verified by western blot and immunofluorescence analysis (Fig. IV-13 b, -14). Whereas ARP3-specific siRNA abolished JMY-f.l.-mediated slight induction of SRF, JMY truncations were able to induce the SRF reporter 10- up to 15-fold despite ARP3 knockdown (Fig. IV-29). SRF activation by overexpression of JMY CA-mutants was slightly decreased upon ARP3 siRNA transfection but still significantly increased compared with expression of full length JMY. These results demonstrated an impact of JMY WH2 domains on MRTF-SRF activity which is independently of ARP2/3 interaction.

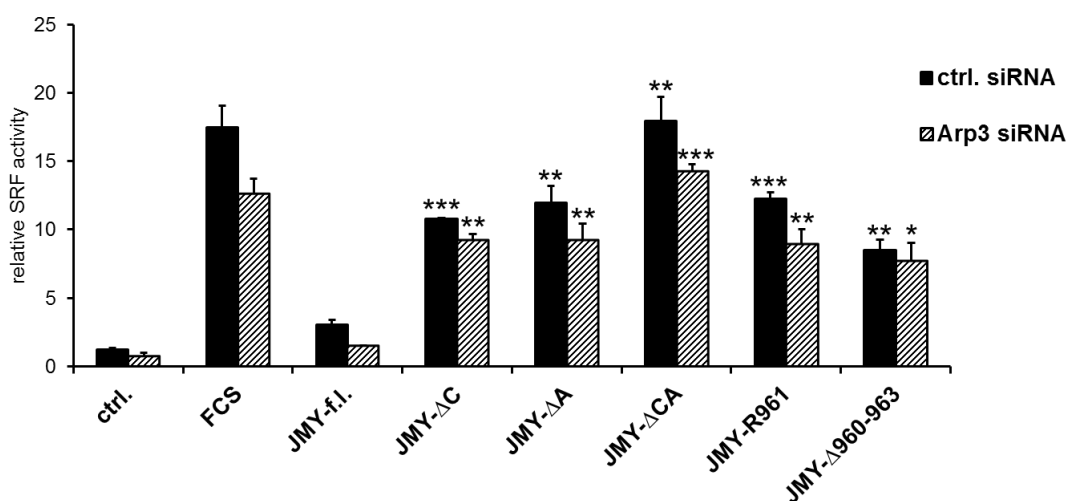


Figure IV-29: C-terminal truncated JMY induces MRTF-SRF activity despite siRNA-mediated ARP3 knockdown. NIH 3T3 cells were transiently transfected with the indicated siRNAs for 24 hours following starvation and co-transfection with reporter plasmids and the indicated JMY constructs. Transfection with vector control (ctrl.) and serum-stimulation for 7 hours (FCS) were as controls. Overexpression of JMY truncations induced SRF activity independently of the ARP2/3 complex in comparison to full length JMY. All data were normalized to the control which was set to 1. Significance was related to untreated full length JMY. Error bars, s.e.m., n = 3 (* p ≤ 0.05, ** p ≤ 0.01, *** p ≤ 0.001 according to an unpaired two sample student's t-test).

Moreover, the ARP2/3 inhibitors CK-666 or CK-548 completely abolished basal SRF activity of control cells and reduced serum-induction to 50% (Fig. IV-30). However, MRTF-SRF activity mediated by JMY mutants was not diminished to comparable extent upon CK-666 treatment. The decreasing effect of CK-548 was more intensive. But, JMY-induced reporter activity still represented 5- to 15-fold induction compared with the serum-starved control (ctrl.). In comparison to full length JMY, expression of

truncated variants considerably induced the SRF reporter 8- to 15-fold despite CK-666 and 5- to 8-fold despite CK-548 treatment. The impact of full length JMY on SRF activity was unimproved by the inhibitors. FCS-mediated SRF activity was also marginal decreased to 50%. These results demonstrated JMY-induced MRTF-SRF activity which was partially independent of ARP2/3-mediated actin polymerization. Furthermore, the central acidic region of JMY showed inhibitory regulation of the full length protein.

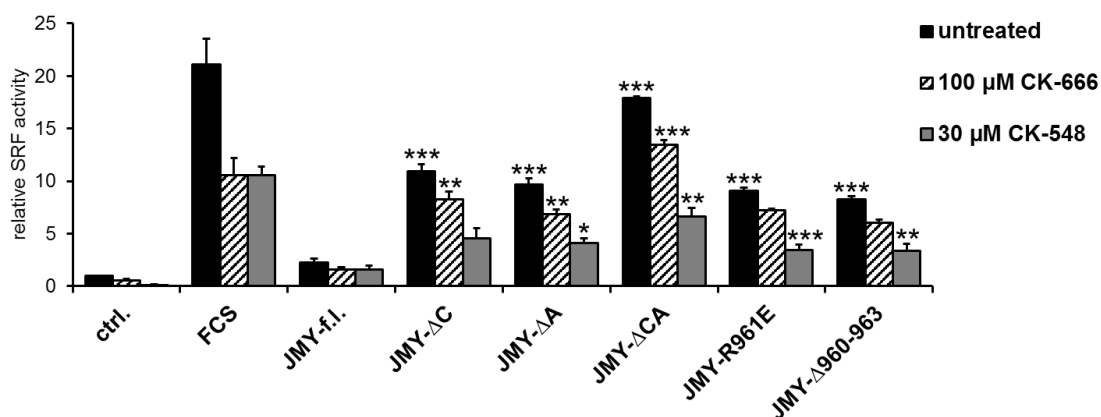


Figure IV-30: C-terminal truncated JMY induces MRTF-SRF activity despite CK-666- or CK-548-mediated ARP2/3 inhibition. Serum-starved NIH 3T3 cells were co-transfected with reporter plasmids and the indicated JMY constructs following treatment with 100 μM CK-666 or 30 μM CK-548 for 7 hours. Transfection with vector control (ctrl.) and serum-stimulation for 7 hours (FCS) were as controls. Overexpression of JMY truncations induced SRF activity independently of the ARP2/3 complex in comparison to the full length construct. All data were normalized to the control which was set to 1. Significance was related to untreated full length JMY. Error bars, s.e.m., n = 3 (* p ≤ 0.05, ** p ≤ 0.01, *** p ≤ 0.001 according to an unpaired two sample student's t-test).

Additionally, the actin de-polymerization drug Latrunculin B was used to increase the cellular G-actin pool. As a control, serum-induced activation of the MRTF-SRF reporter was completely blocked by Latrunculin B treatment (Fig. IV-31). In contrast, Latrunculin failed to abolish SRF induction mediated by expression of full length JMY and JMY mutants. MRTF-SRF activation by these constructs was only decreased to a remaining level of 5- to 13-fold despite drug treatment. These results, together with the data from the siRNA-mediated ARP3 knockdown and the inhibition by CK-666 and CK-548 confirmed the hypothesis that JMY was able to act on actin:MRTF complexes directly through WH2 (V) domains and independently of ARP2/3-mediated actin nucleation. Aside from this, the data exposed a more structural feature of JMY which could be due to conformational auto-inhibition.

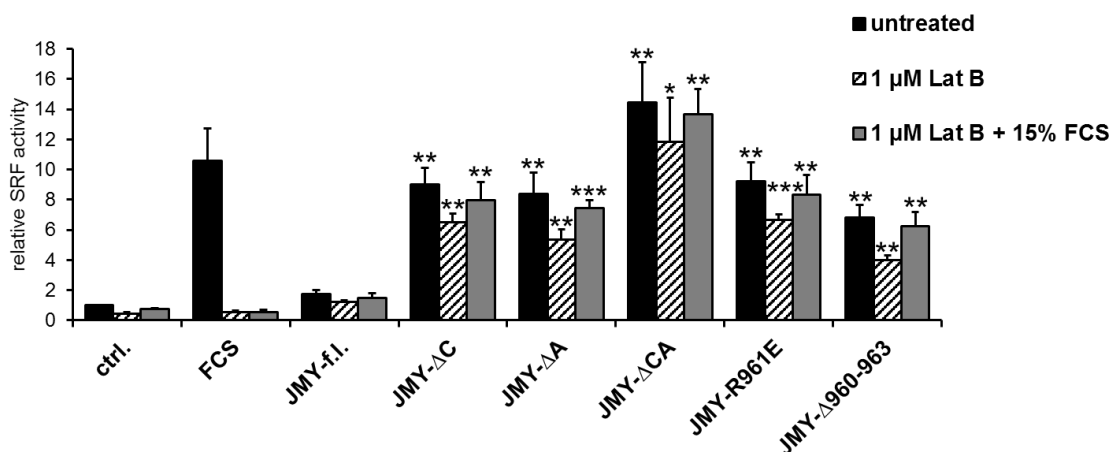


Figure IV-31: C-terminal truncated JMY induces MRTF-SRF activity despite Latrunculin B treatment. Serum-starved NIH 3T3 cells were co-transfected with reporter plasmids and the indicated JMY constructs following treatment with 1 μ M Latrunculin B for 7 hours. Transfection with vector control (ctrl.) and serum-stimulation for 7 hours (FCS) were as controls. Overexpression of JMY truncations induced SRF activity despite Latrunculin B treatment in comparison to the full length construct. All data were normalized to the control which was set to 1. Significance was related to untreated full length JMY. Error bars, s.e.m., n = 3 (* $p \leq 0.05$, ** $p \leq 0.01$, *** $p \leq 0.001$ according to an unpaired two sample student's t-test).

V Discussion

V.1 Nuclear Actin Polymerization

The cytoskeleton component actin has a prominent role on regulating nuclear gene expression via the MRTF-SRF transcription module. Thereby, actin dynamics critically affect transcriptional activity of target genes. The most important regulatory step is the dissociation of an inhibitory G-actin:MRTF complex in response to depletion of the monomeric actin pool (Miralles *et al*, 2003; Olson & Nordheim, 2010). Actin-regulated MRTF-A activation is known to occur in the cytoplasm as well as inside the nucleus (Vartiainen *et al*, 2007). Although there are numerous reports for G-actin, nuclear actin filament polymerization has long been controversial due to difficulties in staining and lack of functional correlations (Gonsior *et al*, 1999; Schoenenberger *et al*, 2005; Jockusch *et al*, 2006).

To address regulation of actin:MRTF complexes in the nuclear compartment, F-actin formation inside the nucleus should be visualized. By use of NLS-fused, filament enhancing actin mutants (G15S, S14C, V159N) and the F-actin markers LifeAct-GFP and phalloidin the presence of filamentous actin could be clearly demonstrated inside the nucleus of NIH 3T3 fibroblasts by this study (Fig. IV-1, VIII-1). Moreover, in cooperation with the group of Bernd Knöll, bioinformatics and comparison of various cell types led to the characterization of the architecture of nuclear F-actin structures as conserved networks of curved fibers and rods (Fig. IV-1, VIII-1) (Kokai *et al*, 2014). In addition, stimulation of MRTF-SRF-related gene expression by NLS-actin-G15S, -S14C and -V159N could be proved. This provided evidence on the principle ability for actin to polymerize inside the interphase nucleus and to form filamentous structures which opened new aspects on actin regulation and actin-related biological functions. At the same time, Baarlink and colleagues confirmed these findings by publishing the detection of rapid nuclear actin polymerization in response to serum-stimulation (Baarlink *et al*, 2013). They assumed that the integral part of physiological, serum-responsive MRTF-SRF induction is mediated by the activation of nuclear mDia formins. However, it is controversial that formins are the essential regulators for nuclear actin polymerization and MRTF activation as the observed actin networks are extremely transient and disassembled within seconds.

Similar to the nucleator mDia, the WH2-containing nucleation-promoting factor (NPF) N-WASP was already shown to activate MRTF-SRF-mediated transcription (Sotiropoulos *et al*, 1999; Copeland & Treisman, 2002; Baarlink *et al*, 2013). We therefore proposed to analyze representative WH2-containing NPF to be involved in nuclear actin assemblies and nuclear actin:MRTF complex regulation. However, transient expression of NLS-fused N-WASP, WAVE2 and JMY failed to induce activity of the MRTF-SRF transcription module in mouse fibroblasts (data not shown). Moreover, immunofluorescence analysis revealed atypical cytoplasmic and nuclear actin staining and non-physiological cell morphology indicating a cell damaging impact of these constructs (data not shown). Although N-WASP and JMY both are known to function also in the nuclear compartment, the results did not advance in a promising direction (Zuchero & Coutts, 2009; Coutts *et al*, 2009; Wu *et al*, 2006; Park & Takenawa, 2011; Yamaguchi *et al*, 2005). Thus, it requires optimized NLS-fused NPF constructs to further investigate NPF-mediated regulation of nuclear actin:MRTF complexes.

V.2 MRTF-A Activation by N-WASP and WAVE2

Transcriptional activity of the MRTF-SRF module is controlled by actin dynamics and the complex formation of MRTF with globular actin. MRTF-A is sufficient for SRF activation upon dissociation from inhibitory actin monomers (Miralles *et al*, 2003; Posern & Treisman, 2006). WH2 (V) domains of various nucleation-promoting factors (NPF) were shown to bind actin at the same surface like MRTF-A RPEL motifs indicating a role of WH2 domains on MRTF-A activation by mutually exclusive actin-binding (Mouilleron *et al*, 2008).

N-WASP and WAVE2 are widely expressed WH2-containing NPF and act in the regulatory actin pathway upon activation by the Rho-GTPases Cdc42 and Rac1, respectively. Overexpression of N-WASP and WAVE2 in this study induced MRTF-SRF-dependent reporter activity and increased the mRNA expression level of *smooth muscle actin* (*Acta2*) (Fig. IV-3). N-WASP was already shown earlier to activate SRF-dependent gene transcription through its VCA domain, the WH2 (V) domain and the central acidic (CA) region, indicating a role of WH2-containing proteins on the actin-MRTF-SRF pathway (Sotiropoulos *et al*, 1999). We could now also confirmed this for WAVE2. Activity of the SRF co-factor MRTF-A depends on its nuclear accumulation

upon dissociation from G-actin. N-WASP and WAVE2 both affected repressive actin:MRTF complexes thereby inducing MRTF-A nuclear translocation (Fig. IV-4).

Interestingly, WH2-containing JMY did not activate the MRTF-A-SRF module to a robust level (Fig. IV-21). Since auto-inhibition, mediated by intramolecular folding, was already speculated for the full length protein, JMY seemed to be regulated differentially compared with N-WASP and WAVE2 and was therefore analyzed separately (Firat-Karalar *et al*, 2011).

N-WASP and WAVE2 both modulate actin polymerization through interaction of their central acidic (CA) region with the ARP2/3 complex (Campellone & Welch, 2010). However, the hypothesized mutually exclusive binding of WH2 domains and MRTF-A focused on a polymerization-independent mechanism as previously shown for the actin-sequestering protein thymosin- β 4 which represents one single WH2 domain (Hinkel *et al*, 2014; Morita & Hayashi, 2013; Posern *et al*, unpublished). Hence, the CA region of N-WASP and WAVE2 had to be mutated for impaired ARP2/3 interaction to analyze a direct impact of WH2 domains on actin:MRTF complexes.

V.3 MRTF-A Activation by Competition with WH2 (V) Domains for Actin-binding

Polymerization-independent competition of WH2 domain-containing N-WASP or WAVE2 with MRTF-A for actin-binding was investigated using central acidic (CA) mutant constructs. For murine N-WASP it was known that arginine 474 (R474), which is located in the C domain, is crucial for ARP2/3 interaction and activation. Additionally, it contacts the N-WASP GTPase-binding domain (GBD) thereby inducing intramolecular auto-inhibition until activation by Cdc42. The N-WASP A domain additionally enhances activation of the ARP2/3 complex (Kim *et al*, 2000; Marchand *et al*, 2001). Thus, R474E, Δ A and Δ CA variants of N-WASP and WAVE2 were generated as potentially constitutive active and ARP2/3-deficient constructs.

In an *in vitro* co-immunoprecipitation assay N-WASP- and WAVE2-R474E and - Δ A competed with purified MRTF-A (2-261) RPEL motifs for actin-binding (Fig. IV-6). The experimental setup excluded ARP2/3- or polymerization-dependent effects thereby postulating a direct competition of N-WASP and WAVE2 WH2 (V) domains. The results could be confirmed by a similar behavior of isolated N-WASP or WAVE2

WH2 domains (Weissbach *et al*, 2016; thesis of F. Schikora, in preparation). While the impact on actin:MRTF complex dissociation in this assay was more pronounced for WAVE2 both NPF were unable to disrupt actin-RPEL-association when lacking the entire central acidic region (Δ CA). Previous findings on purified WH2 domains underlined a functional importance for proper length of domains as well as linker regions. We thus speculate that the Δ CA constructs have compromised WH2 domains, resulting in diminished activity of N-WASP- and WAVE2- Δ CA (Qualmann & Kessels, 2009). Full length N-WASP was not able to compete with MRTF-A for actin-binding in the immunoprecipitation assay, possibly due to its intramolecular inhibition (Kim *et al*, 2000). In contrast, full length N-WASP induced activity of the MRTF-SRF reporter plasmid as well as target gene transcription (Fig. IV-12). These divergent findings suggest an ARP2/3-mediated effect in the latter case, which is absent in the biochemical competition assay. Although most of the other constructs displayed an impact on actin:MRTF-A complexes by significantly decreasing the amount of actin-bound MRTF (Fig. IV-6) the reverse precipitation of actin:NPF complexes was not successful (data not shown). It remains to be determined whether this reflected their function as G-actin carrier during filament elongation in which binding to actin is very transient or whether experimental conditions negatively affected binding affinities during precipitation (Pollard & Cooper, 2009).

Complex disruption by N-WASP and WAVE2 mutants often correlated with nuclear accumulated MRTF (Fig. IV-7, -8). Both NPF induced translocation of MRTF-A despite impaired ARP2/3 interaction indicating a direct role of their WH2 domains. However, the impact was only moderate when the entire CA region was deleted. The predominant view on MRTF-A activation as a result of altered actin dynamics and a depleted G-actin pool did not explain the effect of ARP2/3-deficient NPF (Miralles *et al*, 2003; Olson & Nordheim, 2010). MRTF-A release and nuclear accumulation upon mutant expression was present also in the absence of any obvious alterations in the F-actin level (Fig. IV-10, -11).

Sufficient MRTF-A nuclear translocation upon WAVE2-full length and -mutant expression could be confirmed by a strong induction of the SRF-reporter (Fig. IV-12 b). However, in the same context the activation by N-WASP-R474E and - Δ A was low (Fig. IV-12 a). From that it has to be clarified whether differences in the affinities of WH2 domains played a role or N-WASP and WAVE2 constructs differed for structural reasons. According to previous findings, Δ CA of both NPF represented functional

inefficient constructs. Nevertheless, reporter activation upon expression of isolated V and VCA fragments verified a direct impact of WH2 domains on actin:MRTF complexes (Weissbach *et al*, 2016; thesis of F. Schikora, in preparation). Due to transient transfection technique induction of mRNA expression levels of the SRF target genes *smooth muscle actin (Acta2)*, *vinculin (Vcl)* and *integrin $\alpha 5$ (Itga5)* in general was low and more pronounced for full length constructs (Fig. IV-12 c, d).

MRTF-A activation by N-WASP and WAVE2 mutants provided evidence that the actin-MRTF-SRF pathway underlies a more complex regulation than simple alterations in the G-/F-actin ratio. The postulated mutually exclusive binding of MRTF and WH2 domains independently of actin nucleation could be maintained by the findings that N-WASP and WAVE2 induced MRTF-SRF reporter activity despite inhibition of the ARP2/3 complex by siRNA-mediated knockdown or CK-666 or upon treatment with Latrunculin B (Fig. IV-13, -15, -16). ARP3-siRNA decreased the impact of full length N-WASP and WAVE2 but was not sufficient to abolish NPF-mediated SRF activity (Fig. IV-13 a). Similarly, treatment with the ARP2/3 inhibitor CK-666 only slightly reduced SRF induction to a robust remaining level (Fig. IV-15). Interestingly, the de-polymerization drug Latrunculin B dramatically reduced serum-stimulated SRF-reporter induction but did not block the impact of N-WASP and WAVE2 (Fig. IV-16). Moreover, Latrunculin binds the ATP pocket of an actin monomer which enhances simultaneous binding of MRTF-A RPEL motifs or WH2 domains to actin (Mouilleron *et al*, 2011; Sotiropoulos *et al*, 1999; Descot *et al*, 2009). MRTF-A activation despite Latrunculin treatment suggested a competitive binding of WH2-containing N-WASP or WAVE2. In contrast, serum-stimulated MRTF-SRF activation was fully restricted to actin polymerization, blocked by pre-treatment with Latrunculin B.

Moreover, experiments with polymerization-deficient actin R62D confirmed the assumption that actin:MRTF complex disruption was not fully restricted to polymerization events (Weissbach *et al*, 2016; thesis of F. Schikora, in preparation). Amongst others, findings on regulating MRTF-A activity underlined a role for ERK1/2-mediated phosphorylation of MRTF-A serine 454 as well as for an C-terminal interaction with filamin A (Muehlich *et al*, 2008; Kircher *et al*, 2015). Both could be excluded in this study by using the purified RPEL domain MRTF-A (2-261) (Fig. IV-6). Nevertheless, recent findings uncovered multiple other serum-inducible phosphorylation sites, located at the N-terminus of MRTF-A, which are responsible for

regulating transcriptional activity (Panayiotou *et al*, 2016). For instance the formation of actin:RPEL complexes is inhibited upon ERK-mediated phosphorylation of MRTF serine 98. In contrast, phosphorylation of serine 33 inhibits MRTF activation by increasing its nuclear export. Thus, protein modifications concerning the N-terminal MRTF-A RPEL motifs could also play a role on regulating actin:MRTF complexes independently of altered actin dynamics.

De-novo association of actin and purified MRTF RPEL motifs was considerably reduced following serum-stimulation which suggested insignificance for altered G-/F-actin levels but relevance of molecular competition processes (Fig. IV-17, VIII-4). Furthermore, co-immunoprecipitation studies with ectopic cell lysates, pre-treated with serum, similarly showed impaired complex formation of MRTF-A (2-261) with actin WT as well as polymerization-deficient actin R62D (Fig. IV-18, -19 a, VIII-5). One explanation could be the presence of a serum-inducible and transferable competitor, possibly WH2 (V)-containing proteins. A putative *trans*-acting factor X could compete actin:MRTF complexes through binding to either actin or MRTF-A, given by the experimental setup in Figure IV-18 and VIII-5. Thus serum-stimulation would decrease actin:MRTF complexes and simultaneously increase actin:X or MRTF:X complexes. A proteome-wide mass spectrometry-based screening of proteins differentially bound to actin and MRTF-A upon serum-stimulation therefore could help to identify the putative transferable competitor. In addition, the screening should include further stimuli, such as LPA, to investigate the presence of multiple *trans*-acting factors. Expected candidates has to be signal-inducible, widely expressed and regulated. Transcriptionally induced factors could be excluded due to the time-restriction of the experiment (Fig. IV-18). Otherwise, serum-mediated cellular processes are versatile. Thus complex disruption could also be mediated through differential actin-binding properties, for instance following MICAL-2-induced actin oxidation (Lundquist *et al*, 2014). For the first instance, attempts to identify a possible *trans*-acting competitor could eliminate an influence of protein phosphorylation and pointed towards a non-enzymatic factor (Fig. IV-19 b). However, this kind of identification approach did not significantly advance in a promising direction and requires further investigation. Screenings for protein modifications, including phosphorylation, oxidation, glycosylation or acetylation, on actin or MRTF-A as a function of serum-starvation and -stimulation would be recommendable. It remains to be addressed whether inducible WH2 (V) domains and WH2-containing proteins come into consideration.

Beside the common model for actin-MRTF-SRF-related gene transcription it has been possible to demonstrate activation of MRTF-A which is independent of actin alterations but rather regulated by representative WH2-containing N-WASP and WAVE2 in this study. From there, a direct competitive mechanism could be assumed. The challenge will be to identify critical WH2-containing proteins as there are more than 80 known in mammals until now. The number is even raising based on bioinformatics and they all display a vast diversity of cellular functions (Weiß & Schultz, 2015). Common identification methods, like siRNA-specific domain knockout or knockdown, are not practicable due to the fact that WH2 (V) domains hardly exhibit sequence homology. Consequently, a specific siRNA would be required for each WH2 domain of each WH2-containing protein. Moreover, it remains difficult to determine correct domain borders because WH2 domains are intrinsically disordered (Dominguez, 2007; Guharoy *et al*, 2013). Varying actin binding-affinities of the various WH2 domains is not negligible as well. Beside differences in their actin affinity the K_d of multiple WH2 domains within one protein also differ (Renault *et al*, 2013). Compared with N-WASP, WAVE2 has a higher affinity to actin which is consistent with a more pronounced impact of WAVE2 on actin:MRTF complex disruption and MRTF activation (Fig. IV-6, -8, -12) (Chereau *et al*, 2005). Moreover, the actin-affinity of MRTF-A (2-261) is higher compared with N-WASP which enabled the disruption of actin:N-WASP-WH2 complexes by MRTF-A (2-261) (Weissbach *et al*, 2016; thesis of F. Schikora, in preparation). But N-WASP is more affine to actin than to the ARP2/3 complex thus mutually exclusive actin-binding independently of ARP2/3 interaction was considerably detectable (Marchand *et al*, 2001). WH2 domain proteins like COBL or SPIRE2 exhibit strong actin affinities resulting in more potent binding competition and MRTF-A activation (Campellone & Welch, 2010; Renault *et al*, 2008; Weissbach *et al*, 2016; thesis of F. Schikora, in preparation). However, COBL and SPIRE2 are tissue-specific and not regulated by other factors which excluded both WH2 proteins as widespread inducible MRTF activators (Ahuja *et al*, 2007; Quinlan *et al*, 2005). In contrast, N-WASP and WAVE2 are ubiquitously present in several cell types and they are signal-inducible regulated by GTPases of the Rho-family (Kim *et al*, 2000; Eden *et al*, 2002). Despite lacking the ARP2/3 interaction site N-WASP and WAVE2 as well as their isolated WH2 (V) domains were able to induce MRTF-A activity (Weissbach *et al*, 2016; thesis of F. Schikora, in preparation). This highlighted both WH2-containing NPF as attractive candidates for mutually exclusive binding, but experimental evidence for

their physiological involvement in specific signal transduction pathway has yet to be obtained. Further investigations therefore need to focus on the *in vivo* kinetics and dynamics of endogenous WH2 domain proteins and actin:MRTF complexes which will be challenging. Visualization of live-cell, intracellular complex formation and disruption would give interesting insights, also into the subcellular localization of complementation events. This in turn is just viable by using non-endogenous, optogenetic tools like fluorescence-labeled proteins or biosensors. For the first instance, we attempted to visualize the association and dissociation of actin and MRTF in living NIH 3T3 cells using a YFP-based biosensor system (Nagai *et al*, 2001; Michel *et al*, 2011). We created these sensors as they contain a central, interchanged and permuted YFP with an N-terminal fused MRTF-A RPEL motif and C-terminal fused actin R62D. The YFP-specific sensor emission should vary as a function of RPEL:actin association or dissociation. Initial experiments using complex-enhancing Latrunculin B and complex-inhibiting Cytochalasin D indeed showed very slight treatment-dependent differences in YFP emission which were hard to detect (data not shown). Thus NPF-mediated impacts on biosensor emission could be even more challenging. Further approaches to visualize life-cell complex formation and disruption could include three chromophore fluorescence resonance energy transfer (FRET) or complementation of multicolor luciferases (Okamoto & Hayashi, 2006; Hida *et al*, 2009). Both techniques are based on differential chromophore labeling of the different complex partners. Accordingly, each complex combination will be detected by a distinct emission or color. Moreover, it would be possible to detect both complex formation and competition-mediated disruption, due to a reversible chromophore interaction. In contrast, bimolecular fluorescence complementation (BiFC) underlies an irreversible chromophore association and would therefore only visualize complex formation but no competition (Hu & Kerppola, 2003).

Nevertheless, this study demonstrated that the molecular mechanisms on actin:MRTF-A complex disruption are more complex than previously thought and that WH2 domains and WH2 domain-containing proteins are able to activate MRTF-A by a direct competition for actin-binding. Transcriptional activity of MRTF-A in turn critically affects tumor cell migration and metastasis by regulating processes like adhesion, migration and invasion of cancer cells (Medjkane *et al*, 2009; Leitner *et al*, 2011; Morita *et al*, 2007). Therefore, the detailed molecular understanding of MRTF regulation is relevant to open new aspects on tumor biology and cancer cell therapy.

V.4 JMY CA-Region mediates intramolecular Inhibition

Following initial experiments, the WH2 (V) protein JMY was not considered as a promising candidate for a crucial signal transducer due to its minor impact on MRTF-A transcriptional activation and nuclear accumulation (Fig. IV-21, -22). However, JMY could play a role for WH2 domain proteins especially on nuclear actin:MRTF-A complexes. Its subcellular localization is controlled by mutually exclusive binding of G-actin and importin- α/β to the nuclear localization signal of JMY (Renault *et al*, 2013; Zuchero *et al*, 2012). Because of a tandem repeat of three WH2 domains, JMY facilitates actin filament formation both *de novo* from pure G-actin and via ARP2/3 interaction (Zuchero & Coutts, 2009; Zuchero *et al*, 2012; Renault *et al*, 2013). Thus, the disability of full length JMY to activate MRTF-A was even more remarkable (Fig. IV-21, -22).

The analysis of JMY constructs shown in this study, with truncations in their central acidic (CA) region, proposed conformational auto-inhibition of the full length protein. In an *in vitro* immunoprecipitation assay JMY was not efficient to dissociate actin:MRTF complexes unless parts of the CA region were deleted suggesting an inhibiting role for the CA domain (Fig. IV-24, -25). In line with this, an inhibitory mechanism was already assumed since the activity of full length JMY was suppressed compared with its isolated VCA domain (Firat-Karalar *et al*, 2011). While JMY- Δ CA was unable to act on actin:MRTF complexes in the immunoprecipitation it still strongly induced nuclear MRTF-A accumulation and transcriptional activation of the MRTF-SRF module (Fig. IV-26, -27, -28). The inconsistency between both approaches could be due to the transient transfection methodology and low transfection efficiency which is critical for evaluating the competition assay but less decisive for immunofluorescence-based analysis of only positive transfected cells. Furthermore, JMY- Δ C, - Δ A, -R961E and - Δ 960-963 considerably induced MRTF-SRF activity (Fig. IV-28). The impact on MRTF activation of JMY constructs was rising with the extent of C-terminal deletions suggesting that the CA region caused intramolecular folding and inhibition of MRTF-A activation. Moreover, JMY activity was restricted to three WH2 (V) domains, because JMY- Δ VCA did not increase the MRTF-SRF reporter at all. Thus, a proper domain length and correct domain borders seemed to be crucial for JMY function as previously mentioned for WH2-containing N-WASP and WAVE2 (Qualmann & Kessels, 2009). These findings additionally lead to the hypothesis of a direct impact of WH2 domains on MRTF-A activation by mutually exclusive

actin-binding.

JMY is able to act independently of the ARP2/3 complex (Zuchero *et al*, 2012). From there, JMY- Δ C, Δ A, Δ CA, -R961E and Δ 960-963 strongly induced the MRTF-SRF reporter despite ARP2/3 knockdown or ARP2/3 inhibitor treatment (Fig. IV-29, -30). JMY-mediated MRTF-A activation was uncoupled of actin polymerization since there was no significant alteration of the F-actin level detectable (Fig. VIII-6, -7). Treatment with de-polymerizing Latrunculin B dramatically reduced serum-induced MRTF-SRF activity but did not diminish the impact of JMY truncations (Fig. IV-31). The minor impact of full length JMY was even more unchanged. Latrunculin contacts the nucleotide-binding site on G-actin thereby enhancing repressive actin:MRTF-A complexes (Mouilleron *et al*, 2011; Sotiropoulos *et al*, 1999; Descot *et al*, 2009). Thus, MRTF-A activation despite Latrunculin treatment suggested a competitive binding of JMY WH2 domains, if they are accessible in an open protein conformation, as proposed for JMY truncations. Additionally, these findings could be confirmed by a similar behavior of isolated JMY WH2 domains which are unrelated to any nucleating activity or auto-inhibition (thesis of F. Schikora, in preparation).

In this study, it was possible to demonstrate new insights on structure-related properties of JMY including intramolecular folding mediated by the central acidic region. As a more recently found NPF JMY characterization as yet is meager and its regulation by structural auto-inhibition is still speculated (Burianek & Soderling, 2013). It remains to identify the interacting amino acids or domains which are responsible for intramolecular folding of full length JMY. Genetic tools, like further JMY constructs carrying various point-mutations within the VCA domain, therefore could be helpful. Moreover, elucidating the crystal structure of the different JMY constructs would be informative to address folding-mediated protein regulation. Potential regulatory interaction partners should be investigated as well by performing screening approaches such as co-immunoprecipitation analysis and proteome-wide mass spectrometry-based screening. This study provides a starting point for detailed molecular characterization of JMY which is a relative new NPF of the WASP family and may contribute to physiological activation of MRTF-A. Similar to N-WASP and WAVE2, JMY therefore also comes into consideration to open new aspects on MRTF-mediated tumor biology.

VI Bibliography

- Ahuja R, Pinyol R, Reichenbach N, Custer L, Klingensmith J, Kessels MM & Qualmann B (2007) Cordon-bleu is an actin nucleation factor and controls neuronal morphology. *Cell* 131: 337–50.
- Aldrich RA, Steinberg AG & Campbell DC (1954) Pedigree demonstrating a sex-linked recessive condition characterized by draining ears, eczematoid dermatitis and bloody diarrhea. *Pediatrics* 13: 133–9.
- Ammer AG & Weed SA (2008) Cortactin branches out: roles in regulating protrusive actin dynamics. *Cell Motil. Cytoskeleton* 65: 687–707.
- Antón IM, Jones GE, Wandosell F, Geha R, Ramesh N, Tapon N, Hall A, Derry JM, al. et, Symons M, al. et, Kolluri R, al. et, Aspenstrom P, al. et, Miki H, al. et, Rohatgi R, al. et, Higgs HN, et al (2007) WASP-interacting protein (WIP): working in polymerisation and much more. *Trends Cell Biol.* 17: 555–62.
- Aravind L, Koonin E V., Baxevanis AD, Landsman D, Aravind L, Landsman D, Aasland R, al. et, Gregory SL, al. et, Aasland R, al. et, Romig H, al. et, Gohring F, al. et, Altschul SF, al. et, Tatusov RL, al. et, et al (2000) SAP – a putative DNA-binding motif involved in chromosomal organization. *Trends Biochem. Sci.* 25: 112–114.
- Baarlink C, Wang H & Grosse R (2013) Nuclear actin network assembly by formins regulates the SRF coactivator MAL. *Science* 340: 864–7.
- Banzai Y, Miki H, Yamaguchi H & Takenawa T (2000) Essential Role of Neural Wiskott-Aldrich Syndrome Protein in Neurite Extension in PC12 Cells and Rat Hippocampal Primary Culture Cells *. *J. Biol. Chem.* 275: 11987–11992.
- Bear JE, Rawls JF & Saxe CL (1998) SCAR, a WASP-related protein, isolated as a suppressor of receptor defects in late Dictyostelium development. *J. Cell Biol.* 142: 1325–35.
- Benesch S, Lommel S, Steffen A, Stradal TEB, Scaplehorn N, Way M, Wehland J & Rottner K (2002) Phosphatidylinositol 4,5-biphosphate (PIP₂)-induced vesicle movement depends on N-WASP and involves Nck, WIP, and Grb2. *J. Biol. Chem.* 277: 3771–6.
- Bettinger BT, Gilbert DM & Amberg DC (2004) Actin up in the nucleus. *Nat. Rev. Mol. Cell Biol.* 5: 410–5.
- Bosticardo M, Marangoni F, Aiuti A, Villa A & Grazia Roncarolo M (2009) Recent advances in understanding the pathophysiology of Wiskott-Aldrich syndrome. *Blood* 113: 6288–95.
- Boxer LM, Prywes R, Roeder RG & Kedes L (1989) The sarcomeric actin CArG-binding factor is indistinguishable from the c-fos serum response factor. *Mol. Cell. Biol.* 9: 515–522.

- Burianek LE & Soderling SH (2013) Under lock and key: spatiotemporal regulation of WASP family proteins coordinates separate dynamic cellular processes. *Semin. Cell Dev. Biol.* 24: 258–66.
- Burtnick LD, Urosev D, Irobi E, Narayan K & Robinson RC (2004) Structure of the N-terminal half of gelsolin bound to actin: roles in severing, apoptosis and FAF. *EMBO J.* 23: 2713–22.
- Campellone KG & Welch MD (2010) A nucleator arms race: cellular control of actin assembly. *Nat. Rev. Mol. Cell Biol.* 11: 237–51.
- Cen B, Selvaraj A, Burgess RC, Hitzler JK, Ma Z, Morris SW & Prywes R (2003) Megakaryoblastic leukemia 1, a potent transcriptional coactivator for serum response factor (SRF), is required for serum induction of SRF target genes. *Mol. Cell. Biol.* 23: 6597–608.
- Chen Z, Borek D, Padrick SB, Gomez TS, Metlagel Z, Ismail AM, Umetani J, Billadeau DD, Otwinowski Z & Rosen MK (2010) Structure and control of the actin regulatory WAVE complex. *Nature* 468: 533–8.
- Chereau D, Kerff F, Graceffa P, Grabarek Z, Langsetmo K & Dominguez R (2005) Actin-bound structures of Wiskott – Aldrich syndrome protein (WASP) - homology domain 2 and the implications for filament assembly. *Proc. Natl. Acad. Sci. U. S. A.* 102: 16644–16649.
- Chirgwin JM, Przybyla AE, MacDonald RJ & Rutter WJ (1979) Isolation of biologically active ribonucleic acid from sources enriched in ribonuclease. *Biochemistry* 18: 5294–9.
- Chomczynski P & Sacchi N (1987) Single-step method of RNA isolation by acid guanidinium thiocyanate-phenol-chloroform extraction. *Anal. Biochem.* 162: 156–159.
- Copeland JW & Treisman R (2002) The Diaphanous-related Formin mDial Controls Actin Polymerization. *Mol. Cell. Biol.* 13: 4088–4099.
- Coutts AS, Weston L & La Thangue NB (2009) A transcription co-factor integrates cell adhesion and motility with the p53 response. *Proc. Natl. Acad. Sci. U. S. A.* 106: 19872–7.
- Dalton S, Marais R, Wynne J & Treisman R (1993) Isolation and characterization of SRF accessory proteins. *Philos. Trans. R. Soc. Lond. B. Biol. Sci.* 340: 325–32.
- Dalton S & Treisman R (1992) Characterization of SAP-1, a protein recruited by serum response factor to the c-fos serum response element. *Cell* 68: 597–612.
- Derry JM, Ochs HD, Francke U, Ammann AJ, Hong R, Brochstein JA, Gillio AP, Ruggiero M, Kernan NA, Emanuel D, Laver J, Small T, O'Reilly RJ, Cicchetti P, Mayer BJ, Theil G, Baltimore D, Creighton TE, Basile G de Saint, Arveiler B, et al (1994) Isolation of a novel gene mutated in Wiskott-Aldrich syndrome. *Cell* 78: 635–44.
- Descot A, Hoffmann R, Shaposhnikov D, Reschke M, Ullrich A & Posern G (2009) Negative regulation of the EGFR-MAPK cascade by actin-MAL-mediated Mig6/Errfi-1 induction. *Mol. Cell* 35: 291–304.
- Dominguez R (2007) The beta-Thymosin/WH2 Fold: Multifunctionality and Structure. *Ann. N. Y. Acad. Sci.* 1112: 86–94.

- Dominguez R (2010) Structural insights into de novo actin polymerization. *Curr Opin Struct Biol.* 20: 217–225.
- Dopie J, Skarp K-P, Rajakylä EK, Tanhuanpää K & Vartiainen MK (2012) Active maintenance of nuclear actin by importin 9 supports transcription. *Proc. Natl. Acad. Sci. U. S. A.* 109: E544-52.
- Eden S, Rohatgi R, Podtelejnikov A V, Mann M & Kirschner MW (2002) Mechanism of regulation of WAVE1-induced actin nucleation by Rac1 and Nck. *Nature* 418: 790–3.
- Felgner PL, Gadek TR, Holm M, Roman R, Chan HW, Wenz M, Northrop JP, Ringold GM & Danielsen M (1987) Lipofection: a highly efficient, lipid-mediated DNA-transfection procedure. *Proc. Natl. Acad. Sci. U. S. A.* 84: 7413–7.
- Firat-Karalar EN, Hsiue PP & Welch MD (2011) The actin nucleation factor JMY is a negative regulator of neuritogenesis. *Mol. Biol. Cell* 22: 4563–74.
- Firestone GL & Winguth SD (1990) Immunoprecipitation of proteins. *Methods Enzymol.* 182: 688–700.
- Fried S, Matalon O, Noy E & Barda-Saad M (2014) WIP: more than a WASp-interacting protein. *J. Leukoc. Biol.* 96: 713–27.
- Geeves MA & Holmes KC (2005) The Molecular Mechanism of Muscle Contraction. *Adv. Protein Chem.* 71: 161–193.
- Geneste O, Copeland JW & Treisman R (2002) LIM kinase and Diaphanous cooperate to regulate serum response factor and actin dynamics. *J. Cell Biol.* 157: 831–8 A.
- Gineitis D & Treisman R (2001) Differential Usage of Signal Transduction Pathways Defines Two Types of Serum Response Factor Target Gene. *J. Biol. Chem.* 276: 24531–24539.
- Goley ED, Rodenbusch SE, Martin AC, Welch MD, Belmont LD, Patterson GML, Drubin DG, Beltzner CC, Pollard TD, Blanchoin L, Amann KJ, Higgs HN, Marchand JB, Kaiser DA, Pollard TD, Blanchoin L, Pollard TD, Hitchcock-DeGregori SE, Cooper JA, Walker SB, et al (2004) Critical conformational changes in the Arp2/3 complex are induced by nucleotide and nucleation promoting factor. *Mol. Cell* 16: 269–79.
- Goley ED & Welch MD (2006) The ARP2/3 complex: an actin nucleator comes of age. *Nat. Rev. Mol. Cell Biol.* 7: 713–726.
- Gonsior SM, Platz S, Buchmeier S, Scheer U, Jockusch BM & Hinssen H (1999) Conformational difference between nuclear and cytoplasmic actin as detected by a monoclonal antibody. *J. Cell Sci.* 809: 797–809.
- Graceffa P & Dominguez R (2003) Crystal structure of monomeric actin in the ATP state. Structural basis of nucleotide-dependent actin dynamics. *J. Biol. Chem.* 278: 34172–80.
- Greenberg ME & Ziff EB (1984) Stimulation of 3T3 cells induces transcription of the c-fos proto-oncogene. *Nature* 311: 433–8.
- Grummt I (2006) Actin and myosin as transcription factors. *Curr. Opin. Genet. Dev.* 16: 191–6.
- Guettler S, Vartiainen MK, Miralles F, Larijani B & Treisman R (2008) RPEL motifs link the serum response factor cofactor MAL but not myocardin to Rho signaling via actin binding. *Mol. Cell. Biol.* 28: 732–42.

- Guharoy M, Szabo B, Contreras Martos S, Kosol S & Tompa P (2013) Intrinsic structural disorder in cytoskeletal proteins. *Cytoskelet.* 70: 550–71.
- Gunning PW, Ghoshdastider U, Whitaker S, Popp D & Robinson RC (2015) The evolution of compositionally and functionally distinct actin filaments. *J. Cell Sci.* 128: 2009–19.
- Harlow E & Lane D (1988) *Antibodies: A laboratory manual* New York: Cold Spring Harbor Laboratory Press.
- Hayashi K & Morita T (2012) Differences in the nuclear export mechanism between myocardin and myocardin-related transcription factor A. *J. Biol. Chem.* 288: 5743–55.
- Henzel MJ (2014) The F-act's of nuclear actin. *Curr. Opin. Cell Biol.* 28: 84–9.
- Heuser JE & Kirschner MW (1980) Filament organization revealed in platinum replicas of freeze-dried cytoskeletons. *J. Cell Biol.* 86: 212–34.
- Hida N, Awais M, Takeuchi M, Ueno N, Tashiro M, Takagi C, Singh T, Hayashi M, Ohmiya Y & Ozawa T (2009) High-sensitivity real-time imaging of dual protein-protein interactions in living subjects using multicolor luciferases. *PLoS One* 4: e5868.
- Hill CS, Wynne J, Treisman R, Ammerer G, Bannister AJ, Gottlieb TM, Kouzarides T, Jackson SP, Bigay J, Deterre P, Pfister C, Chabre M, Boguski MS, McCormick F, Bruhn L, Sprague GJ, Chant J, Stowers L, Chong LD, Traynor KA, et al (1995) The Rho family GTPases RhoA, Rac1, and CDC42Hs regulate transcriptional activation by SRF. *Cell* 81: 1159–1170.
- Hinkel R, Trenkwalder T, Petersen B, Husada W, Gesenhues F, Lee S, Hannappel E, Bock-Marquette I, Theisen D, Leitner L, Boekstegers P, Cierniewski C, Müller OJ, le Noble F, Adams RH, Weini C, Nordheim A, Reichart B, Weber C, Olson E, et al (2014) MRTF-A controls vessel growth and maturation by increasing the expression of CCN1 and CCN2. *Nat. Commun.* 5: 3970.
- Ho H-YH, Rohatgi R, Lebensohn AM, Le Ma L, Li J, Gygi SP, Kirschner MW, Allen P., Anton I., Fuente M. de la, Sims T., Freeman S, Ramesh N, Hartwig J., Dustin M., Geha R., Aspenstrom P, Carlier M., Nioche P, Broutin-L'Hermite I, et al (2004) Toca-1 mediates Cdc42-dependent actin nucleation by activating the N-WASP-WIP complex. *Cell* 118: 203–16.
- Hofmann MA & Brian DA (1991) Sequencing PCR DNA amplified directly from a bacterial colony. *Biotechniques* 11: 30–1.
- Hofmann WA, Stojiljkovic L, Fuchsova B, Vargas GM, Mavrommatis E, Philimonenko V, Kysela K, Goodrich JA, Lessard JL, Hope TJ, Hozak P & de Lanerolle P (2004) Actin is part of pre-initiation complexes and is necessary for transcription by RNA polymerase II. *Nat. Cell Biol.* 6: 1094–101.
- Hu C-D & Kerppola TK (2003) Simultaneous visualization of multiple protein interactions in living cells using multicolor fluorescence complementation analysis. *Nat Biotechnol.* 21: 539–545.
- Hu P, Wu S & Hernandez N (2004) A role for beta-actin in RNA polymerase III transcription. *Genes Dev.* 18: 3010–5.

- Innocenti M, Gerboth S, Rottner K, Lai FPL, Hertzog M, Stradal TEB, Frittoli E, Didry D, Polo S, Disanza A, Benesch S, Di Fiore PP, Carlier M-F & Scita G (2005) Abi1 regulates the activity of N-WASP and WAVE in distinct actin-based processes. *Nat. Cell Biol.* 7: 969–76.
- Innocenti M, Zucconi A, Disanza A, Frittoli E, Areces LB, Steffen A, Stradal TEB, Di Fiore PP, Carlier M-F & Scita G (2004) Abi1 is essential for the formation and activation of a WAVE2 signalling complex. *Nat. Cell Biol.* 6: 319–27.
- Iyer D, Belaguli N, Flück M, Rowan BG, Wei L, Weigel NL, Booth FW, Epstein HF, Schwartz RJ & Balasubramanyam A (2003) Novel phosphorylation target in the serum response factor MADS box regulates alpha-actin transcription. *Biochemistry* 42: 7477–86.
- Jockusch BM, Schoenenberger C-A, Stetefeld J & Aebi U (2006) Tracking down the different forms of nuclear actin. *Trends Cell Biol.* 16: 391–6.
- Kabsch W, Mannherz HG, Suck D, Pai EF & Holmes KC (1990) Atomic structure of the actin:DNase I complex. *Nature* 347: 37–44.
- Kalita K, Kharebava G, Zheng J-J & Hetman M (2006) Role of megakaryoblastic acute leukemia-1 in ERK1/2-dependent stimulation of serum response factor-driven transcription by BDNF or increased synaptic activity. *J. Neurosci.* 26: 10020–32.
- Kalita K, Kuzniewska B & Kaczmarek L (2012) MKLs: co-factors of serum response factor (SRF) in neuronal responses. *Int. J. Biochem. Cell Biol.* 44: 1444–7.
- Kim a S, Kakalis LT, Abdul-Manan N, Liu G a & Rosen MK (2000) Autoinhibition and activation mechanisms of the Wiskott-Aldrich syndrome protein. *Nature* 404: 151–8.
- Kircher P, Hermanns C, Nossek M, Drexler MK, Grosse R, Fischer M, Sarikas A, Penkava J, Lewis T, Prywes R, Gudermann T & Muehlich S (2015) Filamin A interacts with the coactivator MKL1 to promote the activity of the transcription factor SRF and cell migration. *Sci. Signal.* 8: ra112.
- Kirkbride KC, Hong NH, French CL, Clark ES, Jerome WG & Weaver AM (2012) Regulation of late endosomal/lysosomal maturation and trafficking by cortactin affects Golgi morphology. *Cytoskeleton (Hoboken)*. 69: 625–43.
- Knöll B, Kretz O, Fiedler C, Alberti S, Schütz G, Frotscher M & Nordheim A (2006) Serum response factor controls neuronal circuit assembly in the hippocampus. *Nat. Neurosci.* 9: 195–204.
- Kokai E, Beck H, Weissbach J, Arnold F, Sinske D, Sebert U, Gaiselmann G, Schmidt V, Walther P, Münch J, Posern G & Knöll B (2014) Analysis of nuclear actin by overexpression of wild-type and actin mutant proteins. *Histochem. Cell Biol.* 141: 123–135.
- Kovacs EM, Verma S, Ali RG, Ratheesh A, Hamilton NA, Akhmanova A & Yap AS (2011) N-WASP regulates the epithelial junctional actin cytoskeleton through a non-canonical post-nucleation pathway. *Nat. Cell Biol.* 13: 934–43.
- Kowalski JR, Egile C, Gil S, Snapper SB, Li R & Thomas SM (2005) Cortactin regulates cell migration through activation of N-WASP. *J. Cell Sci.* 118: 79–87.
- Laemmli UK (1970) Cleavage of structural proteins during the assembly of the head of bacteriophage T4. *Nature* 227: 680–5.

- Lappalainen P & Drubin DG (1997) Cofilin promotes rapid actin filament turnover in vivo. *Nature* 388: 78–82.
- Leitner L, Shaposhnikov D, Mengel A, Descot A, Julien S, Hoffmann R & Posern G (2011) MAL/MRTF-A controls migration of non-invasive cells by upregulation of cytoskeleton-associated proteins. *J. Cell Sci.* 124: 4318–31.
- Li J, Zhu X, Chen M, Cheng L, Zhou D, Lu MM, Du K, Epstein JA & Parmacek MS (2005) Myocardin-related transcription factor B is required in cardiac neural crest for smooth muscle differentiation and cardiovascular development. *Proc. Natl. Acad. Sci. U. S. A.* 102: 8916–21.
- Li S, Chang S, Qi X, Richardson JA & Olson EN (2006) Requirement of a myocardin-related transcription factor for development of mammary myoepithelial cells. *Mol. Cell. Biol.* 26: 5797–808.
- Livak KJ & Schmittgen TD (2001) Analysis of relative gene expression data using real-time quantitative PCR and the 2(-Delta Delta C(T)) Method. *Methods* 25: 402–8.
- Lommel S, Benesch S, Rottner K, Franz T, Wehland J & Kühn R (2001) Actin pedestal formation by enteropathogenic *Escherichia coli* and intracellular motility of *Shigella flexneri* are abolished in N-WASP-defective cells. *EMBO Rep.* 2: 850–7.
- Lundquist MR, Storaska AJ, Liu T-C, Larsen SD, Evans T, Neubig RR & Jaffrey SR (2014) Redox modification of nuclear actin by MICAL-2 regulates SRF signaling. *Cell* 156: 563–76.
- Ma Z, Morris SW, Valentine V, Li M, Herbrick JA, Cui X, Bouman D, Li Y, Mehta PK, Nizetic D, Kaneko Y, Chan GC, Chan LC, Squire J, Scherer SW & Hitzler JK (2001) Fusion of two novel genes, RBM15 and MKL1, in the t(1;22)(p13;q13) of acute megakaryoblastic leukemia. *Nat. Genet.* 28: 220–1.
- Machesky LM, Atkinson SJ, Ampe C, Vandekerckhove J & Pollard TD (1994) Purification of a cortical complex containing two unconventional actins from *Acanthamoeba* by affinity chromatography on profilin-agarose. *J. Cell Biol.* 127: 107–15.
- Marchand JB, Kaiser DA, Pollard TD & Higgs HN (2001) Interaction of WASP/Scar proteins with actin and vertebrate Arp2/3 complex. *Nat. Cell Biol.* 3: 76–82.
- McDonald D, Carrero G, Andrin C, de Vries G & Hendzel MJ (2006) Nucleoplasmic beta-actin exists in a dynamic equilibrium between low-mobility polymeric species and rapidly diffusing populations. *J. Cell Biol.* 172: 541–52.
- Medjkane S, Perez-Sanchez C, Gaggioli C, Sahai E & Treisman R (2009) Myocardin-related transcription factors and SRF are required for cytoskeletal dynamics and experimental metastasis. *Nat. Cell Biol.* 11: 257–68.
- Mercher T, Coniat MB, Monni R, Mauchauffe M, Nguyen Khac F, Gressin L, Mugneret F, Leblanc T, Dastugue N, Berger R & Bernard OA (2001) Involvement of a human gene related to the *Drosophila* spen gene in the recurrent t(1;22) translocation of acute megakaryocytic leukemia. *Proc. Natl. Acad. Sci. U. S. A.* 98: 5776–9.
- Miano JM, Long X & Fujiwara K (2007) Serum response factor: master regulator of the actin cytoskeleton and contractile apparatus. *Am. J. Physiol. Cell Physiol.* 292: C70–81.

- Michel M, Raabe I, Kupinski AP, Pérez-Palencia R & Bökel C (2011) Local BMP receptor activation at adherens junctions in the *Drosophila* germline stem cell niche. *Nat. Commun.* 2: 1–12.
- Miki H, Suetsugu S & Takenawa T (1998) WAVE, a novel WASP-family protein involved in actin reorganization induced by Rac. *EMBO J.* 17: 6932–41.
- Miralles F, Posern G, Zaromytidou A-I & Treisman R (2003) Actin Dynamics Control SRF Activity by Regulation of Its Coactivator MAL. *Cell* 113: 329–342.
- Miralles F & Visa N (2006) Actin in transcription and transcription regulation. *Curr. Opin. Cell Biol.* 18: 261–266.
- Mitchison T & Kirschner M (1984) Dynamic instability of microtubule growth. *Nature* 312: 237–42.
- Mizushima S & Nagata S (1990) pEF-BOS, a powerful mammalian expression vector. *Nucleic Acids Res.* 18: 5322.
- Mokalled MH, Johnson A, Kim Y, Oh J & Olson EN (2010) Myocardin-related transcription factors regulate the Cdk5/Pctaire1 kinase cascade to control neurite outgrowth, neuronal migration and brain development. *Development* 137: 2365–74.
- Morita T & Hayashi K (2013) G-actin sequestering protein thymosin- β 4 regulates the activity of myocardin-related transcription factor. *Biochem. Biophys. Res. Commun.* 437: 331–5.
- Morita T, Mayanagi T & Sobue K (2007) Dual roles of myocardin-related transcription factors in epithelial mesenchymal transition via slug induction and actin remodeling. *J. Cell Biol.* 179: 1027–42.
- Mouilleron S, Guettler S, Langer C a, Treisman R & McDonald NQ (2008) Molecular basis for G-actin binding to RPEL motifs from the serum response factor coactivator MAL. *EMBO J.* 27: 3198–208.
- Mouilleron S, Langer CA, Guettler S, McDonald NQ & Treisman R (2011) Structure of a pentavalent G-actin*MRTF-A complex reveals how G-actin controls nucleocytoplasmic shuttling of a transcriptional coactivator. *Sci. Signal.* 4: ra40.
- Muehlich S, Wang R, Lee S-M, Lewis TC, Dai C & Prywes R (2008) Serum-induced phosphorylation of the serum response factor coactivator MKL1 by the extracellular signal-regulated kinase 1/2 pathway inhibits its nuclear localization. *Mol. Cell. Biol.* 28: 6302–13.
- Mullins RD, Heuser JA & Pollard TD (1998) The interaction of Arp2/3 complex with actin: nucleation, high affinity pointed end capping, and formation of branching networks of filaments. *Proc. Natl. Acad. Sci. U. S. A.* 95: 6181–6.
- Nagai T, Sawano A, Park ES & Miyawaki A (2001) Circularly permuted green fluorescent proteins engineered to sense Ca²⁺. *Proc. Natl. Acad. Sci. U. S. A.* 98: 3197–202.
- Nolen BJ, Tomasevic N, Russell A, Pierce DW, Jia Z, McCormick CD, Hartman J, Sakowicz R & Pollard TD (2009) Characterization of two classes of small molecule inhibitors of Arp2/3 complex. *Nature* 460: 1031–4.

- Norman C, Runswick M, Pollock R, Treisman R, Almendral JM, Sommer D, Macdonald-Bravo H, Burckhardt J, Perera J, Bravo R, Anderson WF, Ohlendorf DH, Takeda Y, Matthews BW, Baldwin A, Sharp PA, Bankier AT, Weston KM, Barrell BG, Bender A, et al (1988) Isolation and properties of cDNA clones encoding SRF, a transcription factor that binds to the c-fos serum response element. *Cell* 55: 989–1003.
- Oda T, Iwasa M, Aihara T, Maéda Y & Narita A (2009) The nature of the globular- to fibrous-actin transition. *Nature* 457: 441–5.
- Oh J, Richardson JA & Olson EN (2005) Requirement of myocardin-related transcription factor-B for remodeling of branchial arch arteries and smooth muscle differentiation. *Proc. Natl. Acad. Sci. U. S. A.* 102: 15122–7.
- Okamoto K & Hayashi Y (2006) Visualization of F-actin and G-actin equilibrium using fluorescence resonance energy transfer (FRET) in cultured cells and neurons in slices. *Nat. Protoc.* 1: 911–9.
- Olave IA, Reck-Peterson SL & Crabtree GR (2002) Nuclear actin and actin-related proteins in chromatin remodeling. *Annu. Rev. Biochem.* 71: 755–81.
- Olson EN & Nordheim A (2010) Linking actin dynamics and gene transcription to drive cellular motile functions. *Nat. Rev. Mol. Cell Biol.* 11: 353–65.
- Padrick SB, Doolittle LK, Brautigam CA, King DS & Rosen MK (2011) Arp2/3 complex is bound and activated by two WASP proteins. *Proc. Natl. Acad. Sci. U. S. A.* 108: E472–9.
- Panayiotou R, Miralles F, Pawlowski R, Diring J, Flynn HR, Skehel M & Treisman R (2016) Phosphorylation acts positively and negatively to regulate MRTF-A subcellular localisation and activity. *Elife* 5: 1–24.
- Park SJ & Takenawa T (2011) Neural Wiskott-Aldrich Syndrome Protein Is Required for Accurate Chromosome Congression and Segregation. *Mol. Cells* 31: 515–521.
- Paunola E, Mattila PK & Lappalainen P (2002) WH2 domain: a small, versatile adapter for actin monomers. *FEBS Lett.* 513: 92–97.
- Pawłowski R, Rajakylä EK, Vartiainen MK & Treisman R (2010) An actin-regulated importin α/β -dependent extended bipartite NLS directs nuclear import of MRTF-A. *EMBO J.* 29: 3448–58.
- Pellegrini L, Tan S & Richmond TJ (1995) Structure of serum response factor core bound to DNA. *Nature* 376: 490–498.
- Pfirrmann T, Lokapally A, Andréasson C, Ljungdahl P & Hollemann T (2013) SOMA: A Single Oligonucleotide Mutagenesis and Cloning Approach. *PLoS One* 8: e64870.
- Philimonenko V V, Zhao J, Iben S, Dingová H, Kyselá K, Kahle M, Zentgraf H, Hofmann WA, de Lanerolle P, Hozák P & Grummt I (2004) Nuclear actin and myosin I are required for RNA polymerase I transcription. *Nat. Cell Biol.* 6: 1165–72.
- Philippart U, Schrott G, Dieterich C, Müller JM, Galgóczy P, Engel FB, Keating MT, Gertler F, Schüle R, Vingron M, Nordheim A, Arsenian S, Weinhold B, Oelgeschlager M, Ruther U, Nordheim A, Buchwalter G, Gross C, Wasylyk B, Chan KK, et al (2004) The SRF target gene Fhl2 antagonizes RhoA/MAL-dependent activation of SRF. *Mol. Cell* 16: 867–80.

- Pipes GCT, Creemers EE & Olson EN (2006) The myocardin family of transcriptional coactivators: versatile regulators of cell growth, migration, and myogenesis. *Genes Dev.* 20: 1545–56.
- Pollard TD (2007) Regulation of actin filament assembly by Arp2/3 complex and formins. *Annu. Rev. Biophys. Biomol. Struct.* 36: 451–77.
- Pollard TD & Cooper J a (2009) Actin, a central player in cell shape and movement. *Science* 326: 1208–12.
- Ponte P, Gunning P, Blau H & Kedes L (1983) Human actin genes are single copy for alpha-skeletal and alpha-cardiac actin but multicopy for beta- and gamma-cytoskeletal genes: 3' untranslated regions are isotype specific but are conserved in evolution. *Mol. Cell. Biol.* 3: 1783–91.
- Posern G, Miralles F, Guettler S & Treisman R (2004) Mutant actins that stabilise F-actin use distinct mechanisms to activate the SRF coactivator MAL. *EMBO J.* 23: 3973–83.
- Posern G, Sotiropoulos A & Treisman R (2002) Mutant Actins Demonstrate a Role for Unpolymerized Actin in Control of Transcription by Serum Response Factor. *Mol. Biol. Cell* 13: 4167–4178.
- Posern G & Treisman R (2006) Actin' together: serum response factor, its cofactors and the link to signal transduction. *Trends Cell Biol.* 16: 588–96.
- Prywes R, Roeder RG, Bell RM, Berridge MJ, Irvine RF, Bravo R, Burckhardt J, Curran T, Muller R, Chandler VL, Maler BA, Yamamoto KR, Cochran BH, Zullo J, Verma IM, Stiles CD, Cooper JA, Bowen-Pope DF, Raines E, Ross R, et al (1986) Inducible binding of a factor to the c-fos enhancer. *Cell* 47: 777–784.
- Qualmann B & Kessels MM (2009) New players in actin polymerization--WH2-domain-containing actin nucleators. *Trends Cell Biol.* 19: 276–85.
- Quinlan ME, Heuser JE, Kerkhoff E & Mullins RD (2005) Drosophila Spire is an actin nucleation factor. *Nature* 433: 382–8.
- Reisler E (1993) Actin molecular structure and function. *Curr. Opin. Cell Biol.* 5: 41–7.
- Renault L, Bugyi B & Carlier M-F (2008) Spire and Cordon-bleu: multifunctional regulators of actin dynamics. *Trends Cell Biol.* 18: 494–504.
- Renault L, Deville C & van Heijenoort C (2013) Structural features and interfacial properties of WH2, β -thymosin domains and other intrinsically disordered domains in the regulation of actin cytoskeleton dynamics. *Cytoskeleton (Hoboken)*. 70: 686–705.
- Richards TA & Cavalier-Smith T (2005) Myosin domain evolution and the primary divergence of eukaryotes. *Nature* 436: 1113–8.
- Rickwood D & Hames BD (1990) Gel Electrophoresis of Nucleic Acids – A Practical Approach. *IRL Press Washingt. D.C.*
- Riedl J, Crevenna AH, Kessenbrock K, Yu JH, Bista M, Bradke F, Jenne D, Holak TA, Werb Z, Sixt M, Wedlich-soldner R, Klopferspitz A, Avenue P & Francisco S (2008) Lifeact: a versatile marker to visualize F-actin. *Nat. Methods* 5: 1–8.
- Rodal AA, Sokolova O, Robins DB, Daugherty KM, Hippenmeyer S, Riezman H, Grigorieff N & Goode BL (2005) Conformational changes in the Arp2/3 complex leading to actin nucleation. *Nat. Struct. Mol. Biol.* 12: 26–31.

- Rosales-Nieves AE, Johndrow JE, Keller LC, Magie CR, Pinto-Santini DM & Parkhurst SM (2006) Coordination of microtubule and microfilament dynamics by *Drosophila* Rho1, Spire and Cappuccino. *Nat. Cell Biol.* 8: 367–76.
- Rotty JD, Wu C & Bear JE (2013) New insights into the regulation and cellular functions of the ARP2/3 complex. *Nat. Rev. Mol. Cell Biol.* 14: 7–12.
- Safer D & Nachmias VT (1994) Beta thymosins as actin binding peptides. *Bioessays* 16: 473–9.
- Saiki RK, Gelfand DH, Stoffel S, Scharf SJ, Higuchi R, Horn GT, Mullis KB & Erlich HA (1988) Primer-directed enzymatic amplification of DNA with a thermostable DNA polymerase. *Science* 239: 487–91.
- Sanger F, Nicklen S & Coulson AR (1992) DNA sequencing with chain-terminating inhibitors. 1977. *Biotechnology* 24: 104–8.
- Schlüter K, Waschbüsch D, Anft M, Hügging D, Kind S, Hänisch J, Lakisic G, Gautreau A, Barnekow A & Stradal TEB (2014) JMY is involved in anterograde vesicle trafficking from the trans-Golgi network. *Eur. J. Cell Biol.* 93: 194–204.
- Schoenenberger C, Buchmeier S, Boerries M, Sütterlin R, Aebi U & Jockusch BM (2005) Conformation-specific antibodies reveal distinct actin structures in the nucleus and the cytoplasm. *J. Struct. Biol.* 152: 157–68.
- Schutt CE, Myslik JC, Rozycki MD, Goonesekere NC & Lindberg U (1993) The structure of crystalline profilin-beta-actin. *Nature* 365: 810–6.
- Selvaraj A & Prywes R (2004) Expression profiling of serum inducible genes identifies a subset of SRF target genes that are MKL dependent. *BMC Mol. Biol.* 5: 13.
- Shen X, Ranallo R, Choi E, Wu C, Boyer LA, Peterson CL, Brachmann CB, Davies A, Cost GJ, Caputo E, Li J, Hieter P, Boeke JD, Cairns BR, Henry NL, Kornberg RD, Cairns BR, Erdjument-Bromage H, Tempst P, Winston F, et al (2003) Involvement of Actin-Related Proteins in ATP-Dependent Chromatin Remodeling. *Mol. Cell* 12: 147–155.
- Shikama N, Lee CW, France S, Delavaine L, Lyon J, Krstic-Demonacos M, La Thangue NB, Arany Z, Newsome D, Oldread E, Livingston DM, Eckner R, Attardi LD, Lowe SW, Brugarolos J, Jacks T, Avantaggiati ML, Ogryzko V, Gardner K, Giordano A, et al (1999) A novel cofactor for p300 that regulates the p53 response. *Mol. Cell* 4: 365–76.
- Shiota J, Ishikawa M, Sakagami H, Tsuda M, Baraban JM & Tabuchi A (2006) Developmental expression of the SRF co-activator MAL in brain: role in regulating dendritic morphology. *J. Neurochem.* 98: 1778–88.
- Shore P & Sharrocks AD (1995) The MADS-box family of transcription factors. *Eur. J. Biochem.* 229: 1–13.
- Smith PK, Krohn RI, Hermanson GT, Mallia AK, Gartner FH, Provenzano MD, Fujimoto EK, Goeke NM, Olson BJ & Klenk DC (1985) Measurement of protein using bicinchoninic acid. *Anal. Biochem.* 150: 76–85.
- Sotiropoulos A, Gineitis D, Copeland J & Treisman R (1999) Signal-Regulated Activation of Serum Response Factor Is Mediated by Changes in Actin Dynamics. *Cell* 98: 159–169.

- Steffen A, Rottner K, Ehinger J, Innocenti M, Scita G, Wehland J & Stradal TEB (2004) Sra-1 and Nap1 link Rac to actin assembly driving lamellipodia formation. *EMBO J.* 23: 749–59.
- Stewart DM, Treiber-Held S, Kurman CC, Facchetti F, Notarangelo LD & Nelson DL (1996) Studies of the expression of the Wiskott-Aldrich syndrome protein. *J. Clin. Invest.* 97: 2627–34.
- Stradal TE & Scita G (2006) Protein complexes regulating Arp2/3-mediated actin assembly. *Curr. Opin. Cell Biol.* 18: 4–10.
- Stradal TEB & Wehland J (2005) Aktindynamik und WASP / WAVE-Proteine. *BIOspektrum* 11: 5–8.
- Straub FB (1942) Actin. In *Institute of Medical Chemistry University Szeged, Szent-Györgyi A* (ed) pp 1–15.
- Straub FB & Feuer G (1989) Adenosinetriphosphate. The functional group of actin. 1950. *Biochim. Biophys. Acta* 1000: 180–95.
- Stritt C & Knöll B (2010) Serum response factor regulates hippocampal lamination and dendrite development and is connected with reelin signaling. *Mol. Cell. Biol.* 30: 1828–37.
- Stritt C, Stern S, Harting K, Manke T, Sinske D, Schwarz H, Vingron M, Nordheim A & Knöll B (2009) Paracrine control of oligodendrocyte differentiation by SRF-directed neuronal gene expression. *Nat. Neurosci.* 12: 418–27.
- Student (1908) *The Probable Error of a Mean* 6th ed. Biometrika.
- Sun HQ, Yamamoto M, Mejillano M & Yin HL (1999) Gelsolin, a Multifunctional Actin Regulatory Protein. *J. Biol. Chem.* 274: 33179–33182.
- Sun Q, Chen G, Streb JW, Long X, Yang Y, Stoeckert CJ & Miano JM (2006a) Defining the mammalian CARGome. *Genome Res.* 16: 197–207.
- Sun S-C, Wang Z-B, Xu Y-N, Lee S-E, Cui X-S & Kim N-H (2011) Arp2/3 complex regulates asymmetric division and cytokinesis in mouse oocytes. *PLoS One* 6: e18392.
- Sun Y, Boyd K, Xu W, Ma J, Jackson CW, Fu A, Shillingford JM, Robinson GW, Hennighausen L, Hitzler JK, Ma Z & Morris SW (2006b) Acute myeloid leukemia-associated Mkl1 (Mrtf-a) is a key regulator of mammary gland function. *Mol. Cell. Biol.* 26: 5809–26.
- Symons M, Derry JM, Karlak B, Jiang S, Lemahieu V, McCormick F, Francke U, Abo A, Bagrodia S, Taylor S., Creasy C., Chernoff J, Cerione R., Boguski M., McCormick F, Chant J, Stowers L, Chong L., Traynor-Kaplan A, Bokoch G., et al (1996) Wiskott-Aldrich syndrome protein, a novel effector for the GTPase CDC42Hs, is implicated in actin polymerization. *Cell* 84: 723–34.
- Taylor M, Treisman R, Garrett N & Mohun T (1989) Muscle-specific (CArG) and serum-responsive (SRE) promoter elements are functionally interchangeable in *Xenopus* embryos and mouse fibroblasts. *Development* 106: 67–78.
- Ti S-C, Jurgenson CT, Nolen BJ & Pollard TD (2011) Structural and biochemical characterization of two binding sites for nucleation-promoting factor WASp-VCA on Arp2/3 complex. *Proc. Natl. Acad. Sci. U. S. A.* 108: E463-71.

- Todaro GJ & Green H (1963) Quantitative studies of the growth of mouse embryo cells in culture and their development into established lines. *J. Cell Biol.* 17: 299–313.
- Tomasevic N, Jia Z, Russell A, Fujii T, Hartman JJ, Clancy S, Wang M, Beraud C, Wood KW & Sakowicz R (2007) Differential regulation of WASP and N-WASP by Cdc42, Rac1, Nck, and PI(4,5)P2. *Biochemistry* 46: 3494–502.
- Treisman R (1994) Ternary complex factors: growth factor regulated transcriptional activators. *Curr. Opin. Genet. Dev.* 4: 96–101.
- Treisman R (1995) Journey to the surface of the cell: Fos regulation and the SRE. *EMBO J.* 14: 4905–4913.
- Treisman R, Adamson ED, Meek J, Edwards SA, Aviv H, Volloch Z, Bastos R, Levy S, Banerji J, Rusconi S, Schaffner W, Banerji J, Olson L, Schaffner W, Bastos R, Volloch Z, Aviv H, Bravo R, Burckhardt J, Curran T, et al (1985) Transient accumulation of c-fos RNA following serum stimulation requires a conserved 5' element and c-fos 3' sequences. *Cell* 42: 889–902.
- Treisman R, Bienz M, Pelham HRB, Borgmeyer U, Nowock J, Sippel AE, Brent R, Ptashne M, Chen EY, Seeburg P, Cochran BH, Reffel AC, Stiles CD, Cochran BH, Zullo J, Verma IM, Stiles CD, Curran T, Peters G, Beveren C Van, et al (1986) Identification of a protein-binding site that mediates transcriptional response of the c-fos gene to serum factors. *Cell* 46: 567–574.
- Vandekerckhove J & Weber K (1978) At least six different actins are expressed in a higher mammal: An analysis based on the amino acid sequence of the amino-terminal tryptic peptide. *J. Mol. Biol.* 126: 783–802.
- Vartiainen MK, Guettler S, Larijani B & Treisman R (2007) Nuclear actin regulates dynamic subcellular localization and activity of the SRF cofactor MAL. *Science* 316: 1749–52.
- Veltman DM & Insall RH (2010) WASP family proteins: their evolution and its physiological implications. *Mol. Biol. Cell* 21: 2880–93.
- Wang D, Chang PS, Wang Z, Sutherland L, Richardson JA, Small E, Krieg PA, Olson EN, Aravind L, Koonin EV, Belaguli NS, Sepulveda JL, Nigam V, Charron F, Nemer M, Schwartz RJ, Black BL, Olson EN, Chang PS, Li L, et al (2001) Activation of Cardiac Gene Expression by Myocardin, a Transcriptional Cofactor for Serum Response Factor. *Cell* 105: 851–862.
- Wang D-Z, Li S, Hockemeyer D, Sutherland L, Wang Z, Schrott G, Richardson JA, Nordheim A & Olson EN (2002) Potentiation of serum response factor activity by a family of myocardin-related transcription factors. *Proc. Natl. Acad. Sci. U. S. A.* 99: 14855–60.
- Wang Z, Wang D-Z, Pipes GCT & Olson EN (2003) Myocardin is a master regulator of smooth muscle gene expression. *Proc. Natl. Acad. Sci. U. S. A.* 100: 7129–34.
- Weiß CL & Schultz J (2015) Identification of divergent WH2 motifs by HMM-HMM alignments. *BMC Res. Notes* 8: 18.
- Weissbach J, Schikora F, Weber A, Kessels M & Posern G (2016) Myocardin-Related Transcription Factor A Activation by Competition with WH2 Domain Proteins for Actin Binding. *Mol. Cell. Biol.* 36: 1526–39.
- Winder SJ & Ayscough K. (2005) Actin-binding proteins. *J. Cell Sci.* 118: 651–654.

- Wu X, Yoo Y, Okuhama NN, Tucker PW, Liu G & Guan J-L (2006) Regulation of RNA-polymerase-II-dependent transcription by N-WASP and its nuclear-binding partners. *Nat. Cell Biol.* 8: 756–63.
- Yamaguchi H, Lorenz M, Kempiak S, Sarmiento C, Coniglio S, Symons M, Segall J, Eddy R, Miki H, Takenawa T & Condeelis J (2005) Molecular mechanisms of invadopodium formation: the role of the N-WASP-Arp2/3 complex pathway and cofilin. *J. Cell Biol.* 168: 441–52.
- Yoshio T, Morita T, Tsujii M, Hayashi N & Sobue K (2010) MRTF-A/B suppress the oncogenic properties of v-ras- and v-src-mediated transformants. *Carcinogenesis* 31: 1185–93.
- Zencheck WD, Xiao H, Nolen BJ, Angeletti RH, Pollard TD & Almo SC (2009) Nucleotide- and activator-dependent structural and dynamic changes of arp2/3 complex monitored by hydrogen/deuterium exchange and mass spectrometry. *J. Mol. Biol.* 390: 414–27.
- Zuchero J & Coutts A (2009) p53-cofactor JMY is a multifunctional actin nucleation factor. *Nat. cell* 11: 451–459.
- Zuchero JB, Belin B & Mullins RD (2012) Actin binding to WH2 domains regulates nuclear import of the multifunctional actin regulator JMY. *Mol. Biol. Cell* 23: 853–63.

VII Abbreviation List

A	acidic domain
Abi 1	Abelson interactor
ABP	actin-binding proteins
<i>Acta2</i>	smooth muscle actin, actin alpha 2
ADP	adenosine diphosphate
APS	ammonium persulfate
<i>Arc</i>	activity-regulated cytoskeleton-associated
ARP2/3 complex	actin-related protein-2/3 complex
ATP	adenosine triphosphate
BCA	bicinchoninic acid
BiFC	bimolecular fluorescence complementation
bp	base pair
BSA	bovine serum albumin
C	central/connecting domain
CAP	adenylyl-cyclase-associated protein
CArG box	consensus SRF-binding site (CC(A/T) ₆ GG)
CArG-like element	non-consensus SRF-binding site
cDNA	complementary DNA
<i>c-fos</i>	proto-oncogene
cpGFP	circularly permuted GFP
Co-IP	co-immunoprecipitation
CRIB	Cdc42 and Rac interactive binding
CT	cycle threshold
DMEM	Dubelcco's modified Eagle medium
DMSO	di-methyl-sulfoxide
DNA	deoxyribonucleic acid
DRF	Diaphanous-related formins
GEF	guanine nucleotide exchange factors
eGFP	enhanced green fluorescent protein
GFP	green fluorescent protein
GMF	glia maturation factor (GMF)
E	glutamic acid
<i>E. coli</i>	<i>Escherichia coli</i>
EDTA	Ethylenediaminetetraacetic acid
EGF	epithelial growth factor
<i>Egr1</i>	early growth response 1 gene
Elk-1	Ets-like transcription factor 1
EMT	epithelial-mesenchymal transition
ERK	extracellular signal-regulated kinase

Ets	E twenty six
FACS	fluorescence-activated cell sorting
FBS	fetal bovine serum
FCS	fetal calf serum
FH	formin homology domains
f.l.	full length
FRET	fluorescence resonance energy transfer
HA	hemagglutinin
HEPES	4-(2-hydroxyethyl)-1-piperazineethansulfonic acid
HPRT	hypoxanthine phosphoribosyl-transferase
HS1	hematopoietic-specific protein 1
IEG	immediate early genes
<i>Itga5</i>	integrin alpha 5
JMY	junction-mediating and regulatory protein
kb	kilobase
K_d	dissociation constant
kDa	kilodalton
LatB	Latrunculin B
LB	lysogeny broth
LPA	lysophosphatidic acid
MACS	magnetic cell separation
MADS box	DNA-binding motif, identified in MCM1, AG, DEFA, SRF
MAL	megakaryocytic acute leukemia
MAPK	mitogen-activated protein kinase
mDia	murine Diaphanous
Mkl	megakaryoblastic leukemia
MRTF	myocardin-related transcription factors
MYOCD	myocardin
NAD^+	Nicotinamide adenine dinucleotide
Nck1,2	non-catalytic kinase 1, 2
NES	nuclear export signal
Net	Erp/Sap-2/Elk-3
NLS	nuclear localization signal
NPF	nucleation promoting factor
N-WASP	neuronal WASP
OTT	one twenty two
PAGE	polyacrylamide gel electrophoresis
PBS	phosphate buffered saline
PCR	polymerase chain reaction
PICK1	protein interacting with C kinase 1
PVDF	polyvinylidene fluoride
qRT-PCR	reverse transcription-quantitative PCR
R	Arginine
RBM15	RNA-binding motif protein-15

RFP	red fluorescent protein
RIPA	radio-immunoprecipitation assay buffer
RNA	ribonucleic acid
ROCK	Rho-associated kinase
RPEL	actin-binding domain with consensus sequence RPxxxEL
rpm	rounds per minute
SAP	SAF-A/B, Acinus, PIAS DNA-binding domain
Sap-1	SRF accessory protein 1
SDS	sodium dodecyl sulfate
SEM	standard error of the mean
SH3	Src homology 3
SHD	SCAR homology domain
SILAC	stable isotope labeling by amino acids in cell culture
siRNA	small interfering RNA
SRE	serum response element
SRF	serum response factor
SOMA	Single Oligonucleotide Mutagenesis and Cloning Approach
TAD	transcriptional transactivation domain
TCF	ternary complex factor
TECEP	Tris-(2-carboxyethyl)-phosphine hydrochloride solution
TEMED	N,N,N,N-Tetramethylethylenediamine
TGF- β	transforming growth factor β
TNF α	tumor necrosis factor α
TOCA1	transducer of Cdc42-depenent actin assembly
UV	ultraviolet
V	verprolin homology domain (WH2)
<i>Vcl</i>	vinculin
WAS	Wiskott-Aldrich syndrome
WASH	WASP and SCAR homologue
WASP	Wiskott-Aldrich syndrome protein
WAVE	WASP family verprolin-homologous protein
WB	western blot
WCR	WAVE regulatory complex
WH2	WASP homology 2 domain (V)
WHAMM	WASP homologue associated with actin, membranes and microtubules
WIP	WASP-interacting protein
WT	wildtype
YFP	yellow fluorescent protein

VIII Appendix

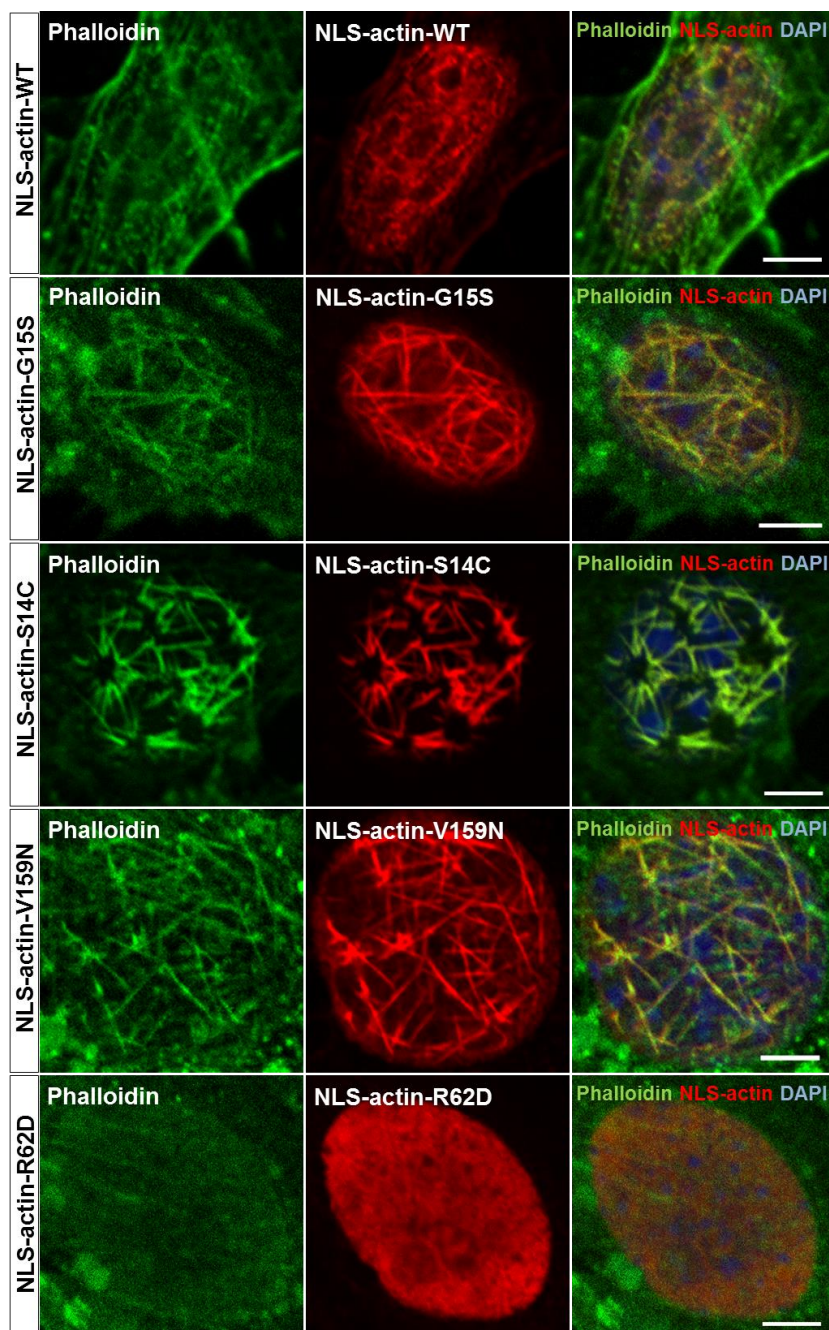


Figure VIII-1: Analysis of nuclear actin networks through phalloidin staining. NIH 3T3 fibroblasts were transfected with the indicated actin mutants, fixed, counterstained with DAPI (blue) and phalloidin (green), immune-stained against Flag-tag for the localization of the expressed actins (red) and analyzed by confocal microscopy. Cells expressing NLS-actin-WT/-G15S/-S14C/-V159N showed phalloidin- and Flag-positive nuclear F-actin bundles with an increased straight shape from actin-WT to actin-V159N. Polymerization-deficient NLS-actin-R62D was negative for phalloidin- or Flag-positive actin bundles and showed a uniform distribution over the nucleoplasm. *Scale bars, 5 μ m.*

N-WASP 1 -----MSS 3
WAVE2 1 -----mpLVT 5
JMY -----

N-WASP 4 GQQPPRRV-----TNV-----gsl11tPQENESLFSFLGKKCVTMSSAVVQlyA---ADRCMWA 55
WAVE2 6 RNIEPRHLcrqtlpsdtselecrTnitlanvirqlgsl---SKYAEDIFGEICTQASAFASRVNSlaervdrVQVKVTQL 82
JMY -----

N-WASP 56 KKCSGVACLVKDNPQRSYFLRIFDIKDGKLL---WEQEL-----YNNFVYNSPRGYFHFHAFAGDTCQVALNFANEEEE- 123
WAVE2 83 DPKEEEVSIQGINTRKAF--RSSTTQDQKLF---DRNSLPVPVLETYNSCDAPPPINLSPYRDDGKEALKFYTNPSYF 156
JMY 1 -----MSfaLEETLESDWAVRPHVFDEREKHKFVFIWAWNEIEGKFAITCHNRTAQ 52

N-WASP 124 ---AKKFRKAVTDLLGRQRKSEKRRDAPNGPNLPMATVDIKNPEITTNRFYGSQVNNI SHTK---EKKKGKA-KK-K 193
WAVE2 157 FDLWKEKMLQDTKDIMKEKRKHKEKNDPNRGNVNRKIKTRKEWEKMKMGQEFVE--SKER---LGPSGYS-ST-L 228
JMY 53 RQSGSREQAGTPASDGSRGPGSPAARGRSEAAAATAALRSPGPRKSQAWAEGGSPRSARSLKgdppRGPAGRGpESPL 132

N-WASP 194 RLTKADIGTPSNFQIHVGVWDpNTGFDLNNLDPELKNLFDmCGISeAQlKdREtSKVIYDFIEKtGGVEAVKNE----- 268
WAVE2 229 VYQNGSIGSVENVDAASYPPPPQSDSASSPSPFSEDNLPPPPAEFSYPADNQRGSVLAGPKRTSMVSPSHPPPA----- 303
JMY 133 RSPARAKASPLRRSAESRDATASATPAPPAPPVPPVSSVRVVSASGAVSEEEIEVLEMVREDEAPQPLPDSEQPPPSAAELE 212

N-WASP 269 -----LRRQAPP-----PPPPSRGGPPPPPPPHSS-----GPPPPPARGRGAPP----- 308
WAVE2 304 -----PPLSSPP-----GPKGFAPPAPPAPPMPMS-----VFPPLPSMGFGSPG----- 343
JMY 213 -----SPAEecswAGLFSFQDLRAVHQQLCSVNSqLEPCLPVFFPEEPGmwt-----vlfq 263

N-WASP -----
WAVE2 -----
JMY 264 g-----apemteqeI-----dalcyqlqvyI-----ghgldtcgwkiI-----sq 298

N-WASP	-----	
WAVE2	-----	
JMY	vlfte-----tddpeey-----eslseirq--kgyeevlqarrrriqellld--khktiesmve-----lildlyq	354
N-WASP	-----	
WAVE2	-----	
JMY	MEDE----AYSSIAEATTEL-----YQYLLQPFQDMRE--LMLRRQIQIKI--SMENDYLGPRRIESLQKED----	413
N-WASP	-----	
WAVE2	-----	
JMY	ADWQRKAHMAVLSIQDLTVKY-----FEITAKAQKAVYDRMRADQKKFKASWAAAAER-----MEKLQYAVS	476
N-WASP	-----	
WAVE2	-----	
JMY	KETLQMMRAKEICLEQ-----KKHALKEEMQSLQGGTEAI---ARLD-----QLESDYDILQQLY---EVQF	533
N-WASP	-----	
WAVE2	-----	
JMY	EILKCEELLTLTAQLESIKRLISEKRDEVV---YYDTYESMEamLEKEEMAA-----SVH---AQREELQKLOQKARQL	600
N-WASP	-----	
WAVE2	-----	
JMY	EARRGRVSAKKAYLRNKKEICIAKHHEKFQQRFOSEDEYRAHHTIQIKRDKLHDEEERKSAWVSQERQRTLDRLRTFKQR	680
N-WASP	-----	
WAVE2	-----	
JMY	YPGQvilkstrlrrvaHSRRRKSTASpvpcceeqchslptvllqgqektevggggs-qlgpsqtapQSLVqledtsseqllest	759

N-WASP	309	PPPS-----RAPTAAPPPPPPSRP-----GVVVPPPPNRMYPSP-----PPALPSSA	351
WAVE2	344	TP-----PPSPPSFP-----PHPFAAPP-----PPPPAAD	372
JMY	760	SLPP-----RAVVSSELPFQASAPLLTSI-----dpkpcsvTID-----FLPPPLpptppPPPPPPP	811
N-WASP	352	PSGPP-----	356
WAVE2	373	YFMPP-----	377
JMY	812	PPPPPlpvakngastTAETLEKDALRTegnersIPKSASAPAAHLF--DSSQLVSArkkLrktveg---lqrrrvssp	885
N-WASP	357	-----PPPPPSMAGSTAPPPPPPPPP-----FGPPPPGLFSDGDHQPAPSGNKAALLDQIREGAQL	415
WAVE2	378	-----PPLSQPSGGA--PPPPPPPP-----PGPPPLPFGADGQPAAPPPPPSEATKPK-----	426
JMY	886	MDEVLASLKR-----SFHLKKVEQRTLPFPFDE-----	914
Δ474-476 / Δ960-963			
N-WASP	416	KKVEqnsrpscGRDALLDQIRQ--G---IQLKSVSD---GQESTPPT-----PAPTSgIVGALMEVMCKSSKAI-HS-	480
WAVE2	427	-----sslpaVSDARSDLLSAIRQ--G---FQLRRVEE---QREQEK-----RDVVGNVDVATILSFRIAV-EY-	480
JMY	915	-----DDSNNILAQIRK--G---VKLKKVQKEVL--RESFT-----LLPDTDPLTRSIHEALRIKEAS----	966
N-WASP	481	-----SDEdedDDEEDEFDDDEWED	501
WAVE2	481	-----SDSE--DDSEFEDEDD-WSD	497
JMY	967	-----PES---EDEEALPCTDWEN	983

Figure VIII-2: Amino acid alignment of murine full length N-WASP, WAVE2 and JMY. Computer based alignment of the indicated full length NPF showed structural homology of WH2 (V) domains (gray), the central region (C) (green) and the acidic region (A) (purple). Structural homology highlighted a highly conserved arginine (R) (red) located at the C-terminus of all three proteins. *Arrows* indicate positions of inserted STOP codons and initiation positions of deletions or point mutations.

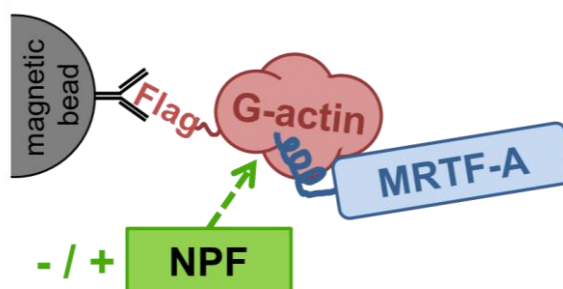


Figure VIII-3: Schematics of anti-Flag co-immunoprecipitation assay of Flag-actin:MRTF-A complexes. Co-immunoprecipitation of Flag-actin complexed with MRTF-A was mediated by anti-Flag magnetic beads. Supplementation of overexpressed WH2 (V)-containing nucleation promoting factors (NPF) was done to analyze the impact of the NPF on complex dissociation.

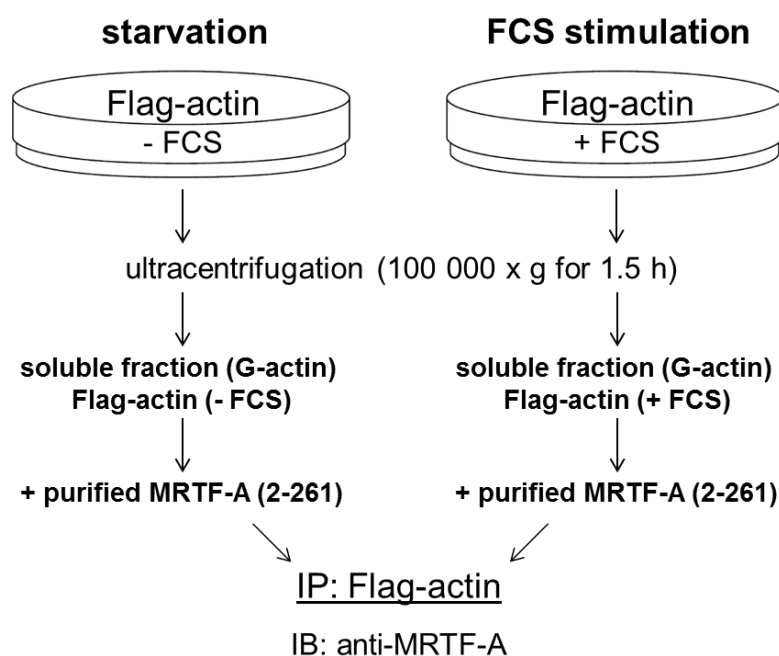


Figure VIII-4: Experimental setup for co-immunoprecipitation of ultra-centrifuged Flag-actin and purified MRTF-A. Serum-starved NIH 3T3 cells (-FCS) were transiently transfected with Flag-actin. Serum-stimulation with 15% FCS (+FCS) was for 1 hour before harvesting. Flag-actin expressing cells were harvested in G-actin buffer (soluble fraction buffer) and ultra-centrifuged at 100 000 x g for 1.5 hours. Ultra-centrifuged supernatants were mixed with purified MRTF-A (2-261) and incubated with anti-Flag magnetic beads for another 1.5 hours under constant rotation. Precipitated Flag-actin was analyzed for the amount of bound MRTF-A (2-261) using anti-MRTF-A and anti-Flag antibody.

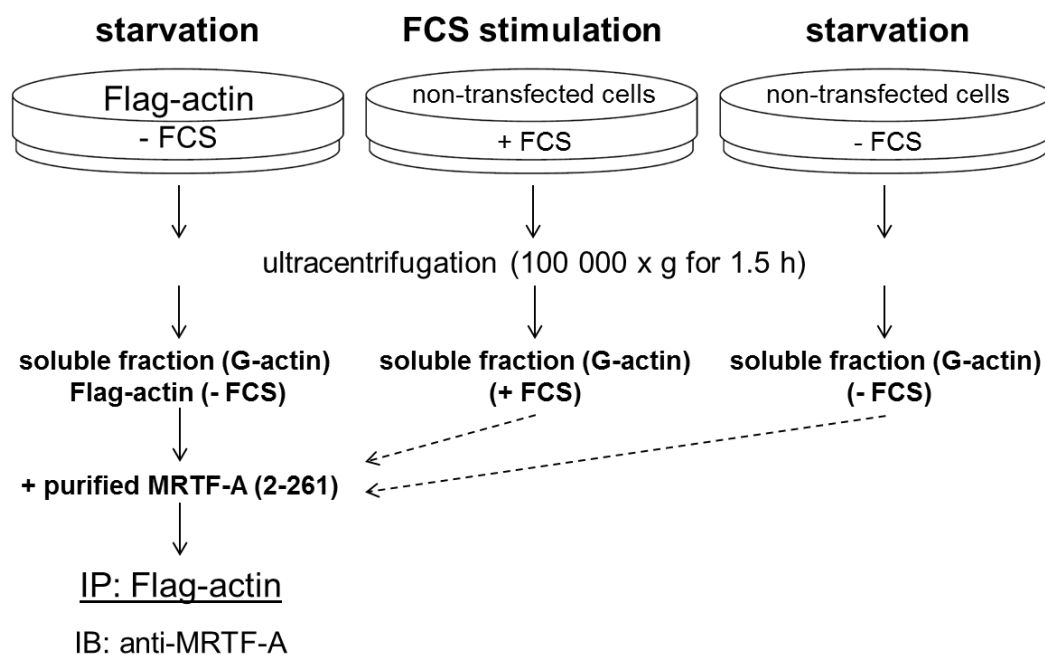


Figure VIII-5: Schematics of the experimental setup of anti-Flag co-immunoprecipitation to identify a *trans*-acting factor. Serum-starved NIH 3T3 cells were either transiently transfected with Flag-actin (Flag-actin, -FCS) or remained non-transfected (non-transfected cells, -FCS). Serum-stimulation of non-transfected cells with 15% FCS (non-transfected cells, +FCS) was for 1 hour before harvesting. Cells were harvested in G-actin buffer (soluble fraction buffer) and ultra-centrifuged at 100 000 x g for 1.5 hours. Ultra-centrifuged supernatant of Flag-actin-expressing cells was mixed with the supernatant of non-transfected starved cells (-FCS) and purified MRTF-A (2-261) as control. Serum-stimulation was analyzed by mixing the supernatant of Flag-actin-expressing cells with the supernatant of non-transfected FCS stimulated cells (+FCS) and purified MRTF-A (2-261). The lysate mixes were incubated with anti-Flag magnetic beads for 1.5 hours under constant rotation. Precipitated Flag-actin was analyzed for the amount of bound MRTF-A (2-261) using anti-MRTF-A and anti-Flag antibody.

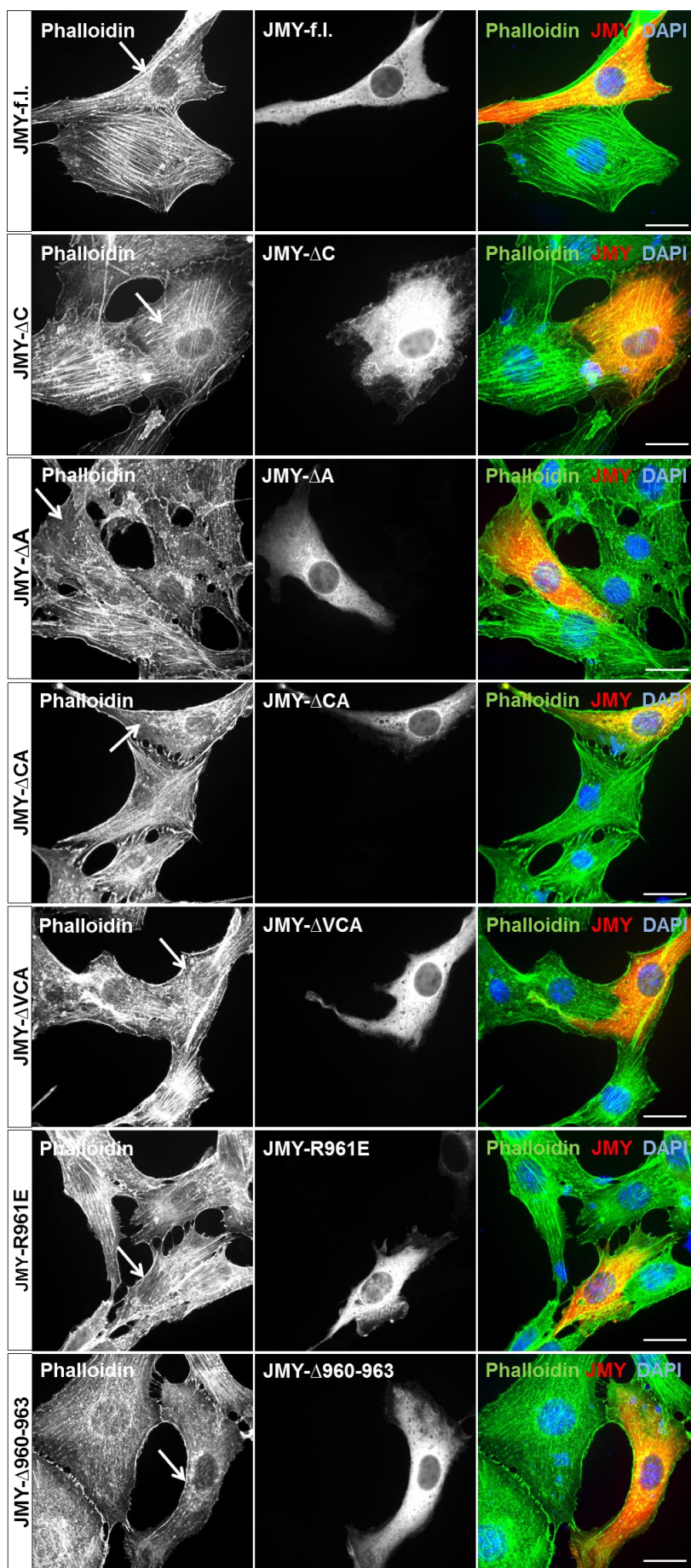
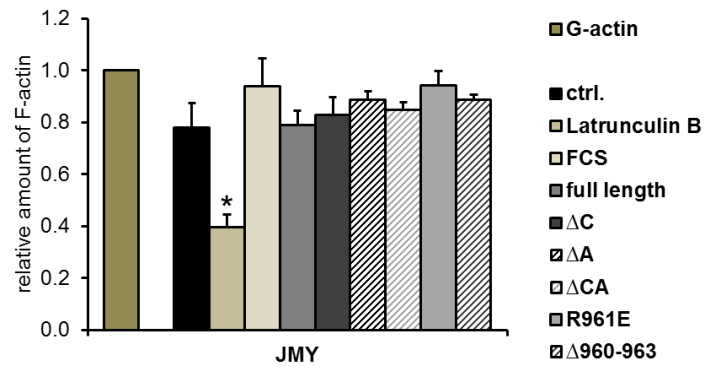


Figure VIII-6: Overexpression of JMY did not induce enhanced actin polymerization. Serum-starved NIH 3T3 cells were transiently transfected with the indicated myc-tagged JMY constructs and analyzed for the actin cytoskeleton by epifluorescence microscopy. Transfected cells were fixed, counterstained with DAPI (blue) and immunostained with anti-myc antibody for the localization of myc-expressing cells (red) and phalloidin (green) to visualize F-actin. *Arrows* indicate myc-expressing cells. *Scale bars*, 20 μm .



VIII-7: Quantification of the proportionality of G- and F-actin upon overexpression of JMY constructs. Serum-starved NIH 3T3 cells were transiently transfected with the indicated myc-tagged JMY constructs and analyzed for the actin cytoskeleton by cell fractionation via ultracentrifugation. F-actin levels were normalized to G-actin which was set to 1. Non-transfected, non-treated cells (ctrl.) and treatment with 1 μ M Latrunculin B or 15% serum (FCS) for 1 hour were as controls. *Error bars*, s.e.m., n = 3 (* $p \leq 0.05$, ** $p \leq 0.01$, *** $p \leq 0.001$ according to an unpaired two sample student's t-test).

IX List of Publications

Parts of this dissertation were published in the following peer-reviewed works:

Weissbach J., Schikora F., Weber A., Kessels M., Posern G. 2016. MRTF-A activation by competition with WH2 domain proteins for actin binding. *Molecular and Cellular Biology* 01097-15.

Kokai E., Beck H., Weissbach J., Arnold F., Sinske D., Sebert U., Gaiselmann G., Schmidt V., Walther P., Münch J., Posern G., Knöll B. 2014. Analysis of nuclear actin by overexpression of wild-type and actin mutant proteins. *Histochemistry and Cell Biology* 141:123-135.

X Acknowledgements

First, I would like to thank Prof. Guido Posern for giving me the opportunity to work on this interesting project in his laboratory, for the support, the scientific input and his general mentoring as well as the continuing willingness to discuss.

I thank Prof. Mechthild Hatzfeld from the University of Halle who kindly accepted to take on the task of second proof reader. Furthermore, I would like to express my gratitude for being a member of my thesis advisory committee.

I thank Prof. Bernd Knöll from the University of Ulm who kindly accepted to take on the task of third proof reader and for being a member of my thesis advisory committee.

I would like to thank all former and current members of the Posern group, Dmitry Shaposhnikov, Ulrich Blache, Anja Ehrenfordt, Falk Pohl, Janine Obendorf, Stefanie Beinicke, Anja Weber, Astrid Vess, Anurag Singh, Franziska Schikora, Sara Werner and Ingo Holstein for the familiar working atmosphere, the scientific and also non-scientific experiences and for making our group probably the coolest one in the whole institute. You are awesome lab mates!

Thereby, my special thanks goes to Anja for her help and her continuing technical but mainly ethical support as well as to Dmitry, Ulrich and Astrid for their advice and helpful discussions. My project partner Franziska I want to thank for supporting each other throughout all stages of our PhD period.

Herbert Neuhaus, the “unofficial member of the Posern group”, I would like to thank for sharing his scientific and non-scientific experiences, for his support, the helpful discussions and his advice.

I thank all members of the Institute for Physiological Chemistry including the Section of Pathobiochemistry (Molecular Medicine) in Halle for their cooperativeness.

To my family, I am grateful for their loving support during my PhD thesis, my duration of study, my whole life! Christoph, thanks for your love and being there for me at all times!

This work was financially supported by the Deutsche Forschungsgemeinschaft (DFG).

Eidesstattliche Erklärung

Hiermit erkläre ich an Eides statt, dass die vorliegende Arbeit selbstständig und nur unter Verwendung der angegebenen Literatur und Hilfsmittel angefertigt wurde. Es wurden keine anderen Quellen und Hilfsmittel verwendet. Die, den benutzten Werken wörtlich oder sinngemäß entnommenen Stellen, sind als solche kenntlich gemacht. Ich versichere weiterhin, dass die Arbeit in gleicher oder ähnlicher Form noch keiner anderen Prüfungsbehörde vorgelegt wurde.

Halle (Saale), Oktober 2016

Julia Weißbach

Lebenslauf

Lebenslauf

Dipl.-Biol. Julia Weißbach

geboren am: 24. Juni 1987 in Querfurt

wohnhaft in: Albert-Schweitzer-Straße 30,
06114 Halle (Saale)

Staatsangehörigkeit: deutsch

Berufliche Tätigkeit

- seit 06/2012 Wissenschaftliche Mitarbeiterin in der Medizinischen Fakultät am Institut für Physiologische Chemie (Prof. Dr. Guido Posern) der Martin-Luther-Universität Halle-Wittenberg, Halle (Saale)
Thema: The Role of WH2-containing Proteins in regulating Actin-MRTF-SRF mediated Transcription
- 10/2011 – 06/2012 Wissenschaftliche Mitarbeiterin in der Medizinischen Fakultät der Klinik und Poliklinik für Innere Medizin I, Abteilung Molekulare Gastroenterologie (Prof. Dr. med. Thomas Seufferlein) am Universitätsklinikum, Halle (Saale)
Thema: Das Armadillo Protein p0071 als neuer Regulator des Proteintransports vom *trans*-Golgi-Netzwerk zur Plasmamembran

Praktische Tätigkeit

- 07/2010 – 05/2011 Diplomarbeit am Institut für Biologie, Institutsbereich Genetik, Abteilung Entwicklungsgenetik (Prof. Dr. Gunter Reuter) der Martin-Luther-Universität Halle-Wittenberg, Halle (Saale)
Thema: SNP-Kartierung und molekulare Analyse neuer *Su(var)*-Gene bei *Drosophila melanogaster*
Bewertung: 1,3

Lebenslauf

- 08/2009 – 09/2009 Forschungsgruppenpraktikum am Institut für Biologie, Institutsbereich Genetik, Abteilung Entwicklungsgenetik (Prof. Dr. Gunter Reuter) der Martin-Luther-Universität Halle-Wittenberg, Halle (Saale)
Thema: SNP-Kartierung von *Su(var)-2-8* bei *Drosophila melanogaster*
- 10/2008 Immunologisches Vertiefungspraktikum am Institut für Medizinische Immunologie (Dr. rer. nat. Rudolf Lichtenfels) der Martin-Luther-Universität Halle-Wittenberg, Halle (Saale)
Thema: Proteomex-Screening von Nierenzellkarzinom- und Normalzelllinien zur diagnostischen Früherkennung

Ausbildung

- 10/2005 – 05/2011 Studium der Biologie an der Martin-Luther-Universität Halle-Wittenberg mit Vertiefungsrichtung Genetik
Abschluss: Diplom mit Note: 1,4
- 02/2003 – 06/2005 Staatliches Gymnasium „Klosterschule“ in Roßleben (Thüringen)
Abschluss: Allgemeine Hochschulreife mit Note 1,8
- 09/1999 – 02/2003 Gymnasium in Querfurt
- 09/1997 – 07/1999 Sekundarschule in Schmon
- 08/1993 – 07/1997 Grundschule in Ziegelroda

Halle (Saale), Oktober 2016

Julia Weißbach